UNIVERSIDADE DE SÃO PAULO
Instituto de Ciências Matemáticas e de Computação

New families of linear and partially linear quantile regression models under reparameterized Marshall-Olkin distributions

Isaac Esteban Cortés Olmos

Tese de Doutorado do Programa Interinstitucional de Pós-Graduação em Estatística (PIPGEs)

ICMC USP SÃO CARLOS

Isaac Esteban Cortés Olmos

New families of linear and partially linear quantile regression models under reparameterized Marshall-Olkin distributions

Thesis submitted to the Institute of Mathematics and Computer Science – ICMC-USP and to the Department of Statistics – DEs-UFSCar – in accordance with the requirements of the Statistics Interagency Graduate Program, for the degree of Doctor in Statistics. *FINAL VERSION*

Concentration Area: Statistics

Advisor: Prof. Dr. Mário de Castro Andrade Filho

USP – São Carlos
September 2023

Ficha catalográfica elaborada pela Biblioteca Prof. Achille Bassi
e Seção Técnica de Informática, ICMC/USP,
com os dados inseridos pelo(a) autor(a)

C828n

Cortés, Isaac Esteban
New families of linear and partially linear quantile regression models under reparameterized Marshall-Olkin distributions / Isaac Esteban Cortés; orientador Mário de Castro Andrade Filho. -- São Carlos, 2023.
128 p.

Tese (Doutorado - Programa Interinstitucional de Pós-graduação em Estatística) -- Instituto de Ciências Matemáticas e de Computação, Universidade de São Paulo, 2023.

1. Quantile regression. 2. Global influence. 3. Local influence. 4. Residual analysis. 5. P-splines. I. de Castro Andrade Filho, Mário , orient. II. Título.

Bibliotecários responsáveis pela estrutura de catalogação da publicação de acordo com a AACR2:
Gláucia Maria Saia Cristianini - CRB - 8/4938
Juliana de Souza Moraes - CRB - 8/6176

Isaac Esteban Cortés Olmos

Novas famílias de modelos de regressão quantílica linear e parcialmente linear sob distribuições Marshall-Olkin reparametrizadas

Tese apresentada ao Instituto de Ciências Matemáticas e de Computação – ICMC-USP e ao Departamento de Estatística – DEs-UFSCar, como parte dos requisitos para obtenção do título de Doutor em Estatística – Programa Interinstitucional de Pós-Graduação em Estatística. *VERSÃO REVISADA*

Área de Concentração: Estatística

Orientador: Prof. Dr. Mário de Castro Andrade Filho

USP – São Carlos
Setembro de 2023

UNIVERSIDADE FEDERAL DE SÃO CARLOS

Centro de Ciências Exatas e de Tecnologia
Programa Interinstitucional de Pós-Graduação em Estatística

Folha de Aprovação

Defesa de Tese de Doutorado do candidato Isaac Esteban Cortés Olmos, realizada em 31/07/2023.

Comissão Julgadora:

Prof. Dr. Mário de Castro Andrade Filho (USP)

Profa. Dra. Katiane Silva Conceição (USP)

Prof. Dr. Francisco José de Azevedo Cysneiros (UFPE)

Prof. Dr. Fernanda de Bastiani (UFPE)

Profa. Dra. Larissa Avila Matos (UNICAMP)

O Relatório de Defesa assinado pelos membros da Comissão Julgadora encontra-se arquivado junto ao Programa Interinstitucional de Pós-Graduação em Estatística.

ACKNOWLEDGEMENTS

First, I want to thank the only true God, Jesus Christ, for giving me the strength and intelligence to develop this dissertation. I'd also like to express my gratitude to my brothers in Christ, along with my family, who have been my true support throughout both good and bad times.

My heartfelt thanks to my supervisor, Mário de Castro, for the countless suggestions provided during the development of this dissertation. I would also like to express my gratitude to Professor Diego Gallardo for his valuable input on the dissertation topic.

I would like to thank: Francisco Csyneiros, Katiane Silva Conceição, Fernanda de Bastiani and Larissa Avila Matos for their suggestions in this dissertation work.

Finally, I would like to express my gratitude to my colleagues and classmates at the university. Without their tremendous help, companionship, and patience, I would not have been able to complete this academic journey.

This study was financed in part by the Coordenação de Aperfeiçoamento de Pessoal de Nível Superior - Brasil (CAPES) - Finance Code 001

RESUMO

CORTÉS, I. E. **Novas famílias de modelos de regressão quantílica linear e parcialmente linear sob distribuições Marshall-Olkin reparametrizadas**. 2023. 130 p. Tese (Doutorado em Estatística – Programa Interinstitucional de Pós-Graduação em Estatística) – Instituto de Ciências Matemáticas e de Computação, Universidade de São Paulo, São Carlos – SP, 2023.

Nesta tese, propomos famílias de modelos de regressão quantílica linear e parcialmente linear, onde a variável resposta segue uma distribuição Marshall-Olkin reparametrizada com suporte na reta real. Esta distribuição apresenta uma grande flexibilidade que surge ao aplicar a metodologia Marshall-Olkin as distribuições da família de locação-escala, logo reparametrizando o parâmetro de locação em função do quantil. Por esse motivo, o nome da nova distribuição é Marshall-Olkin reparametrizada, que contém parâmetros de quantil, escala e assimetria. A primeira família tem uma estrutura semelhante aos modelos lineares generalizados, que permite a utilização do método da máxima verossimilhança. Consequentemente, calculamos as expressões do vetor escore e da matriz de informação observada para realizar a inferência estatística. A adequação dos modelos e observações discrepantes são estudadas por meio de três tipos de resíduos. Para avaliar a sensibilidade das estimativas são desenvolvidas medidas de influência global e local. A segunda família é uma extensão da primeira família por adicionar a descrição da relação não linear entre os quantis da variável resposta e uma variável contínua por meio de B-splines. Nesta família as ferramentas de inferência estatística são baseadas na função de log-verossimilhança penalizada. Também, analogamente à primeira família são apresentados os resíduos e as medidas de influência global e local. São considerados dois exemplos de aplicações que ilustram a utilidade das famílias propostas para conjuntos de dados na área de saúde e nutrição.

Palavras-chave: Regressão quantílica, Estimadores de máxima verossimilhança, Influência global, Influência local, Análise residual, Estimadores de máxima verossimilhança penalizada, P-splines.

ABSTRACT

CORTÉS, I. E. **New families of linear and partially linear quantile regression models under reparameterized Marshall-Olkin distributions**. 2023. 130 p. Tese (Doutorado em Estatística – Programa Interinstitucional de Pós-Graduação em Estatística) – Instituto de Ciências Matemáticas e de Computação, Universidade de São Paulo, São Carlos – SP, 2023.

In this dissertation, we propose families of linear and partially linear quantile regression models, where the response variable follows a reparameterized Marshall-Olkin distribution with support on the real line. This distribution presents great flexibility and arises from applying the Marshall-Olkin methodology to distributions of the location-scale family and then reparameterizing the location parameter as a function of the quantile. For this reason, the new distribution's name is reparameterized Marshall-Olkin, which contains quantile, scale and skewness parameters. The first family has a structure similar to the generalized linear models that enable the use of the maximum likelihood method. Consequently, we calculate the expressions of the score vector and the observed information matrix to perform the statistical inference. The adequacy of models and outlier observations are studied through three types of residuals. In order to assess the sensitivity of the estimates, measures of global and local influence are developed. The second family is an extension of the first family by adding the description of the nonlinear relationship between the quantiles of the response variable and a continuous variable through B-splines. In this family, statistical inference tools are based on the penalized log-likelihood function. Also, analogously to the first family, the residuals and measures of global and local influence are presented. Two examples of applications are considered that illustrate the usefulness of the proposed families for data sets in the areas of health and nutrition.

Keywords: Quantile regression, Maximum likelihood estimators, Global influence, Local influence, Residual analysis, Penalized maximum likelihood estimators, P-splines.

LIST OF FIGURES

LIST OF ALGORITHMS

LIST OF TABLES

CONTENTS

CHAPTER

1

INTRODUCTION

Regression analysis describes the linear relationship between the conditional mean of a response variable and a set of predictor variables. The fit and modeling of the conditional mean have been done using simple linear regression, multiple linear regression, and regression with heteroscedastic errors. These regressions employ weighted least squares and maximum likelihood (ML) methods to estimate the parameters. Draper and Smith (1998) and Gordon (2015) have illustrated how important it is to use these tools in disciplines like Economics, Business Administration and the Social Sciences. However, studying only the conditional mean has its limitations, as the three relevant limitations mentioned by Hao and Naiman (2007).

The first limitation of traditional regression is that it does not allow for the analysis of noncentral locations of the response variable to address specific issues of interest. For instance, in studies of economic inequality, there is an interest in modeling the extremes of income, including the poor (lower tail) and the wealthy (upper tail). Another example from the health field involves the study of individuals with low weight (lower tail) and obesity (upper tail) using the body mass index (BMI).

The assumptions of the traditional regression is the second limitation. These assumptions in real life are difficult to satisfy. For example, homoscedasticity does not occur often. Additionally, the response variable commonly has heavier tails than the normal distribution. Finally, the conditional mean is strongly influenced by outliers that make the mean an inappropriate measure.

Finally, the third limitation of traditional regression is that it does not allow us to cover investigations that focus on studying beyond how predictor variables affect the location and scale parameters of the response variable. It is currently necessary to analyze the effects of the predictor variables on the skewness and, if possible, the kurtosis of the response variable.

Quantile regression (QR) models introduced by Koenker and Jr (1978) allow specifying the changes of the conditional quantiles by a set of linear predictors. In this way, its flexibility helps to a great extent to solve problems such as economic inequality and the body mass index

mentioned above. Two of its outstanding advantages are its robustness to the influence of outlier observations (HUNTER; LANGE, 2000) and the ability to provide a complete description of the conditional distribution of the response (DAVINO; FURNO; VISTOCCO, 2013).

Recently, some authors have studied alternative distributions to perform QR. For example, in the context of positively supported responses, Noufaily and Jones (2013) and Sánchez *et al.* (2021) studied the generalized gamma and Birnbaum-Saunders distributions, respectively. Korkmaz and Korkmaz (2023), Mazucheli *et al.* (2020) and Jodra and Jimenez-Gamero (2020) investigated the unit log-log, unit-Weibull and exponential-geometric distributions with support in the unit interval, respectively. In addition, Morales *et al.* (2017) and Gallardo *et al.* (2020) proposed an asymmetric family of distributions and the power skew-normal, both with support in the real line, respectively. The structure of these models has the advantage of the easy interpretation of the parameters that allow the application of the ML methodology to obtain the estimates and carry out analysis of global and local influence.

In this dissertation, we propose new families of linear and partially linear QR models for distributions with quantile, scale and skewness parameters, named reparameterized Marshall-Olkin (RPMO) distributions (CORTÉS; CASTRO; GALLARDO, 2023). These distributions with support on the real line arise by applying the Marshall-Olkin methodology (MARSHALL; OLKIN, 1997) to the family of location-scale distributions and then reparameterizing the location parameter in terms of the quantile. The family of linear QR models can be used to deal with the three limitations of traditional regression. Its structure is similar to generalized linear models (GLM) (NELDER; WEDDERBURN, 1972). Therefore, the ML method allows for obtaining estimates and developing global and local diagnostics.

The family of partially linear QR models is an extension of the linear QR models. They are useful in situations where predictors have linear effects on the quantiles of the response variable while another variable has a nonlinear effect. Thus, the models allow the capture of more complex data viewed in Astronomy, Biology, Medicine, Economics, and Finance, among others.

Cai and Xiao (2012), in different contexts, note that nonparametric and semiparametric regression models (which are a general case of partially linear models) have garnered the attention of researchers due to their greater flexibility compared to linear QR models. Some important references that illustrate the points mentioned include Cai (2002), Gooijer and Zerom (2003) and Cai, Gu and Li (2009).

The main contribution of this dissertation is to develop the process of estimation and statistical inference on the parameters for the families of linear and partially linear QR models under RPMO distributions. Moreover, to adopt techniques of global and local influence for the same families.

This dissertation is structured into six chapters as follows. Chapter 2 introduces the RPMO family of distributions and analyzes their skewness and kurtosis. It then formulates the linear QR model and discusses the ML methodology for estimating the model parameters. Moreover, it adopts three types of residuals, two methods of global influence, and three schemes of methods of local influence. In Chapter 3, the behavior of ML estimators is assessed through simulation studies and presents an application example. Chapter 4 proposes a family of partially linear QR models for RPMO distributions. This chapter is also devoted to performing statistical inference on parameters and extending measures of local and global influence. Chapter 5 studies the properties of penalized ML estimators through simulation. Additionally, this chapter illustrates the methodologies investigated in Chapter 4. Finally, in Chapter 6, we provide some final comments on the main results and some ideas for future work.

1.1 Preliminaries

Marshall and Olkin (1997) propose a widely used method for generating new probability distributions. This method involves introducing a new parameter to an existing distribution and includes the original distribution as a particular case. The resulting distribution offers greater flexibility in modeling various types of data.

The cumulative density function resulting from the application of the Marshall-Olkin (MO) methodology is given by

$$G(y;\alpha) = \frac{F_0(y)}{\alpha + (1-\alpha)F_0(y)},\ y \in \mathbb{R}, \alpha \in \mathbb{R}^+, \tag{1.1}$$

where F_0 represents the baseline cumulative distribution function and α the new parameter. It is evident that Equation (1.1) provides a means to derive new parametric distributions. Consequently, the probability density function corresponding to Equation (1.1) can be expressed as

$$g(y;\alpha) = \frac{\alpha f_0(y)}{[\alpha + (1-\alpha)F_0(y)]^2},\ y \in \mathbb{R}, \alpha \in \mathbb{R}^+, \tag{1.2}$$

with f_0 representing the baseline probability density function. In the literature, some interesting specific cases of (1.2) discussed involve taking f_0 to be normal (GARCÍA; GÓMEZ-DÉNIZ; VÁZQUEZ-POLO, 2010), Cauchy (JACOB; JAYAKUMAR, 2012) and other distributions belonging to the location-scale family (RUBIO; STEEL, 2012).

CHAPTER

2

REPARAMETERIZED MARSHALL-OLKIN REGRESSION MODELS

This chapter presents the family of RPMO distributions for modeling data with support on the real line. Subsequently, an analysis of the skewness and kurtosis of these distributions is conducted. Additionally, the QR model is formulated, defining a structure similar to that of GLM. This formulation naturally leads us to employ ML methodology for deriving the score vector, ML estimators, and the observed information matrix in order to perform statistical inferences.

Furthermore, diagnostic analysis methods for the QR model of the RPMO family are developed. First, three types of residuals are adopted. Secondly, the expressions of likelihood displacement and generalized Cook's distance are proposed as global influence. Third, three perturbation schemes in the model or data are specified as local influence.

2.1 Reparameterized Marshall-Olkin distributions

This section defines the probability density function (pdf) of the RPMO family of distributions. Then, some properties are studied, such as the cumulative distribution function (cdf) and the quantile function (qf).

Definition 2.1. We will say that a random variable Y has a RPMO distribution if its pdf is given by

$$g(y;\xi_q,\sigma,\alpha) = \frac{\alpha f_0(u_q)}{\sigma\left[\alpha+(1-\alpha)F_0(u_q)\right]^2}, \quad y\in\mathbb{R}, \tag{2.1}$$

where

$$u_q = \frac{y-\xi_q}{\sigma} + F_0^{-1}\left(\frac{\alpha q}{1+q\alpha-q}\right),$$

$\xi_q \in \mathbb{R}$, $\sigma \in \mathbb{R}^+$ and $\alpha \in \mathbb{R}^+$ are the q-quantile, scale and skewness parameters, respectively. Also, f_0 and F_0 are the baseline pdf and cdf belonging to the location-scale family. We denote it by $Y \sim \text{RPMO}(\xi_q, \sigma, \alpha, f_0)$.

The set of distributions with a pdf given in Equation (2.1) is referred to as the RPMO family. Consequently, Table 1 displays the expressions of f_0 and F_0 for the family members, along with their corresponding notations. It's worth noting that the logistic distribution, which belongs to the location-scale family, is not included in the table. This omission is due to the Arnold-Groeneveld skewness measure being zero for any value of α, as discussed in Rubio and Steel (2012). This indicates that the α parameter does not modify the skewness of the logistic distribution and, as a result, it is excluded from the RPMO family.

Table 1 – Expressions of f_0 and F_0 of the baseline models and their respective notations in the RPMO family.

Baseline Model	$f_0(u_q)$	$F_0(u_q)$	New Model
Gumbel	$\exp\left(-u_q - \exp\left(-u_q\right)\right)$	$\exp\left(-\exp\left(-u_q\right)\right)$	RPMOG
Student's-t	$\frac{\Gamma\left(\frac{\vartheta+1}{2}\right)}{\sqrt{\pi\vartheta}\Gamma\left(\frac{\vartheta}{2}\right)}\left(1+\frac{u_q^2}{\vartheta}\right)^{-\frac{\vartheta+1}{2}}$	$\frac{1}{2}+\frac{u_q\Gamma\left(\frac{\vartheta+1}{2}\right)}{\sqrt{\pi\vartheta}\Gamma\left(\frac{\vartheta}{2}\right)}{}_2F_1\left(\frac{1}{2},\frac{\vartheta+1}{2};\frac{3}{2},-\frac{u_q^2}{\vartheta}\right)$	RPMOT
Normal	$\frac{1}{\sqrt{2\pi}}\exp\left(-\frac{u_q^2}{2}\right)$	$0.5\left[1+\text{erf}\left(\frac{u_q}{\sqrt{2}}\right)\right]$	RPMON
Cauchy	$\frac{1}{\pi(1+u_q^2)}$	$0.5+\frac{\arctan(u_q)}{\pi}$	RPMOC

Note: ϑ, erf and ${}_2F_1$ denote the degrees of freedom, error function and hypergeometric function, respectively.

One of the advantages of the RPMO family is that its pdf has closed form expressions, which reduce computational costs. Another advantage is that it can be useful for modeling data with support on the real line. Additionally, if $\alpha = 1$ in Equation (2.1), we have the reparameterized pdf of the location-scale family.

Figure 1 illustrates the behavior of the distributions within the RPMO family for $\sigma = 1$, $q = 0.5$ and different values of α and ξ_q. We have highlighted the particular case when $\alpha = 1$ with a red line in the plots. It's worth noting that these distributions exhibit greater flexibility compared to their specific cases. As expected, the family can be used to fit skewed and unimodal data.

Properties 2.1. Let $Y \sim \text{RPMO}(\xi_q, \sigma, \alpha, f_0)$, then the cdf of Y is given by

$$G(y; \xi_q, \sigma, \alpha) = \frac{F_0(u_q)}{\alpha + (1-\alpha)F_0(u_q)}, \tag{2.2}$$

where

$$u_q = \frac{y - \xi_q}{\sigma} + F_0^{-1}\left(\frac{\alpha q}{1 + q\alpha - q}\right).$$

The expression in Equation (2.2), like that of the pdf, has a closed form. Figure 2 illustrates the behavior of the cdf for $\sigma = 1$, $q = 0.5$ and different values of ξ_q and α. It can be observed that for α values smaller than 1 (particular case), the cdf converges more rapidly to 1 , while for α values greater than 1, the CDF converges more slowly to 1.

Properties 2.2. Let $Y \sim \text{RPMO}(\xi_q, \sigma, \alpha)$, then the qf of Y is expressed as

$$Q(p;\xi_q,\sigma,\alpha) = \sigma\left[F_0^{-1}\left(\frac{\alpha p}{1+p\alpha-p}\right) - F_0^{-1}\left(\frac{\alpha q}{1+q\alpha-q}\right)\right] + \xi_q, \tag{2.3}$$

where $p \in (0,1)$ and $q \in (0,1)$. Note that if $p = q$, then $Q(p;\xi_q,\sigma,\alpha) = \xi_q$. Algorithm 1 presents a scheme that generates random numbers to distributions belonging to the RPMO family using the inversion method.

Figure 1 – Plots of the pdfs of the distributions belonging to the RPMO family with $\sigma = 1$, $q = 0.5$ and different values of ξ_q and α.

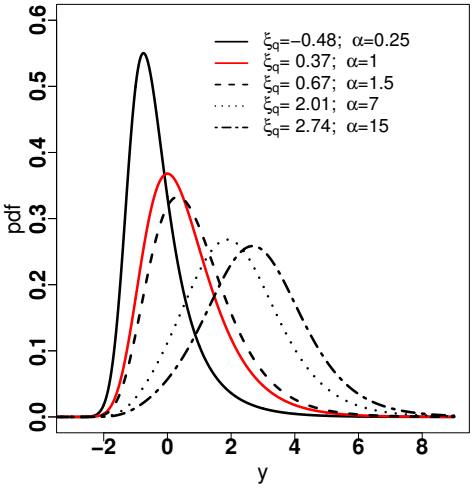

(a) RPMOG

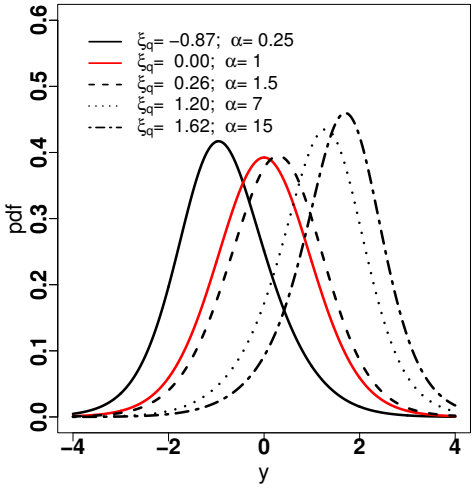

(b) RPMOT with $\vartheta = 15$

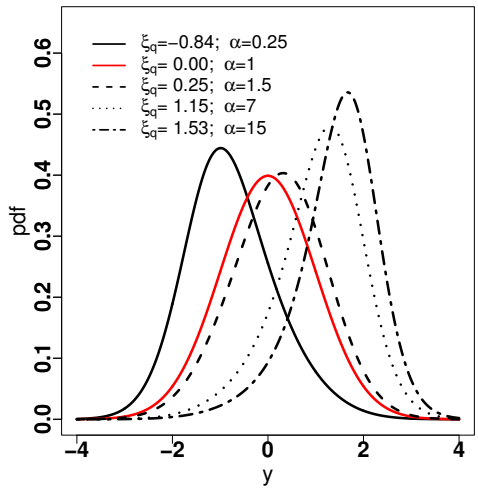

(c) RPMON

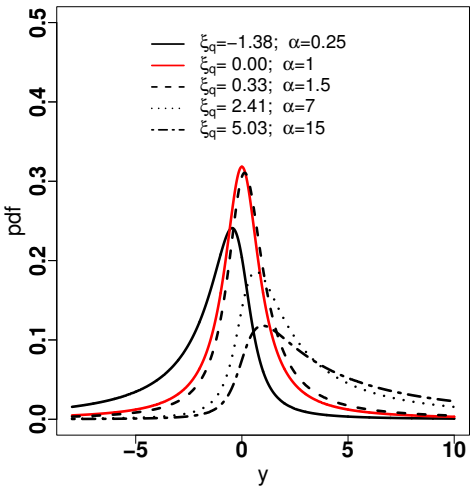

(d) RPMOC

Algorithm 1 – Generation of a random numbers from the distribution RPMO$(\xi_q, \sigma, \alpha, f_0)$

1: Set the values of the probability q and the parameters ξ_q, σ and α.
2: Generate random numbers $U_i \sim U(0,1)$, where U_i denotes the unitary uniform distribution.
3: Evaluate

$$y_i = \sigma\left[F_0^{-1}\left(\frac{U_i\alpha}{1+\alpha U_i - U_i}\right) - F_0^{-1}\left(\frac{\alpha q}{1+q\alpha - q}\right)\right] + \xi_q.$$

4: Repeat (2)-(3) for $i = 1, \ldots, n$.

Figure 2 – Plots of the cdfs of the distributions belonging to the RPMO family with $\sigma = 1$, $q = 0.5$ and different values of ξ_q and α.

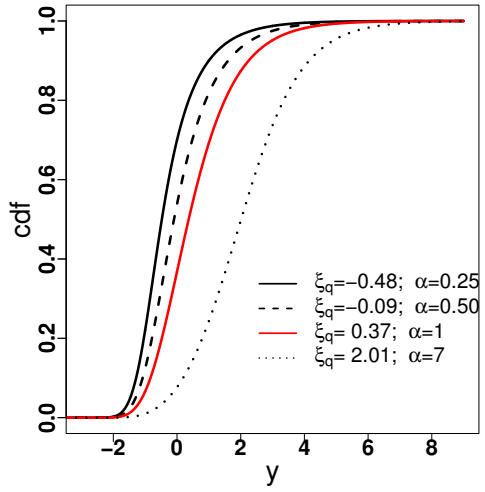

(a) RPMOG

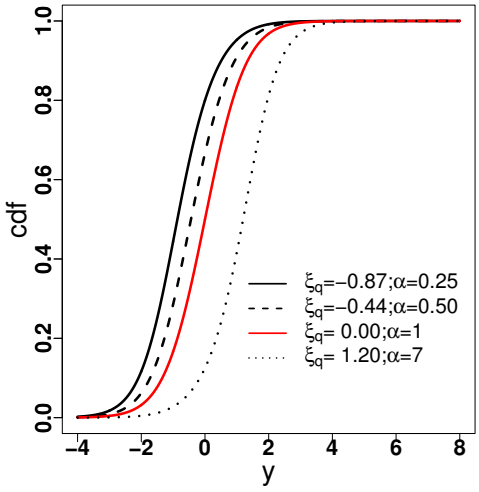

(b) RPMOT with $\vartheta = 15$

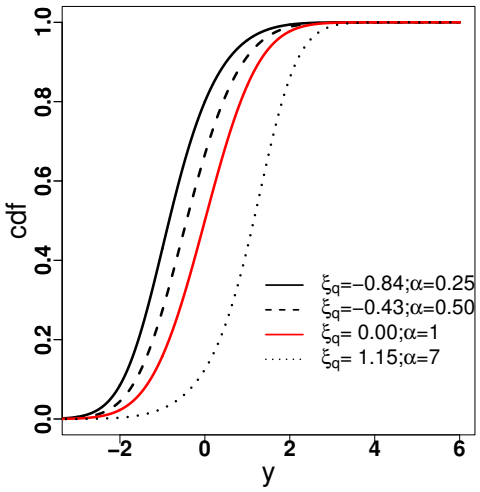

(c) RPMON

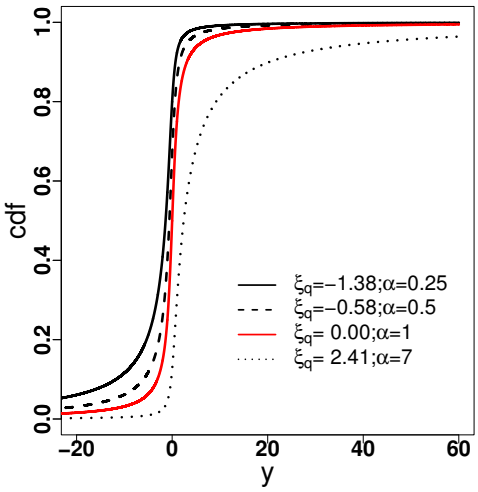

(d) RPMOC

2.2 Skewness and Kurtosis

In this section, we analyze the skewness and kurtosis measures of the distributions through respective plots.

Let $Y \sim \text{RPMO}(\xi_q, \sigma, \alpha, f_0)$, we can assess its skewness behavior numerically using Fisher's skewness coefficient, defined in this family as

$$\tilde{\mu}_3 = \frac{\mathbb{E}\left[(Y - \mathbb{E}[Y])^3\right]}{\left(\mathbb{E}\left[(Y - \mathbb{E}[Y])^2\right]\right)^{3/2}}, \text{ where } \qquad \mathbb{E}[Y^k] = \int_{-\infty}^{\infty} y^k \, g(y; \xi_q, \sigma, \alpha) dy. \tag{2.4}$$

However, the RPMOC distribution lacks finite moments. Therefore, we suggest using Bowley's skewness coefficient, denoted by

$$S_k = \frac{Q(0.75; \xi_q, \sigma, \alpha) + Q(0.25; \xi_q, \sigma, \alpha) - 2Q(0.5; \xi_q, \sigma, \alpha)}{Q(0.75; \xi_q, \sigma, \alpha) - Q(0.25; \xi_q, \sigma, \alpha)}, \tag{2.5}$$

where $Q(p; \xi_q, \sigma, \alpha)$ is the qf defined in Equation (2.3).

Figure 3 shows the skewness coefficients in the distributions for $\sigma = 1$ and $\xi_q = 0$ as a function of $\alpha \in (0, 50]$. Another plot within the figure specifies an interval of α values specifically for the RPMOT distribution. The red line highlights the case when $\alpha = 1$. In this figure, it is evident that the distributions exhibit both negative and positive skewness, except for the RPMOG distribution, which shows only positive skewness. Furthermore, the behavior of the skewness measure in the RPMOG distribution is decreasing, in contrast to the RPMOC distribution. The RPMOT distribution with $\vartheta = 15$ is not monotonic. All figures indicate that the distributions within the family offer higher flexibility than their particular cases.

To assess the kurtosis of the RPMO family, we utilize the Pearson kurtosis coefficient defined by

$$\tilde{\mu}_4 = \frac{\mathbb{E}\left[(Y - \mathbb{E}[Y])^4\right]}{\left(\mathbb{E}\left[(Y - \mathbb{E}[Y])^2\right]\right)^2}. \tag{2.6}$$

On the other hand, we propose the Moors kurtosis coefficient for the RPMOC distribution, denoted as

$$\text{K}_k = \frac{\left[Q(7/8; \xi_q, \sigma, \alpha) - Q(5/8; \xi_q, \sigma, \alpha)\right] + \left[Q(3/8; \xi_q, \sigma, \alpha) - Q(1/8; \xi_q, \sigma, \alpha)\right]}{Q(6/8; \xi_q, \sigma, \alpha) - Q(2/8; \xi_q, \sigma, \alpha)}, \tag{2.7}$$

where $Q(p; \xi_q, \sigma, \alpha)$ is the qf defined in Equation (2.3).

Figure 4 displays the kurtosis coefficient for $\sigma = 1$ and $\xi_q = 0$ as a function of $\alpha \in (0, 50]$. The red line highlights the case when $\alpha = 1$. In the figure, we can observe that the coefficients in the RPMON, RPMOC and RPMOT (with $\vartheta = 15$) distributions exhibit similar behavior. Furthermore, the RPMOG distribution demonstrates a high kurtosis and its coefficient decreases as α increases. All figures indicate that the distributions within the family have higher kurtosis than their particular cases.

Figure 3 – Plots of the skewness coefficient in the RPMO family of distributions against α parameter.

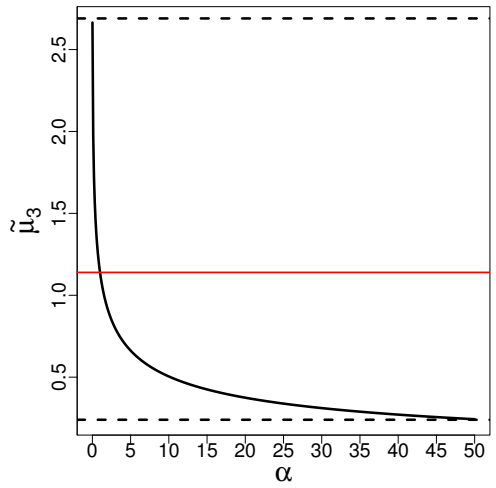

(a) RPMOG

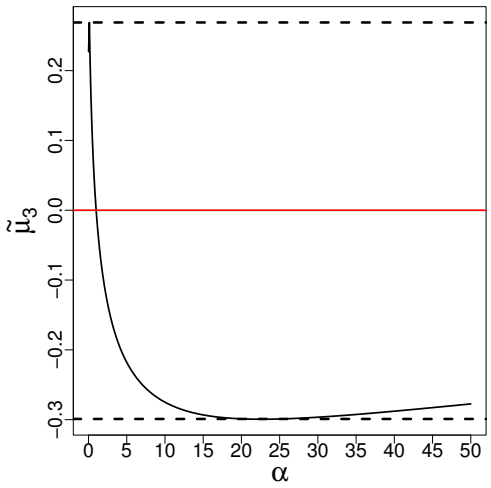

(b) RPMOT with $\vartheta = 15$

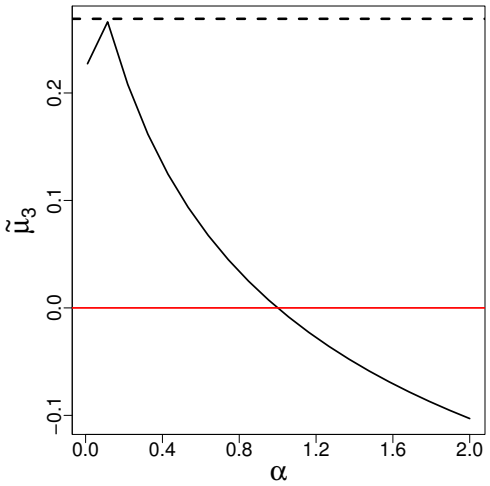

(c) RPMOT with $\vartheta = 15$

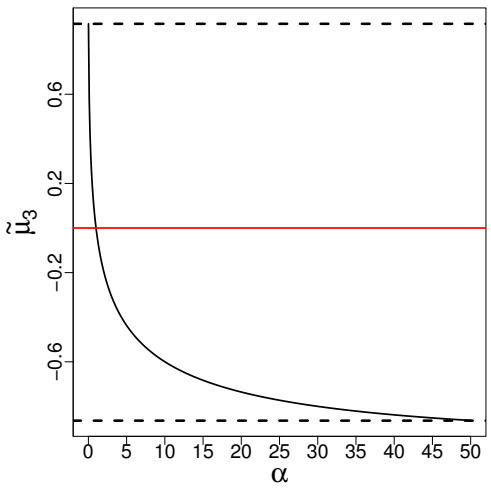

(d) RPMON

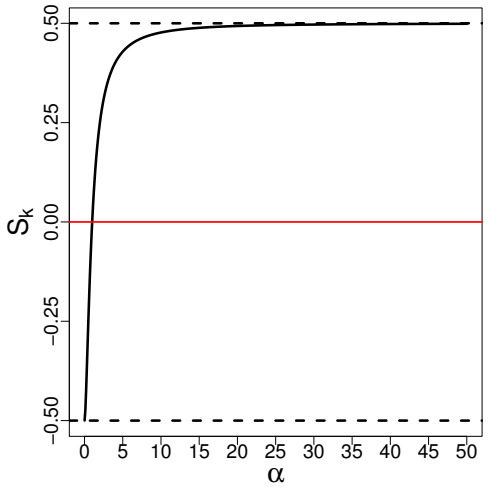

(e) RPMOC

Figure 4 – Plots of the kurtosis coefficient in the RPMO family of distributions against α parameter.

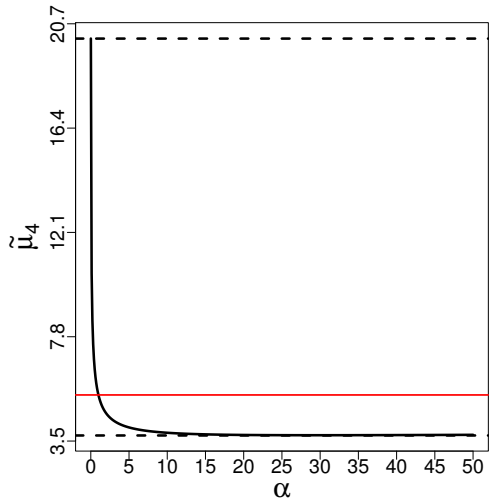

(a) RPMOG

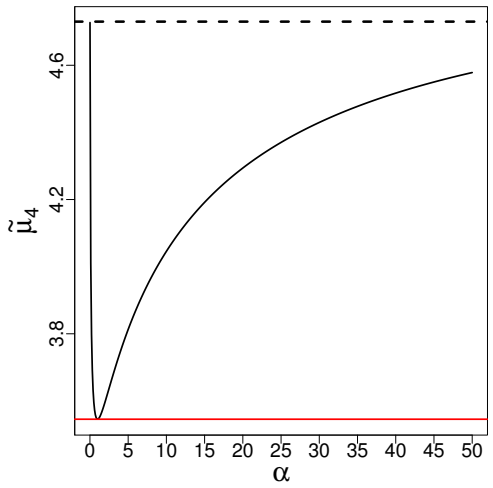

(b) RPMOT with $\vartheta = 15$

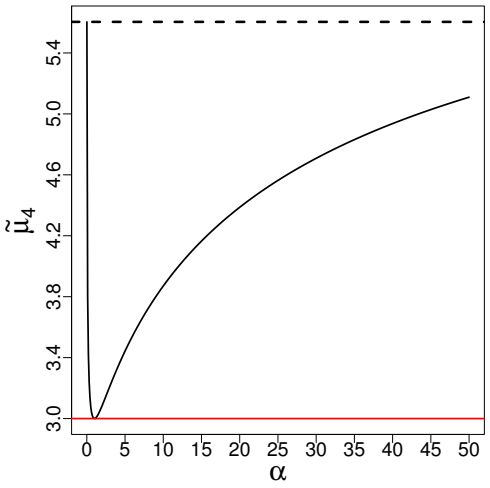

(c) RPMON

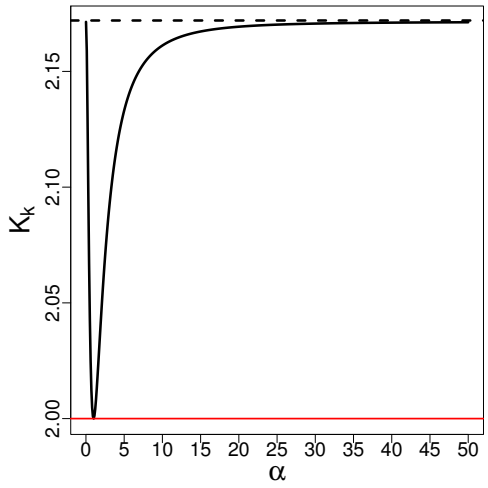

(d) RPMOC

2.3 Quantile regression model

This section formulates the QR model for the RPMO family of distributions.

Let $Y_1,\ldots,Y_n$ be independent random variables, where each Y_i, $i=1,\ldots,n$, follows the pdf given in Equation (2.1) with q-th quantile ξ_{iq}, scale σ_{iq}, and skewness α_{iq} parameters. Then, considering the probability $q\in(0,1)$ fixed, the RPMO model parameters have the following systematic components

$$\xi_{iq}=\eta_{1iq}=\mathbf{x}_{1i}^{\top}\boldsymbol{\beta}_q,\qquad \log(\sigma_{iq})=\eta_{2iq}=\mathbf{x}_{2i}^{\top}\boldsymbol{\nu}_q \text{ and } \qquad \log(\alpha_{iq})=\eta_{3iq}=\mathbf{x}_{3i}^{\top}\boldsymbol{\tau}_q, \tag{2.8}$$

where $\boldsymbol{\beta}_q=(\beta_{1q},\ldots,\beta_{tq})^{\top}$, $\boldsymbol{\nu}_q=(\nu_{1q},\ldots,\nu_{rq})^{\top}$ and $\boldsymbol{\tau}_q=(\tau_{1q},\ldots,\tau_{mq})^{\top}$ are vectors of unknown regression coefficients with $(t+r+m)<n$; η_{1iq}, η_{2iq} and η_{3iq} are the linear predictors; and $\mathbf{x}_{1i}=(x_{1i1},\ldots,x_{1it})^{\top}$, $\mathbf{x}_{2i}=(x_{2i1},\ldots,x_{2ir})^{\top}$ and $\mathbf{x}_{3i}=(x_{3i1},\ldots,x_{3im})^{\top}$ are observations on t, r and m known regressors, for $i=1,\ldots,n$.

In addition, we will assume the following aspects: $\mathbf{y}=(y_1,\ldots,y_n)^{\top}$ is the vector of observed responses; $\boldsymbol{\beta}_q\in\mathbb{R}^t$, $\boldsymbol{\nu}_q\in\mathbb{R}^r$ and $\boldsymbol{\tau}_q\in\mathbb{R}^m$ are functionally independent; and the covariate matrices $\mathbf{X}_1=(\mathbf{x}_{11}^{\top},\ldots,\mathbf{x}_{1n}^{\top})^{\top}$, $\mathbf{X}_2=(\mathbf{x}_{21}^{\top},\ldots,\mathbf{x}_{2n}^{\top})^{\top}$ and $\mathbf{X}_3=(\mathbf{x}_{31}^{\top},\ldots,\mathbf{x}_{3n}^{\top})^{\top}$ have ranks t, r and m, respectively.

2.4 Maximum likelihood estimation

This section mainly derives the score vector, ML estimators, observed information matrix and asymptotic confidence intervals to perform statistical inference.

Let $Y_1,\ldots,Y_n$ be independent random variables such that $Y_i\sim\text{RPMO}(\xi_{iq},\sigma_{iq},\alpha_{iq},f_0)$, then the log-likelihood function for $\boldsymbol{\theta}_q=(\boldsymbol{\beta}_q^{\top},\boldsymbol{\nu}_q^{\top},\boldsymbol{\tau}_q^{\top})^{\top}$ can be written as

$$\begin{aligned}\ell(\boldsymbol{\theta}_q)&=\sum_{i=1}^{n}\ell_i(\xi_{iq},\sigma_{iq},\alpha_{iq}),\text{ where}\\ \ell_i(\xi_{iq},\sigma_{iq},\alpha_{iq})&=\log(\alpha_{iq})+\log(f_0(u_{iq}))-\log(\sigma_{iq})-2\log(\alpha_{iq}+(1-\alpha_{iq})F_0(u_{iq})),\\ u_{iq}&=(y_{iq}-\xi_{iq})/\sigma_{iq}+F_0^{-1}(\alpha_{iq}q/(1+q\alpha_{iq}-q)),\end{aligned} \tag{2.9}$$

for $i=1,\ldots,n$ and $q\in(0,1)$ fixed. The score vector of dimension $(t+r+m)$ is given by $\mathbf{U}(\boldsymbol{\theta}_q)=(\mathbf{U}_{\boldsymbol{\beta}_q}^{\top},\mathbf{U}_{\boldsymbol{\nu}_q}^{\top},\mathbf{U}_{\boldsymbol{\tau}_q}^{\top})^{\top}=\partial\ell(\boldsymbol{\theta}_q)/\partial\boldsymbol{\theta}_q$ whose components are

$$\mathbf{U}_{\boldsymbol{\beta}_q}=\frac{\partial\ell(\boldsymbol{\theta}_q)}{\partial\boldsymbol{\beta}_q}=\mathbf{X}_1^{\top}\mathbf{W}_1\mathbf{A}_1, \tag{2.10}$$

$$\mathbf{U}_{\boldsymbol{\nu}_q}=\frac{\partial\ell(\boldsymbol{\theta}_q)}{\partial\boldsymbol{\nu}_q}=\mathbf{X}_2^{\top}\mathbf{W}_2\mathbf{A}_2 \text{ and} \tag{2.11}$$

$$\mathbf{U}_{\boldsymbol{\tau}_q}=\frac{\partial\ell(\boldsymbol{\theta}_q)}{\partial\boldsymbol{\tau}_q}=\mathbf{X}_3^{\top}\mathbf{W}_3\mathbf{A}_3, \tag{2.12}$$

with

$$\mathbf{W}_1 = \left[b_{iq}\ \delta_{ij}\right], \qquad \mathbf{W}_2 = \left[e_{iq}\ \delta_{ij}\right], \qquad \mathbf{W}_3 = \left[d_{iq}\ \delta_{ij}\right],$$
$$\mathbf{A}_1 = (\dot{\ell}_{\xi_{1q}}, \ldots, \dot{\ell}_{\xi_{nq}})^\top, \quad \mathbf{A}_2 = (\dot{\ell}_{\sigma_{1q}}, \ldots, \dot{\ell}_{\sigma_{nq}})^\top \text{ and } \quad \mathbf{A}_3 = (\dot{\ell}_{\alpha_{1q}}, \ldots, \dot{\ell}_{\alpha_{nq}})^\top,$$

where

$$b_{iq} = \frac{\partial \xi_{iq}}{\partial \eta_{1iq}} = 1, \qquad e_{iq} = \frac{\partial \sigma_{iq}}{\partial \eta_{2iq}} = \exp\left(\eta_{2iq}\right), \qquad d_{iq} = \frac{\partial \alpha_{iq}}{\partial \eta_{3iq}} = \exp\left(\eta_{3iq}\right),$$

δ_{ij} is the Kronecker delta with $i, j = 1, \ldots, n$ and $q \in (0,1)$ fixed. Finally, the elements of the vectors are given by

$$\begin{aligned}
\dot{\ell}_{\xi_{iq}} &= \frac{\partial \ell_i(\xi_{iq}, \sigma_{iq}, \alpha_{iq})}{\partial \xi_{iq}} \\
&= 2\psi_{1iq}\left[\frac{f_0(u_{iq})(1-\alpha_{iq})}{\alpha_{iq} + (1-\alpha_{iq})F_0(u_{iq})}\right] - \psi_{1iq}\left[\frac{f_0'(u_{iq})}{f_0(u_{iq})}\right], \qquad (2.13) \\
\dot{\ell}_{\sigma_{iq}} &= \frac{\partial \ell_i(\xi_{iq}, \sigma_{iq}, \alpha_{iq})}{\partial \sigma_{iq}} \\
&= 2\psi_{1iq}\psi_{2iq}\left[\frac{f_0(u_{iq})(1-\alpha_{iq})}{\alpha_{iq} + (1-\alpha_{iq})F_0(u_{iq})}\right] - \psi_{1iq} - \psi_{1iq}\psi_{2iq}\left[\frac{f_0'(u_{iq})}{f_0(u_{iq})}\right] \qquad (2.14)
\end{aligned}$$

and

$$\begin{aligned}
\dot{\ell}_{\alpha_{iq}} &= \frac{\partial \ell_i(\xi_{iq}, \sigma_{iq}, \alpha_{iq})}{\partial \alpha_{iq}} \\
&= \psi_{3iq} + u_{\alpha_{iq}}\left[\frac{f_0'(u_{iq})}{f_0(u_{iq})}\right] - 2\left[\frac{1 - F_0(u_{iq}) + (1-\alpha_{iq})f_0(u_{iq})u_{\alpha_{iq}}}{\alpha_{iq} + (1-\alpha_{iq})F_0(u_{iq})}\right], \qquad (2.15)
\end{aligned}$$

where

$$\psi_{1iq} = \frac{1}{\sigma_{iq}}, \qquad \psi_{2iq} = \frac{(y_i - \xi_{iq})}{\sigma_{iq}}, \qquad \psi_{3iq} = \frac{1}{\alpha_{iq}}, \qquad u_{\alpha_{iq}} = \frac{\Psi_0 q(1-q)}{(1 + q\alpha_{iq} - q)^2}$$

and

$$\Psi_0 \quad = \quad 1/f_0(F_0^{-1}(\alpha_{iq}q/(1+q\alpha_{iq}-q))) \text{ for } i = 1, \ldots, n \text{ and } q \in (0,1) \text{ fixed.}$$

The first derivative of $f_0(u_{iq})$, denoted by $f_0'(u_{iq})$ in Equations (2.13)-(2.15), depends on the distribution in the family. Table 2 provides the expression for $f_0'(u_{iq})$ in each member of the RPMO family.

Note that in Equations (2.10)-(2.12), the ML estimators of $\boldsymbol{\beta}_q$, $\boldsymbol{\nu}_q$ and $\boldsymbol{\tau}_q$ do not have a closed form. Therefore, the ML estimates denoted by $\widehat{\boldsymbol{\beta}}_q$, $\widehat{\boldsymbol{\nu}}_q$ and $\widehat{\boldsymbol{\tau}}_q$, can be obtained by numerical maximization of the log-likelihood function. To solve this numerical maximization, we adopt the RS algorithm from the *gamlss* package (STASINOPOULOS *et al.*, 2017) in the R programming language (R Core Team, 2022).

Table 2 – Expression of the first derivative $f_0'(u_{iq})$ for each member of the RPMO family.

Distribution	$f_0'(u_{iq})$
RPMOG	$\left[\exp\left(-u_{iq}\right)-1\right] f_0(u_{iq})$
RPMOT	$-u_{iq} f_0(u_{iq}) \left(\frac{\vartheta+1}{\vartheta}\right) \left(1+\frac{u_{iq}^2}{\vartheta}\right)^{-1}$
RPMON	$-u_{iq} f_0(u_{iq})$
RPMOC	$-2 f_0(u_{iq}) \left(\frac{u_{iq}}{1+u_{iq}^2}\right)$

2.4.1 RS algorithm

The RS algorithm (STASINOPOULOS; RIGBY, 2008) consists of an outer iteration that maximizes the log-likelihood function, as expressed in Equation (2.9), with respect to $\widehat{\boldsymbol{\beta}}_q$, $\widehat{\boldsymbol{\nu}}_q$ and $\widehat{\boldsymbol{\tau}}_q$. Additionally, there is an inner iteration to fit a model for each distribution parameter individually while keeping the other parameters fixed at their current values. For the RS algorithm, the quantities needed are

- the score functions

$$\boldsymbol{s}_{1q} = (\dot{\ell}_{\xi_{1q}} b_{1q}, \ldots, \dot{\ell}_{\xi_{nq}} b_{nq})^\top, \; \boldsymbol{s}_{2q} = (\dot{\ell}_{\sigma_{1q}} e_{1q}, \ldots, \dot{\ell}_{\sigma_{nq}} e_{nq})^\top \text{ and } \boldsymbol{s}_{3q} = (\dot{\ell}_{\alpha_{1q}} d_{1q}, \ldots, \dot{\ell}_{\alpha_{nq}} d_{nq})^\top;$$

- the diagonal matrices of iterative weights

$$\mathbf{W}_{11} = \operatorname{diag}(\boldsymbol{s}_{1q} \circ \boldsymbol{s}_{1q}), \qquad \mathbf{W}_{22} = \operatorname{diag}(\boldsymbol{s}_{2q} \circ \boldsymbol{s}_{2q}) \quad \text{and} \quad \mathbf{W}_{33} = \operatorname{diag}(\boldsymbol{s}_{3q} \circ \boldsymbol{s}_{3q}),$$

  where $\circ$ is the Hadamard element by element product;

- and the adjusted dependent variables

$$\boldsymbol{z}_{1q} = \boldsymbol{\eta}_{1q} + \mathbf{W}_{11}^{-1} \boldsymbol{s}_{1q}, \qquad \boldsymbol{z}_{2q} = \boldsymbol{\eta}_{2q} + \mathbf{W}_{22}^{-1} \boldsymbol{s}_{2q} \quad \text{and} \quad \boldsymbol{z}_{3q} = \boldsymbol{\eta}_{3q} + \mathbf{W}_{33}^{-1} \boldsymbol{s}_{3q},$$

  where

$$\boldsymbol{\eta}_{1q} = \mathbf{X}_1 \boldsymbol{\beta}_q, \qquad \boldsymbol{\eta}_{2q} = \exp\left(\mathbf{X}_2 \boldsymbol{\nu}_q\right) \quad \text{and} \quad \boldsymbol{\eta}_{3q} = \exp\left(\mathbf{X}_3 \boldsymbol{\tau}_q\right).$$

Let j represent the iteration index of the outer cycle and i represent the iteration index of the inner cycle. The algorithm is described as follows:

Step 1: Initialize fitted values for distributional parameter vectors of length n: $\boldsymbol{\xi}_q^{(1,1)}$, $\boldsymbol{\sigma}_q^{(1,1)}$ and $\boldsymbol{\tau}_q^{(1,1)}$, respectively. In this context, consider the outputs of the skew-normal, skew-t type I and reverse Gumbel parametric regression models as suggested initial values, with $\boldsymbol{\tau}_q^{(1,1)} = \mathbf{1}$. Then, evaluate the initial linear predictors: $\boldsymbol{\eta}_{1q}^{(1,1)} = \boldsymbol{\xi}_q^{(1,1)}$, $\boldsymbol{\eta}_{2q}^{(1,1)} = \exp\left(\boldsymbol{\sigma}_q^{(1,1)}\right)$ and $\boldsymbol{\eta}_{3q}^{(1,1)} = \exp\left(\boldsymbol{\tau}_q^{(1,1)}\right)$.

Step 2: Start the outer cycle $j = 1, 2, \ldots$ until convergence.

(a) Start the inner cycle $i = 1, \ldots, n$ until convergence.

(i) Evaluate the current $\boldsymbol{s}_{1q}^{(j,i)}$, $\mathbf{W}_{11}^{(j,i)}$ and $\boldsymbol{z}_{1q}^{(j,i)}$.

(ii) Regress the current $\boldsymbol{z}_{1q}^{(j,i)}$ against design matrix $\mathbf{X}_1$ using iterative weights $\mathbf{W}_{11}^{(j,i)}$ to obtain the updated parameters $\boldsymbol{\beta}_q^{(j,i)}$.

(b) End the inner cycle on convergence of $\boldsymbol{\beta}_q^{(j,\cdot)}$ and set $\boldsymbol{\beta}_q^{(j+1,1)} = \boldsymbol{\beta}_q^{(j,\cdot)}$, $\boldsymbol{\eta}_{1q}^{(j+1,1)} = \boldsymbol{\eta}_{1q}^{(j,\cdot)}$ and $\boldsymbol{\xi}_q^{(j+1,1)} = \boldsymbol{\xi}_q^{(j,\cdot)}$; otherwise update i and continue the inner cycle.

(a') Start the inner cycle $i = 1, \ldots, n$ until convergence.

(i) Evaluate the current $\boldsymbol{s}_{2q}^{(j,i)}$, $\mathbf{W}_{22}^{(j,i)}$ and $\boldsymbol{z}_{2q}^{(j,i)}$.

(ii) Regress the current $\boldsymbol{z}_{2q}^{(j,i)}$ against design matrix $\mathbf{X}_2$ using iterative weights $\mathbf{W}_{22}^{(j,i)}$ to obtain the updated parameters $\boldsymbol{\nu}_q^{(j,i)}$.

(b') End the inner cycle on convergence of $\boldsymbol{\nu}_q^{(j,\cdot)}$ and set $\boldsymbol{\nu}_q^{(j+1,1)} = \boldsymbol{\nu}_q^{(j,\cdot)}$, $\boldsymbol{\eta}_{2q}^{(j+1,1)} = \boldsymbol{\eta}_{2q}^{(j,\cdot)}$ and $\boldsymbol{\sigma}_q^{(j+1,1)} = \boldsymbol{\sigma}_q^{(j,\cdot)}$; otherwise update i and continue inner cycle.

(a") Start the inner cycle $i = 1, \ldots, n$ until convergence.

(i) Evaluate the current $\boldsymbol{s}_{3q}^{(j,i)}$, $\mathbf{W}_{33}^{(j,i)}$ and $\boldsymbol{z}_{3q}^{(j,i)}$.

(ii) Regress the current $\boldsymbol{z}_{3q}^{(j,i)}$ against $\mathbf{X}_3$ using iterative weights $\mathbf{W}_{33}^{(j,i)}$ to obtain the updated parameters $\boldsymbol{\tau}_q^{(j,i)}$.

(b") End the inner cycle on convergence of $\boldsymbol{\tau}_q^{(j,\cdot)}$ and set $\boldsymbol{\tau}_q^{(j+1,1)} = \boldsymbol{\tau}_q^{(j,\cdot)}$, $\boldsymbol{\eta}_{3q}^{(j+1,1)} = \boldsymbol{\eta}_{3q}^{(j,\cdot)}$ and $\boldsymbol{\alpha}_q^{(j+1,1)} = \boldsymbol{\alpha}_q^{(j,\cdot)}$; otherwise update i and continue inner cycle.

Step 3: End the outer cycle if the change in the log-likelihood is less than 0.001; otherwise, update j and continue the outer cycle.

2.4.2 Observed information matrix

The observed information matrix for $\widehat{\boldsymbol{\theta}}_q = (\widehat{\boldsymbol{\beta}}_q^\top, \widehat{\boldsymbol{\nu}}_q^\top, \widehat{\boldsymbol{\tau}}_q^\top)^\top$ is calculated from the second partial derivative of $\ell(\boldsymbol{\theta})$ relative to all model parameters. Thus, the matrix for the RPMO family is denoted by

$$\ddot{\ell}(\widehat{\boldsymbol{\theta}}_q) = -\frac{\partial^2 \ell(\boldsymbol{\theta}_q)}{\partial \boldsymbol{\theta}_q \partial \boldsymbol{\theta}_q^\top}\Big|_{\boldsymbol{\theta}_q = \widehat{\boldsymbol{\theta}}_q} = \begin{bmatrix} -\ddot{\ell}_{\boldsymbol{\beta}_q\boldsymbol{\beta}_q} & -\ddot{\ell}_{\boldsymbol{\beta}_q\boldsymbol{\nu}_q} & -\ddot{\ell}_{\boldsymbol{\beta}_q\boldsymbol{\tau}_q} \\ & -\ddot{\ell}_{\boldsymbol{\nu}_q\boldsymbol{\nu}_q} & -\ddot{\ell}_{\boldsymbol{\nu}_q\boldsymbol{\tau}_q} \\ & & -\ddot{\ell}_{\boldsymbol{\tau}_q\boldsymbol{\tau}_q} \end{bmatrix},$$

with

$$\ddot{\ell}_{\boldsymbol{\beta}_q\boldsymbol{\beta}_q} = \frac{\partial^2\ell(\boldsymbol{\theta}_q)}{\partial\boldsymbol{\beta}_q\partial\boldsymbol{\beta}_q^\top}\Big|_{\boldsymbol{\theta}_q=\widehat{\boldsymbol{\theta}}_q} = \mathbf{X}_1^\top\mathbf{W}_4\mathbf{X}_1,$$
$$\ddot{\ell}_{\boldsymbol{\beta}_q\boldsymbol{\nu}_q} = \frac{\partial^2\ell(\boldsymbol{\theta}_q)}{\partial\boldsymbol{\beta}_q\partial\boldsymbol{\nu}_q^\top}\Big|_{\boldsymbol{\theta}_q=\widehat{\boldsymbol{\theta}}_q} = \mathbf{X}_1^\top\mathbf{W}_5\mathbf{X}_2,$$
$$\ddot{\ell}_{\boldsymbol{\beta}_q\boldsymbol{\tau}_q} = \frac{\partial^2\ell(\boldsymbol{\theta}_q)}{\partial\boldsymbol{\beta}_q\partial\boldsymbol{\tau}_q^\top}\Big|_{\boldsymbol{\theta}_q=\widehat{\boldsymbol{\theta}}_q} = \mathbf{X}_1^\top\mathbf{W}_6\mathbf{X}_3,$$
$$\ddot{\ell}_{\boldsymbol{\nu}_q\boldsymbol{\nu}_q} = \frac{\partial^2\ell(\boldsymbol{\theta}_q)}{\partial\boldsymbol{\nu}_q\partial\boldsymbol{\nu}_q^\top}\Big|_{\boldsymbol{\theta}_q=\widehat{\boldsymbol{\theta}}_q} = \mathbf{X}_2^\top\mathbf{W}_7\mathbf{X}_2,$$
$$\ddot{\ell}_{\boldsymbol{\nu}_q\boldsymbol{\tau}_q} = \frac{\partial^2\ell(\boldsymbol{\theta}_q)}{\partial\boldsymbol{\nu}_q\partial\boldsymbol{\tau}_q^\top}\Big|_{\boldsymbol{\theta}_q=\widehat{\boldsymbol{\theta}}_q} = \mathbf{X}_2^\top\mathbf{W}_8\mathbf{X}_3 \text{ and}$$
$$\ddot{\ell}_{\boldsymbol{\tau}_q\boldsymbol{\tau}_q} = \frac{\partial^2\ell(\boldsymbol{\theta}_q)}{\partial\boldsymbol{\tau}_q\partial\boldsymbol{\tau}^\top}\Big|_{\boldsymbol{\theta}_q=\widehat{\boldsymbol{\theta}}_q} = \mathbf{X}_3^\top\mathbf{W}_9\mathbf{X}_3,$$

where

$$\mathbf{W}_4 = [(\ddot{\ell}_{\xi_{iq}}\, b_{iq}^2 + \dot{\ell}_{\xi_{iq}}\, b_{iq}\, b'_{iq})\delta_{ij}], \qquad \mathbf{W}_5 = [(\ddot{\ell}_{\xi_{iq}\sigma_{iq}}\, b_{iq}\, e_{iq})\ \delta_{ij}],$$
$$\mathbf{W}_6 = [(\ddot{\ell}_{\xi_{iq}\alpha_{iq}}\, b_{iq}\, d_{iq})\delta_{ij}], \qquad \mathbf{W}_7 = [\big(\ddot{\ell}_{\sigma_{iq}}\, e_{iq}^2 + \dot{\ell}_{\sigma_{iq}}\, e_{iq}\, e'_{iq}\big)\ \delta_{ij}],$$
$$\mathbf{W}_8 = [(\ddot{\ell}_{\sigma_{iq}\alpha_{iq}}\, e_{iq}\, d_{iq})\delta_{ij}], \qquad \mathbf{W}_9 = [(\ddot{\ell}_{\alpha_{iq}}\, d_{iq}^2 + \dot{\ell}_{\alpha_{iq}}\, d_{iq}\, d'_{iq})\delta_{ij}],$$

and

$$b'_{iq} = \frac{\partial b_{iq}}{\partial\xi_{iq}} = 0, \qquad e'_{iq} = \frac{\partial e_{iq}}{\partial\sigma_{iq}} = 1, \qquad d'_{iq} = \frac{\partial d_{iq}}{\partial\alpha_{iq}} = 1,$$

for $i, j = 1,\ldots,n$ and $q \in (0,1)$ fixed. Lastly, the other elements of the matrices are

$$\begin{aligned}\ddot{\ell}_{\xi_{iq}} &= \frac{\partial^2\ell_i(\xi_{iq},\sigma_{iq},\alpha_{iq})}{\partial^2\xi_{iq}^2} \qquad (2.16)\\ &= \psi_{1iq}^2\left[\frac{f_0''(u_{iq})}{f_0(u_{iq})} - \frac{f_0'^2(u_{iq})}{f_0^2(u_{iq})}\right] + 2\psi_{1iq}^2\left[\frac{f_0(u_{iq})(1-\alpha_{iq})}{\alpha_{iq}+(1-\alpha_{iq})F_0(u_{iq})}\right]^2\\ &\quad - 2\psi_{1iq}^2\left[\frac{f_0'(u_{iq})(1-\alpha_{iq})}{\alpha_{iq}+(1-\alpha_{iq})F_0(u_{iq})}\right],\\ \ddot{\ell}_{\xi_{iq}\sigma_{iq}} &= \frac{\partial^2\ell_i(\xi_{iq},\sigma_{iq},\alpha_{iq})}{\partial\xi_{iq}\partial\sigma_{iq}} \qquad (2.17)\\ &= \psi_{1iq}^2\left[\frac{f_0'(u_{iq})}{f_0(u_{iq})}\right] + \psi_{1iq}^2\psi_{2iq}\left[\frac{f_0''(u_{iq})}{f_0(u_{iq})} - \frac{f_0'^2(u_{iq})}{f_0^2(u_{iq})}\right] - 2\psi_{1iq}^2\left[\frac{f_0(u_{iq})(1-\alpha_{iq})}{\alpha_{iq}+(1-\alpha_{iq})F_0(u_{iq})}\right]\\ &\quad + 2\psi_{1iq}^2\psi_{2iq}\left[\frac{f_0(u_{iq})(1-\alpha_{iq})}{\alpha_{iq}+(1-\alpha_{iq})F_0(u_{iq})}\right]^2 - 2\psi_{1iq}^2\psi_{2iq}\left[\frac{f_0'(u_{iq})(1-\alpha_{iq})}{\alpha_{iq}+(1-\alpha_{iq})F_0(u_{iq})}\right],\end{aligned}$$

$$\ddot{\ell}_{\xi_{iq}\alpha_{iq}} = \frac{\partial^2 \ell_i(\xi_{iq},\sigma_{iq},\alpha_{iq})}{\partial \xi_{iq}\partial \alpha_{iq}} \tag{2.18}$$
$$= 2u_{\alpha_{iq}}\psi_{1iq}\left[\frac{f_0'(u_{iq})(1-\alpha_{iq})}{\alpha_{iq}+(1-\alpha_{iq})F_0(u_{iq})}\right] - u_{\alpha_{iq}}\psi_{1iq}\left[\frac{f_0''(u_{iq})}{f_0(u_{iq})} - \frac{f_0'^2(u_{iq})}{f_0^2(u_{iq})}\right]$$
$$- 2\psi_{1iq}\left[\frac{f_0(u_{iq})(1-\alpha_{iq})}{\alpha_{iq}+(1-\alpha_{iq})F_0(u_{iq})}\right]\left[\frac{1-F_0(u_{iq})+(1-\alpha_{iq})f_0(u_{iq})u_{\alpha_{iq}}}{\alpha_{iq}+(1-\alpha_{iq})F_0(u_{iq})}\right]$$
$$- 2\psi_{1iq}\left[\frac{f_0(u_{iq})}{\alpha_{iq}+(1-\alpha_{iq})F_0(u_{iq})}\right],$$

$$\ddot{\ell}_{\sigma_{iq}} = \frac{\partial^2 \ell_i(\xi_{iq},\sigma_{iq},\alpha_{iq})}{\partial^2 \sigma_{iq}^2} \tag{2.19}$$
$$= \psi_{1iq}^2 + 2\psi_{1iq}^2\psi_{2iq}\left[\frac{f_0'(u_{iq})}{f_0(u_{iq})}\right] - 4\psi_{1iq}^2\psi_{2iq}\left[\frac{f_0(u_{iq})(1-\alpha_{iq})}{\alpha_{iq}+(1-\alpha_{iq})F_0(u_{iq})}\right]$$
$$- 2\psi_{1iq}^2\psi_{2iq}^2\left[\frac{f_0'(u_{iq})(1-\alpha_{iq})}{\alpha_{iq}+(1-\alpha_{iq})F_0(u_{iq})}\right] + 2\psi_{1iq}^2\psi_{2iq}^2\left[\frac{f_0(u_{iq})(1-\alpha_{iq})}{\alpha_{iq}+(1-\alpha_{iq})F_0(u_{iq})}\right]^2$$
$$+ \psi_{1iq}^2\psi_{2iq}^2\left[\frac{f_0''(u_{iq})}{f_0(u_{iq})} - \frac{f_0'^2(u_{iq})}{f_0^2(u_{iq})}\right],$$

$$\ddot{\ell}_{\sigma_{iq}\alpha_{iq}} = \frac{\partial^2 \ell_i(\xi_{iq},\sigma_{iq},\alpha_{iq})}{\partial \sigma_{iq}\partial \alpha_{iq}} \tag{2.20}$$
$$= 2u_{\alpha_{iq}}\psi_{1iq}\psi_{2iq}\left[\frac{f_0'(u_{iq})(1-\alpha_{iq})}{\alpha_{iq}+(1-\alpha_{iq})F_0(u_{iq})}\right] - u_{\alpha_{iq}}\psi_{1iq}\psi_{2iq}\left[\frac{f_0''(u_{iq})}{f_0(u_{iq})} - \frac{f_0'^2(u_{iq})}{f_0^2(u_{iq})}\right]$$
$$- 2\psi_{1iq}\psi_{2iq}\left[\frac{f_0(u_{iq})(1-\alpha_{iq})}{\alpha_{iq}+(1-\alpha_{iq})F_0(u_{iq})}\right]\left[\frac{1-F_0(u_{iq})+(1-\alpha_{iq})f_0(u_{iq})u_{\alpha_{iq}}}{\alpha_{iq}+(1-\alpha_{iq})F_0(u_{iq})}\right]$$
$$- 2\psi_{1iq}\psi_{2iq}\left[\frac{f_0(u_{iq})}{\alpha_{iq}+(1-\alpha_{iq})F_0(u_{iq})}\right],$$

and

$$\ddot{\ell}_{\alpha_{iq}} = \frac{\partial^2 \ell_i(\xi_{iq},\sigma_{iq},\alpha_{iq})}{\partial^2 \alpha_{iq}^2} \tag{2.21}$$
$$= u_{\alpha_{iq}}^2\left[\frac{f_0''(u_{iq})}{f_0(u_{iq})} - \frac{f_0'^2(u_{iq})}{f_0^2(u_{iq})}\right] + u_{\alpha_{iq}\alpha_{iq}}\left[\frac{f_0'(u_{iq})}{f_0(u_{iq})}\right] - 2u_{\alpha_{iq}\alpha_{iq}}\left[\frac{f_0(u_{iq})(1-\alpha_{iq})}{\alpha_{iq}+(1-\alpha_{iq})F_0(u_{iq})}\right]$$
$$+ 4\left[\frac{f_0(u_{iq})u_{\alpha_{iq}}}{\alpha_{iq}+(1-\alpha_{iq})F_0(u_{iq})}\right] - 2u_{\alpha_{iq}}^2\left[\frac{f_0'(u_{iq})(1-\alpha_{iq})}{\alpha_{iq}+(1-\alpha_{iq})F_0(u_{iq})}\right] - \psi_{3iq}^2$$
$$+ 2\left[\frac{1-F_0(u_{iq})+(1-\alpha_{iq})f_0(u_{iq})u_{\alpha_{iq}}}{\alpha_{iq}+(1-\alpha_{iq})F_0(u_{iq})}\right]^2,$$

where

$$u_{\alpha_{iq}\alpha_{iq}} = \frac{q(1-q)}{(1+q\alpha_{iq}-q)^2}\left[\Psi_0' - \frac{2q\Psi_0}{(1+q\alpha_{iq}-q)}\right], \qquad \Psi_0' = \frac{q(q-1)\Psi_1\Psi_0^3}{(1+q\alpha_{iq}-q)^2}$$

and

$$\Psi_1 = f_0'\left(F_0^{-1}\left(\frac{\alpha_{iq}q}{1+q\alpha_{iq}-q}\right)\right) \text{ for } i = 1,\ldots,n \text{ and } q \in (0,1) \text{ fixed.}$$

The expression of the second derivative of $f_0(u_{iq})$, written as $f_0''(u_{iq})$ within Equations (2.16)-(2.21), is shown in Table 3 for each member of the RPMO family.

Table 3 – Expression of $f_0''(u_{iq})$ for each member of the RPMO family.

Distribution	$f_0''(u_{iq})$
RPMOG	$f_0(u_{iq})\left[\exp(-2u_{iq}) - 3\exp(-u_{iq}) + 1\right]$
RPMOT	$-f_0(u_{iq})\left(\frac{\vartheta+1}{\vartheta}\right)\left(1+\frac{u_{iq}^2}{\vartheta}\right)^{-1}\left[1-\frac{2u_{iq}^2}{\vartheta}\left(1+\frac{u_{iq}^2}{\vartheta}\right)^{-1} - \left(\frac{\vartheta+1}{\vartheta}\right)u_{iq}^2\left(1+\frac{u_{iq}^2}{\vartheta}\right)^{-1}\right]$
RPMON	$f_0(u_{iq})\left[u_{iq}^2 - f_0(u_{iq})\right]$
RPMOC	$\frac{2(3u_{iq}^2-1)f_0(u_{iq})}{(1+u_{iq}^2)^2}$

2.4.3 Confidence intervals

Under regularity conditions and a large sample size n, the asymptotic distribution of $(\widehat{\boldsymbol{\theta}}_q - \boldsymbol{\theta}_q)$ is $N(\mathbf{0}, \mathbb{I}^{-1}(\widehat{\boldsymbol{\theta}}_q))$, where $\mathbb{I}(\widehat{\boldsymbol{\theta}}_q)$ is the Fisher's information matrix. Since it is not easy to obtain the analytical expression of this matrix, we use the inverse of the observed information matrix, denoted by $\ddot{\ell}^{-1}(\widehat{\boldsymbol{\theta}}_q)$, to approximate $\mathbb{I}^{-1}(\widehat{\boldsymbol{\theta}}_q)$. Then, the estimated standard errors (SE) of the ML estimators of $\boldsymbol{\theta}$ are obtained by calculating the square root of the diagonal elements of $\ddot{\ell}^{-1}(\widehat{\boldsymbol{\theta}}_q)$.

The asymptotic confidence interval for the j-th element of $\widehat{\boldsymbol{\theta}}_q$, denoted by $\widehat{\theta}_{jq}$, is constructed using the following expression

$$\left(\widehat{\theta}_{jq} - z_{\zeta/2}\sqrt{\ddot{\ell}_{jj}^{-1}(\widehat{\theta}_q)}, \widehat{\theta}_{jq} + z_{\zeta/2}\sqrt{\ddot{\ell}_{jj}^{-1}(\widehat{\theta}_q)}\right), \tag{2.22}$$

where $z_{\zeta/2}$ represent the quantile of the standard normal distribution leaving a probability to the right tail with $\zeta/2$ for $0 < \zeta < 1/2$ and $\ddot{\ell}_{jj}^{-1}(\widehat{\theta}_q)$ is the j-th element of the main diagonal of $\ddot{\ell}^{-1}(\widehat{\boldsymbol{\theta}}_q)$ for $j = 1, \ldots, (t+r+m)$ and $q \in (0,1)$ fixed.

2.5 Residuals

This section proposes three types of residuals in the QR model of the RPMO family: normalized quantile residual (NQR), generalized Cox-Snell residual (GCSR) and martingale-type residual (MTR). The main idea is to study the adequacy of the model and detect outliers.

2.5.1 Normalized quantile residual

Here, we adopt the NQRs proposed by Dunn and Smyth (1996). In our case, this residual is given by

$$\widehat{r}_{iq}^{(1)} = \Phi^{-1}\left(\widehat{G}(y_i; \widehat{\xi}_{iq}, \widehat{\sigma}_{iq}, \widehat{\alpha}_{iq})\right), \tag{2.23}$$

where Φ^{-1} is the inverse cdf of the standard normal distribution, $\widehat{G}$ is the estimated cdf of G defined in Section 2.2, for $i = 1,\ldots,n$ and $q \in (0,1)$ fixed. The NQRs have approximately a standard normal distribution if the model is correctly specified. Note that these residuals can be easily calculated for the QR models of the RPMO family.

Furthermore, we present Scheme 2 to build envelopes for the NQRs. For each observation in the dataset, a random sample of size B based on the known distribution is simulated. Then, the 2.5-*th* and 97.5-*th* percentiles (confidence bands) are calculated to draw lines. If the distribution fits the data perfectly, all points are within the confidence bands.

Scheme 2 – Steps to build envelopes for NQRs.

1: Generate random numbers $y_i^{(b)} \sim \text{RPMO}(\widehat{\xi}_{iq}, \widehat{\sigma}_{iq}, \widehat{\alpha}_{iq}, f_0)$ by using Equation (2.3), for $b = 1,\ldots,B$ and $q \in (0,1)$ fixed.
2: Evaluate $y_i^{(b)}$ in Equation (2.23), that is, compute the residuals

$$\widehat{r}_{iq}^{(1)(b)} = \Phi^{-1}\left(\widehat{G}(y_i^{(b)}; \widehat{\xi}_{iq}, \widehat{\sigma}_{iq}, \widehat{\alpha}_{iq})\right), \text{ for } b = 1,\ldots,B.$$

3: Obtain the 2.5-*th* and 97.5-*th* percentiles for the set of B $\widehat{r}_{iq}^{(1)(b)}$.
4: Repeat (1)-(3) for $i = 1,\ldots,n$.
5: Draw a line joining all 2.5-*th* and 97.5-*th* percentiles obtained, respectively.

2.5.2 Generalized Cox-Snell residual

Cox and Snell (1968) studied the GCSR, whose expression in the QR model of the RPMO family is

$$\widehat{r}_{iq}^{(2)} = -\log\left(1 - \widehat{G}(y_i; \widehat{\xi}_{iq}, \widehat{\sigma}_{iq}, \widehat{\alpha}_{iq})\right), \tag{2.24}$$

for $i = 1,\ldots,n$ and $q \in (0,1)$ fixed. If the model is correctly specified, $\widehat{r}_{iq}^{(2)}$ follows approximately an exponential distribution with a rate parameter equal to one, $\text{Exp}(1)$. One advantage of these residuals is their low computational cost in the R language. Scheme 3 displays how to build the envelopes for the GCSR.

Scheme 3 – Steps to build envelopes for GCSR.

1: Generate random numbers $y_i^{(b)} \sim \text{RPMO}(\widehat{\xi}_{iq}, \widehat{\sigma}_{iq}, \widehat{\alpha}_{iq}, f_0)$ by using Equation (2.3), for $b = 1,\ldots,B$ and $q \in (0,1)$ fixed.
2: Evaluate $y_i^{(b)}$ in Equation (2.24), that is, compute the residuals

$$\widehat{r}_{iq}^{(2)(b)} = -\log\left(1 - \widehat{G}(y_i^{(b)}; \widehat{\xi}_{iq}, \widehat{\sigma}_{iq}, \widehat{\alpha}_{iq})\right), \text{ for } b = 1,\ldots,B.$$

3: Obtain the 2.5-*th* and 97.5-*th* percentiles for the set of B $\widehat{r}_{iq}^{(2)(b)}$.
4: Repeat (1)-(3) for $i = 1,\ldots,n$.
5: Draw a line joining all 2.5-*th* and 97.5-*th* percentiles obtained, respectively.

2.5.3 Martingale-type residual

The third residual, considered by Therneau, Grambsch and Fleming (1990) in the context of survival models, can be written in terms of the GCSR. For this reason, its calculation and implementation have a low computational cost. In our case, the residual is defined as

$$\widehat{r}_{iq}^{(3)} = \text{sign}(1-\widehat{r}_{iq}^{(2)})\left\{-2\left[1-\widehat{r}_{iq}^{(2)}+\log\left(\widehat{r}_{iq}^{(2)}\right)\right]\right\}^{0.5}, \tag{2.25}$$

where $\text{sign}(\cdot)$ denotes the sign function, for $i=1,\ldots,n$ and $q\in(0,1)$ fixed. $\widehat{r}_{iq}^{(3)}$ follows approximately a standard normal distribution, $N(0,1)$, if the model is correctly specified. Analogously to Sections 2.5.1 and 2.5.2, the steps for the construction of envelopes are presented in Scheme 4 .

Scheme 4 – Steps to build envelopes for MTRs.

1: Generate random numbers $y_i^{(b)} \sim \text{RPMO}(\widehat{\xi}_{iq}, \widehat{\sigma}_{iq}, \widehat{\alpha}_{iq}, f_0)$ by using Equation (2.3), for $b=1,\ldots,B$ and $q\in(0,1)$ fixed.
2: Evaluate $y_i^{(b)}$ in Equation (2.25), that is, compute the residuals

$$\widehat{r}_{iq}^{(3)(b)} = \text{sign}(1-\widehat{r}_{iq}^{(2)(b)})\left\{-2\left[1-\widehat{r}_{iq}^{(2)(b)}+\log\left(\widehat{r}_{iq}^{(2)(b)}\right)\right]\right\}^{0.5}, \text{ for } b=1,\ldots,B.$$

3: Obtain the 2.5-th and 97.5-th percentiles for the set of B $\widehat{r}_{iq}^{(3)(b)}$.
4: Repeat (1)-(3) for $i=1,\ldots,n$.
5: Draw a line joining all 2.5-th and 97.5-th percentiles obtained, respectively.

2.6 Global influence

This section introduces two popular measures of case deletion: the likelihood displacement (LD) and the generalized Cook's distance (GCD). These measures allow us to analyze the impact of removing an observation from the dataset on the ML estimates of the parameters.

2.6.1 Likelihood displacement

Here, we study a measure of case deletion that has been defined by Cook and Weisberg (1982) in the context of normal regression models. The expression from this measure is

$$\text{LD}_{(i)q} = 2[\ell(\widehat{\boldsymbol{\theta}}_q) - \ell(\widehat{\boldsymbol{\theta}}_{(i)q})], \tag{2.26}$$

for $i=1,\ldots,n$ and $q\in(0,1)$ fixed, where $\ell(\widehat{\boldsymbol{\theta}}_q)$ and $\ell(\widehat{\boldsymbol{\theta}}_{(i)q})$ are the log-likelihood functions of the complete dataset and without the i-th observation, respectively. If $\widehat{\boldsymbol{\theta}}_{(i)q}$ is far from $\widehat{\boldsymbol{\theta}}_q$ the i-th observation is potentially influential, where $\widehat{\boldsymbol{\theta}}_{(i)q}$ denotes the ML estimate of $\boldsymbol{\theta}_q$ when the i-th observation is dropped.

2.6.2 Generalized Cook's distance

The second case deletion measure considered is a standardized norm of $\widehat{\boldsymbol{\theta}}_{(i)q} - \widehat{\boldsymbol{\theta}}_q$, known in the literature as GCD (COOK; WEISBERG, 1982). In the QR model of the RPMO family, it is denoted by

$$\text{GCD}_{(i)q} = (\widehat{\boldsymbol{\theta}}_{(i)q} - \widehat{\boldsymbol{\theta}}_q)^\top \ddot{\ell}^{-1}(\widehat{\boldsymbol{\theta}}_q)(\widehat{\boldsymbol{\theta}}_{(i)q} - \widehat{\boldsymbol{\theta}}_q), \tag{2.27}$$

where $\ddot{\ell}^{-1}(\widehat{\boldsymbol{\theta}}_q)$ is the inverse of the observed information matrix, $\widehat{\boldsymbol{\theta}}_{(i)q}$ is the ML estimate of $\boldsymbol{\theta}_q$ when the i-th observation is dropped, for $i = 1, \ldots, n$ and $q \in (0,1)$ fixed. Large values of $\text{GCD}_{(i)q}$ indicate that the i-th observation is potentially influential.

2.7 Local Influence

According to Ferreira (2008), by using differential geometry, local influence analysis compares parameter estimates before and after perturbing the data or the model. The methodology can be useful for identifying influential observations by examining the effect of introducing small perturbations into the model or data using an appropriate influence measure.

Here, we perturb the model using a vector $\boldsymbol{\omega}$ of dimension $(n \times 1)$ restricted to some open subset of $\Omega \subset \mathbb{R}^n$. Also, let $\ell(\boldsymbol{\theta}_q|\boldsymbol{\omega})$ be the log-likelihood function corresponding to the perturbed model and assuming there is a non-perturbation vector $\boldsymbol{\omega}_0 \in \Omega$ such that $\ell(\boldsymbol{\theta}_q|\boldsymbol{\omega}_0) = \ell(\boldsymbol{\theta}_q)$ for all $\boldsymbol{\theta}_q$, we evaluate the influence of perturbation $\boldsymbol{\omega}$ on the ML estimator $\widehat{\boldsymbol{\theta}}_q$.

Cook (1986) suggests studying the behavior of the likelihood displacement $\text{LD}(\boldsymbol{\omega}) = 2[\ell(\widehat{\boldsymbol{\theta}}_q) - \ell(\widehat{\boldsymbol{\theta}}_{\boldsymbol{\omega}})]$ around $\boldsymbol{\omega} = \boldsymbol{\omega}_0$, where $\widehat{\boldsymbol{\theta}}_{\boldsymbol{\omega}}$ denotes the ML estimator under $\ell(\boldsymbol{\theta}_q|\boldsymbol{\omega})$. Then, Cook (1986) considers selecting a unit direction $\mathbf{d} \in \Omega$ ($||\mathbf{d}|| = 1$) and plot $\text{LD}(\boldsymbol{\omega}_0 + a\mathbf{d})$ against a, where $a \in \mathbb{R}$. Therefore, the normal curvature for $\boldsymbol{\theta}_q$ in the direction of $\mathbf{d}$ is given by

$$\mathbf{C}_{\mathbf{d}}(\boldsymbol{\theta}_q) = 2|\mathbf{d}^\top \boldsymbol{\Delta}_q^\top \ddot{\ell}^{-1}(\boldsymbol{\theta}_q)\boldsymbol{\Delta}_q \mathbf{d}|, \tag{2.28}$$

where $\boldsymbol{\Delta}_q$ is the matrix of dimension $(t + r + m) \times n$ with elements

$$\Delta_{ji} = \frac{\partial^2 \ell(\boldsymbol{\theta}_q|\boldsymbol{\omega})}{\partial \theta_j \partial \omega_i}\Big|_{\boldsymbol{\theta}_q = \widehat{\boldsymbol{\theta}}_q, \boldsymbol{\omega} = \boldsymbol{\omega}_0} \tag{2.29}$$

for $j = 1, \ldots, (t + r + m)$, $i = 1, \ldots, n$ and $\ddot{\ell}^{-1}(\boldsymbol{\theta}_q)$ is the inverse of the observed information matrix defined in Section 2.4.2. It is also recommended by Cook (1986) to examine the eigenvalues of the matrix $\boldsymbol{\Delta}_q^\top \ddot{\ell}^{-1}(\boldsymbol{\theta}_q)\boldsymbol{\Delta}_q$ to detect those cases that strongly influence on $\text{LD}(\boldsymbol{\omega})$. For this reason, we study the total local influence of the i-th case, expressed as $C_i = C_{\mathbf{d}_i}(\boldsymbol{\theta}_q)$, where $\mathbf{d}_i$ is an $(n \times 1)$ vector of zeros with one in the i-th position.

Next, we present three perturbation schemes, introducing small modifications $\boldsymbol{\omega}$ in the log-likelihood, response variable and skewness parameter. Each scheme shows the development of the calculations of the derivatives to obtain the matrix $\boldsymbol{\Delta}_q$.

2.7.1 Case-weight

In order to identify the individuals that generate a high impact on the ML estimates, the case-weight perturbation scheme is considered. Here, $\boldsymbol{\omega} = (\omega_1, \ldots, \omega_n)^\top$ and $\boldsymbol{\omega}_0 = (1, \ldots, 1)^\top$ are vectors of dimension $(n \times 1)$ with $0 \leq \omega_i \leq 1$ for $i = 1, \ldots, n$. Furthermore, the perturbed log-likelihood function has the form

$$\ell(\boldsymbol{\theta}_q|\boldsymbol{\omega}) = \sum_{i=1}^{n} \omega_i \, \ell_i(\xi_{iq}, \sigma_{iq}, \alpha_{iq}), \text{ where} \tag{2.30}$$
$$\ell_i(\xi_{iq}, \sigma_{iq}, \alpha_{iq}) = \log(\alpha_{iq}) + \log(f_0(u_{iq})) - \log(\sigma_{iq}) - 2\log(\alpha_{iq} + (1-\alpha_{iq})F_0(u_{iq})),$$
$$u_{iq} = (y_i - \xi_{iq})/\sigma_{iq} + F_0^{-1}(\alpha_{iq} q/(1 + q\alpha_{iq} - q)),$$

for $i = 1, \ldots, n$ and $q \in (0,1)$ fixed. Consequently, the matrix $\boldsymbol{\Delta}_q$ is expressed as

$$\boldsymbol{\Delta}_q = \begin{bmatrix} \mathbf{X}_1^\top & \mathbf{W}_1 & \mathbf{M}_1 \\ \mathbf{X}_2^\top & \mathbf{W}_2 & \mathbf{M}_2 \\ \mathbf{X}_3^\top & \mathbf{W}_3 & \mathbf{M}_3 \end{bmatrix},$$

where $\mathbf{M}_1 = \left[\ddot{\ell}_{\xi_{iq}\omega_i}\, \delta_{ij}\right]$, $\mathbf{M}_2 = \left[\ddot{\ell}_{\sigma_{iq}\omega_i}\, \delta_{ij}\right]$ and $\mathbf{M}_3 = \left[\ddot{\ell}_{\alpha_{iq}\omega_i}\, \delta_{ij}\right]$, with $\ddot{\ell}_{\xi_{iq}\omega_i} = \dot{\ell}_{\xi_{iq}}$, $\ddot{\ell}_{\sigma_{iq}\omega_i} = \dot{\ell}_{\sigma_{iq}}$ and $\ddot{\ell}_{\alpha_{iq}\omega_i} = \dot{\ell}_{\alpha_{iq}}$, for $j = 1, \ldots, n$. The elements $\dot{\ell}_{\xi_{iq}}$, $\dot{\ell}_{\sigma_{iq}}$ and $\dot{\ell}_{\alpha_{iq}}$, together with the matrices $\mathbf{W}_1$, $\mathbf{W}_2$ and $\mathbf{W}_3$, are those defined in Section 2.4.

2.7.2 Response variable

This perturbation scheme allows us to evaluate the sensitivity of the ML estimates when small perturbations to the response vector are introduced. Thus, let $\boldsymbol{\omega} = (\omega_1, \ldots, \omega_n)^\top$ and $\boldsymbol{\omega}_0 = (0, \ldots, 0)^\top$ be vectors of dimension $(n \times 1)$, $y_i(\omega_i) = y_i + \omega_i \mathrm{s}_y$, where s_y is the sample standard deviation of $\mathbf{y}$ and $\omega_i \in \mathbb{R}$ for $i = 1, \ldots, n$. Therefore, the perturbed log-likelihood function is given by

$$\ell(\boldsymbol{\theta}_q|\boldsymbol{\omega}) = \sum_{i=1}^{n} \ell_i(\xi_{iq}, \sigma_{iq}, \alpha_{iq}, \omega_i), \tag{2.31}$$
$$\ell_i(\xi_{iq}, \sigma_{iq}, \alpha_{iq}, \omega_i) = \log(\alpha_{iq}) + \log(f_0(u_{iq}^*)) - \log(\sigma_{iq}) - 2\log(\alpha_{iq} + (1-\alpha_{iq})F_0(u_{iq}^*)),$$
$$u_{iq}^* = (y_i(\omega_i) - \xi_{iq})/\sigma_{iq} + F_0^{-1}(\alpha_{iq} q/(1 + q\alpha_{iq} - q)),$$

for $i = 1, \ldots, n$ and $q \in (0,1)$ fixed. Hence, the matrix $\boldsymbol{\Delta}_q$ can be written as

$$\boldsymbol{\Delta}_q = \begin{bmatrix} \mathbf{X}_1^\top & \mathbf{W}_1 & \mathbf{M}_4 \\ \mathbf{X}_2^\top & \mathbf{W}_2 & \mathbf{M}_5 \\ \mathbf{X}_3^\top & \mathbf{W}_3 & \mathbf{M}_6 \end{bmatrix},$$

where $\mathbf{M}_4 = \left[\ddot{\ell}_{\xi_{iq}\omega_i}\ \delta_{ij}\right]$, $\mathbf{M}_5 = \left[\ddot{\ell}_{\sigma_{iq}\omega_i}\ \delta_{ij}\right]$ and $\mathbf{M}_6 = \left[\ddot{\ell}_{\alpha_{iq}\omega_i}\ \delta_{ij}\right]$, whose elements are

$$\begin{aligned}
\ddot{\ell}_{\xi_{iq}\omega_i} &= \frac{\partial^2 \ell_i(\xi_{iq},\sigma_{iq},\alpha_{iq},\omega_i)}{\partial\xi_{iq}\partial\omega_i} \\
&= 2\psi_{8iq}\left[\frac{f_0'(u_{iq}^*)(1-\alpha_{iq})}{\alpha_{iq}+(1-\alpha_{iq})F_0(u_{iq}^*)}\right] - 2\psi_{8iq}\left[\frac{f_0(u_{iq}^*)(1-\alpha_{iq})}{\alpha_{iq}+(1-\alpha_{iq})F_0(u_{iq}^*)}\right]^2 \\
&\quad - \psi_{8iq}\left[\frac{f_0''(u_{iq}^*)}{f_0(u_{iq}^*)} - \frac{f_0'^2(u_{iq}^*)}{f_0^2(u_{iq}^*)}\right], \\
\ddot{\ell}_{\sigma_{iq}\omega_i} &= \frac{\partial^2 \ell_i(\xi_{iq},\sigma_{iq},\alpha_{iq},\omega_i)}{\partial\sigma_{iq}\partial\omega_i} \\
&= 2\psi_{8iq}\left[\frac{f_0(u_{iq}^*)(1-\alpha_{iq})}{\alpha_{iq}+(1-\alpha_{iq})F_0(u_{iq}^*)}\right] - \psi_{8iq}\left[\frac{f_0'(u_{iq}^*)}{f_0(u_{iq}^*)}\right] - 2\psi_{9iq}\left[\frac{f_0(u_{iq}^*)(1-\alpha_{iq})}{\alpha_{iq}+(1-\alpha_{iq})F_0(u_{iq}^*)}\right]^2 \\
&\quad - \psi_{9iq}\left[\frac{f_0''(u_{iq}^*)}{f_0(u_{iq}^*)} - \frac{f_0'^2(u_{iq}^*)}{f_0^2(u_{iq}^*)}\right] + 2\psi_{9iq}\left[\frac{f_0'(u_{iq}^*)(1-\alpha_{iq})}{\alpha_{iq}+(1-\alpha_{iq})F_0(u_{iq}^*)}\right], \\
\ddot{\ell}_{\alpha_{iq}\omega_i} &= \frac{\partial^2 \ell_i(\xi_{iq},\sigma_{iq},\alpha_{iq},\omega_i)}{\partial\alpha_{iq}\partial\omega_i} \\
&= 2\psi_{7iq}\left[\frac{f_0(u_{iq}^*)}{\alpha_{iq}+(1-\alpha_{iq})F_0(u_{iq}^*)}\right] - 2\psi_{7iq}u_{\alpha_{iq}}^*\left[\frac{f_0'(u_{iq}^*)(1-\alpha_{iq})}{\alpha_{iq}+(1-\alpha_{iq})F_0(u_{iq}^*)}\right] \\
&\quad + 2\psi_{7iq}\left[\frac{f_0(u_{iq}^*)(1-\alpha_{iq})}{\alpha_{iq}+(1-\alpha_{iq})F_0(u_{iq}^*)}\right]\left[\frac{1-F_0(u_{iq}^*)+(1-\alpha_{iq})f_0(u_{iq}^*)u_{\alpha_{iq}}^*}{\alpha_{iq}+(1-\alpha_{iq})F_0(u_{iq}^*)}\right] \\
&\quad + \psi_{7iq}u_{\alpha_{iq}}^*\left[\frac{f_0''(u_{iq}^*)}{f_0(u_{iq}^*)} - \frac{f_0'^2(u_{iq}^*)}{f_0^2(u_{iq}^*)}\right],
\end{aligned}$$

where

$$\psi_{7iq} = \frac{s_y}{\sigma_{iq}}, \qquad \psi_{8iq} = \frac{s_y}{\sigma_{iq}^2}, \qquad \psi_{9iq} = \frac{(y_i(\omega_i)-\xi_{iq})s_y}{\sigma_{iq}^3}, \qquad u_{\alpha_{iq}}^* = \frac{\Psi_0 q(1-q)}{(1+q\alpha_{iq}-q)^2}$$

and $\Psi_0 = 1/f_0(F_0^{-1}(\alpha_{iq}q/(1+q\alpha_{iq}-q)))$ for $j = 1,\ldots,n$.

2.7.3 Perturbation of the skewness parameter

Following the idea proposed by Sánchez *et al.* (2021), the skewness parameter is perturbed as $\alpha_{iq}(\omega_i) = \alpha_{iq}/\omega_i$ with $\omega_i > 0$ for $i = 1,\ldots,n$ and q fixed. Hence, the perturbed log-likelihood function is

$$\ell(\boldsymbol{\theta}_q|\boldsymbol{\omega}) = \sum_{i=1}^{n} \ell_i(\xi_{iq},\sigma_{iq},\alpha_{iq}(\omega_i)) \tag{2.32}$$

$$\begin{aligned}
\ell_i(\xi_{iq},\sigma_{iq},\alpha_{iq}(\omega_i)) &= \log(\alpha_{iq}) + \log(\omega_i) + \log(f_0(u_{iq})) - \log(\sigma_{iq}) - 2\log(\rho_i(u_{iq})), \\
\rho_i(u_{iq}) &= \alpha_{iq} + (\omega_i - \alpha_{iq})F_0(u_{iq}),
\end{aligned}$$

where $u_{iq} = (y_i - \xi_{iq})/\sigma_{iq} + F_0^{-1}(\alpha_{iq}q/(\omega_i + q\alpha_{iq} - q\omega_i))$. Taking derivatives of Equation (2.32) with respect to α_{iq} and ω_i, the matrix $\boldsymbol{\Delta}_q$ assumes the form

$$\boldsymbol{\Delta}_q = \begin{bmatrix} \mathbf{X}_3^\top & \mathbf{W}_3 & \mathbf{M}_7 \end{bmatrix},$$

where $\mathbf{M}_7 = \begin{bmatrix} \ddot{\ell}_{\alpha_{iq}\omega_i} & \delta_{ij} \end{bmatrix}$, whose elements are

$$\begin{aligned}
\ddot{\ell}_{\alpha_{iq}\omega_i} = {} & u_{\alpha_{iq}\omega_i}\left[\frac{f_0'(u_{iq})}{f_0(u_{iq})}\right] + u_{\alpha_{iq}}u_{\omega_i}\left[\frac{f_0''(u_{iq})}{f_0(u_{iq})} - \frac{f_0'^2(u_{iq})}{f_0^2(u_{iq})}\right] + 2\left[\frac{f_0(u_{iq})u_{\omega_i} - f_0(u_{iq})u_{\alpha_{iq}}}{\alpha_{iq} + (\omega_i - \alpha_{iq})F_0(u_{iq})}\right] \\
& - 2\left[\frac{(\omega_i - \alpha_{iq})f_0'(u_{iq})u_{\omega_i}u_{\alpha_{iq}}}{\alpha_{iq} + (\omega_i - \alpha_{iq})F_0(u_{iq})}\right] - 2\left[\frac{(\omega_i - \alpha_{iq})f_0(u_{iq})u_{\alpha_{iq}\omega_i}}{\alpha_{iq} + (\omega_i - \alpha_{iq})F_0(u_{iq})}\right] \\
& + 2\left[\frac{1 - F_0(u_{iq}) + (\omega_i - \alpha_{iq})f_0(u_{iq})u_{\alpha_{iq}}}{\alpha_{iq} + (\omega_i - \alpha_{iq})F_0(u_{iq})}\right]\left[\frac{F_0(u_{iq}) + (\omega_i - \alpha_{iq})f_0(u_{iq})u_{\omega_i}}{\alpha_{iq} + (\omega_i - \alpha_{iq})F_0(u_{iq})}\right],
\end{aligned}$$

with

$$u_{\omega_i} = \frac{\Psi_0\alpha_{iq}q(q-1)}{(\omega_i + q\alpha_{iq} - q\omega_i)^2}, \quad u_{\alpha_{iq}} = \frac{\Psi_0\omega_i q(1-q)}{(\omega_i + q\alpha_{iq} - q\omega_i)^2}, \quad \Psi_0 = \frac{1}{f_0(F_0^{-1}(q\alpha_{iq}/(\omega_i + q\alpha_{iq} - q\omega_i)))},$$

and

$$u_{\omega_i\alpha_{iq}} = \left[\frac{\omega_i\alpha_{iq}q^2(q-1)^2}{(\omega_i + q\alpha_{iq} - q\omega_i)^4}\right]\Psi_0^3\, f_0'(F_0^{-1}(q\alpha_{iq}/(\omega_i + q\alpha_{iq} - q\omega_i))) + \Psi_0(q-1)q\left[\frac{(\omega_i - q\omega_i - q\alpha_{iq})}{(\omega_i + q\alpha_{iq} - q\omega_i)^3}\right],$$

for $i = 1, \ldots, n$ and q fixed. In this scheme $\boldsymbol{\omega}_0 = (1, \ldots, 1)^\top$ is the non-perturbation vector.

2.8 Final comments

This chapter introduces the family of RPMO distributions that contain three parameters: quantile, scale and skewness. The family has arisen by applying the MO methodology to the location-scale family and then a quantile parameterization. One of the aspects to highlight about the family is that the expressions of the pdf, cdf and qf are closed, which helps to calculate probabilities simply and simulate random numbers directly through the inversion method. Additionally, the skewness and kurtosis coefficients are analyzed using plots, where we observe that the distributions are most flexible compared to the reparameterized location-scale family.

We formulate the QR model for the RPMO family of distributions with a framework similar to generalized linear models. Based on the log-likelihood function, the expressions of the score vector and the observed information matrix to perform inference were derived. The RS algorithm was adopted to obtain the ML estimates due to its low computational cost.

Furthermore, three types of residuals and their envelopes were adopted to detect outliers and study the adequacy of the models. Then, two measures of case deletion were presented as tools of global influence to identify influential observations. For the same purpose, three perturbation schemes were developed as tools of local influence. All of the above mathematical expressions have a simple structure to be implemented in any mathematical or statistical software.

CHAPTER

3

SIMULATION STUDIES AND DATA ANALYSIS FOR LINEAR QUANTILE REGRESSION MODELS

In this chapter, we present simulation studies to assess the behavior of the ML estimators in the QR model of the RPMON, RPMOG and RPMOT ($\vartheta = 15$) distributions. Furthermore, we illustrate the methodologies proposed in Chapter 2 to a National Health and Nutrition Examination Survey (NHANES) dataset.

3.1 Simulation studies

In order to carry out the studies in this section, we generated 3000 random samples using the qf of Equation (2.3) considering $n \in \{100, 150, 200, \ldots, 5000\}$ and $q \in \{0.1, 0.5, 0.9\}$. The ML estimates were obtained using the RS algorithm of the *gamlss* package in the R language. Moreover, three scenarios were considered, whose structures are as follows:

$$\begin{aligned} \xi_{iq} = \eta_{1iq} &= 2.086 + 0.318x_{1i2} + 0.650x_{1i3}, \\ \log(\sigma_{iq}) = \eta_{2iq} &= 0.782 + 0.008x_{2i2}, \\ \log(\alpha_{iq}) = \eta_{3iq} &= 0.5x_{3i1} - 2x_{3i2}; \end{aligned} \tag{I}$$

$$\begin{aligned} \xi_{iq} = \eta_{1iq} &= 1.347 + 0.322x_{1i2} + 0.858x_{1i3}, \\ \log(\sigma_{iq}) = \eta_{2iq} &= 0.189 + 0.006x_{2i2}, \\ \log(\alpha_{iq}) = \eta_{3iq} &= 0.013x_{3i1} + 0.903x_{3i2}; \text{ and} \end{aligned} \tag{II}$$

$$\begin{aligned} \xi_{iq} = \eta_{1iq} &= -1.240 + 0.306x_{1i2} + 0.699x_{1i3}, \\ \log(\sigma_{iq}) = \eta_{2iq} &= 0.521 + 0.009x_{2i2}, \\ \log(\alpha_{iq}) = \eta_{3iq} &= -0.2x_{3i1} + 0.75x_{3i2}, \end{aligned} \tag{III}$$

where $x_{1i2} \sim \mathrm{N}(100,3)$, $x_{1i3} \sim \mathrm{Bern}(0.5)$, $x_{2i2} \sim \mathrm{N}(0,1)$, $x_{3i1} \sim \mathrm{Logis}(0,1)$ and $x_{3i2} \sim \mathrm{Bern}(0.7)$, for $i = 1,\ldots,n$. Also, $\mathrm{Bern}(p)$ denotes Bernoulli distribution and $\mathrm{Logis}(0,1)$ denotes the standard logistic distribution. Scenarios I, II and III were developed in RPMON, RPMOG and RPMOT ($\vartheta = 15$) distributions, respectively. However, the scenario for the RPMOC distribution is not included because Equation (2.13) has multiple roots that generate problems in finding the ML estimates. The repository <https://github.com/isaaccortes1989/RPMO-GAMLSS-FAMILY> contains the structure of the *gamlss.family* distributions necessary for reproducing and fitting the RPMO family.

Figures 5-9 show the mean of the relative bias (RB), standard deviation (SD), the root of the mean square error (RMSE), mean of the asymptotic standard error (SE) and the coverage probability (CP) of the 95% asymptotic confidence intervals for the components of the vector $\widehat{\boldsymbol{\theta}}_q$ in the RPMON model (Scenario I) according to sample sizes. From Figures 5-8, we note that as the sample size n increases, the RBs, SDs, RMSEs and SEs decrease as expected in standard asymptotic theory. Specifically, in Figure 5, it can be seen that the ML estimators associated with β_{1q} and ν_{2q} are less precise than the others, with a lower performance at $q = 0.1$. Finally, Figure 9 displays that the CPs converge to the nominal values as the sample size n increases.

On the other hand, Figures 32-36 from Appendix A present the plots for the same five measures in Scenario II. It can be seen in Figures 32-35 that the asymptotic behavior of RBs, SDs, RMSEs and SEs is similar to Scenario I. But in this scenario, the ML estimators associated with β_{1q}, ν_{2q} and τ_{1q} are less precise than the others, with a lower performance for $q = 0.5$. Moreover, the CPs in Figure 36 are close to the nominal values used for their construction as n increases.

The plots of the five measures in Scenario III are shown in Figures 37-41 of Appendix A. From the first four figures, we note that the asymptotic behavior of the measures is similar to Scenario II, i.e., the quantities decrease as the sample size n increases. Also, β_{1q}, ν_{2q} and τ_{1q} are the ML estimators that are less precise. In addition, the CPs from Figure 41 indicate that a much larger sample size is required than Scenarios I and II to be close to nominal values.

To observe the behavior of the mean SE in all the parameters as a function of the sample size, we present the plots of $\mathrm{SE}_i/\mathrm{SE}_{i+1}$ and $\sqrt{n_{i+1}/n_i}$ rates for $i = 1,...,98$ correspondent to $n \in \{100,150,200,\ldots,5000\}$. These plots for the three scenarios can be seen in Figures 42-50 (Appendix A) and indicate that the behavior of the mean SE decreases according to $\sqrt{n_{i+1}/n_i}$ rate, as expected in the standard asymptotic theory.

Figure 5 – Mean of the RB on the 3000 estimates of the components $\widehat{\boldsymbol{\beta}}_q$, $\widehat{\boldsymbol{\nu}}_q$ and $\widehat{\boldsymbol{\tau}}_q$ obtained in the RPMON model under different sample sizes.

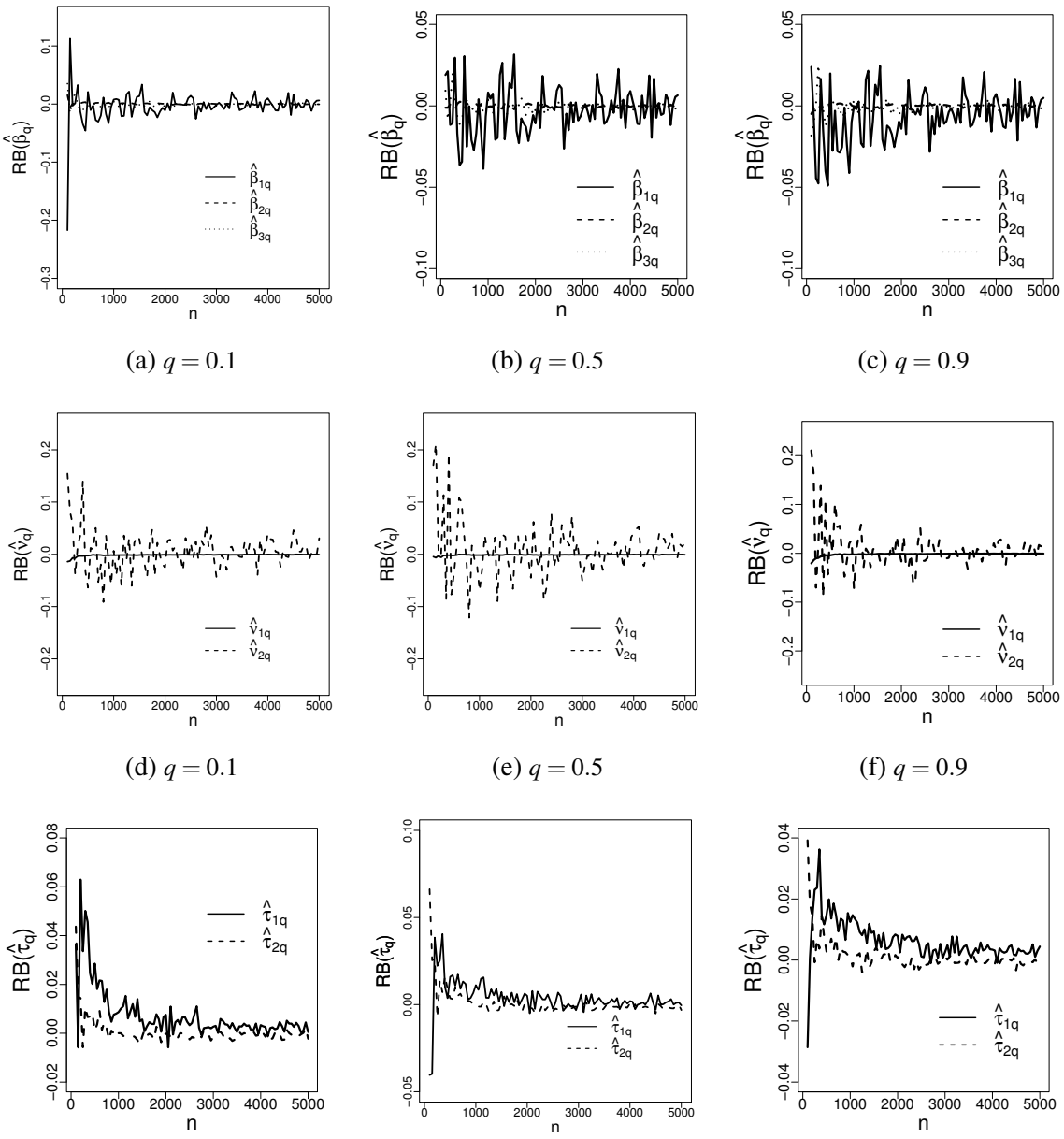

(a) $q = 0.1$ (b) $q = 0.5$ (c) $q = 0.9$

(d) $q = 0.1$ (e) $q = 0.5$ (f) $q = 0.9$

(g) $q = 0.1$ (h) $q = 0.5$ (i) $q = 0.9$

Figure 6 – SD on the 3000 estimates of the components $\widehat{\boldsymbol{\beta}}_q$, $\widehat{\boldsymbol{\nu}}_q$ and $\widehat{\boldsymbol{\tau}}_q$ obtained in the RPMON model under different sample sizes.

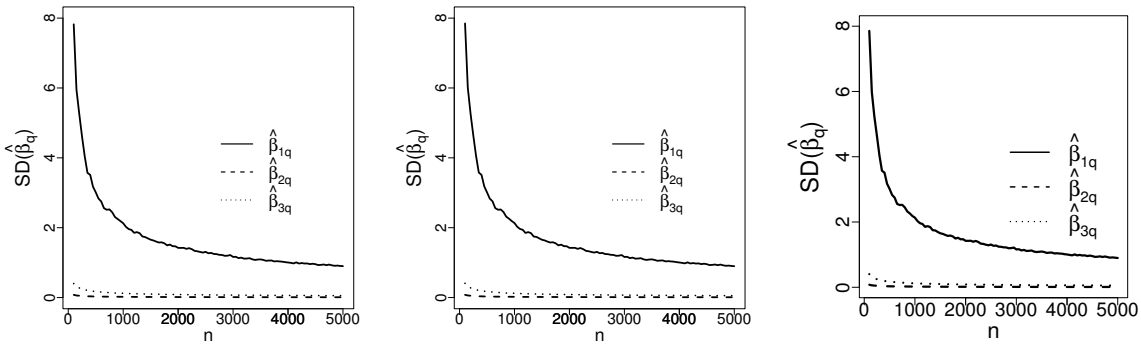

(a) $q = 0.1$ (b) $q = 0.5$ (c) $q = 0.9$

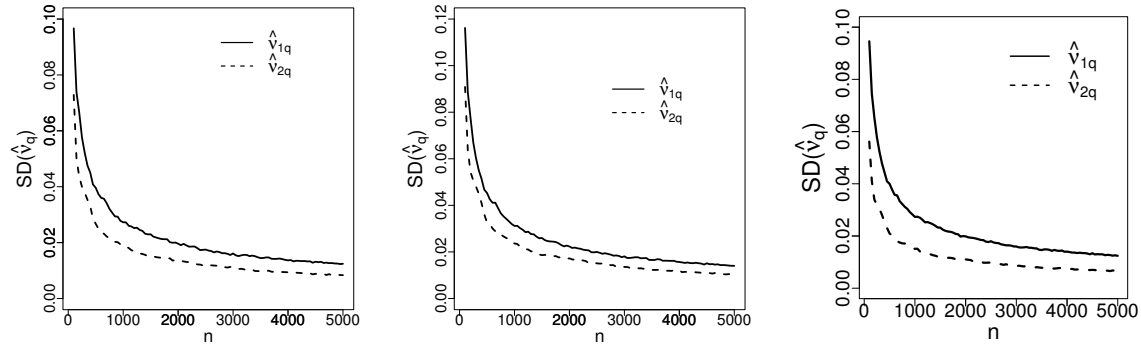

(d) $q = 0.1$ (e) $q = 0.5$ (f) $q = 0.9$

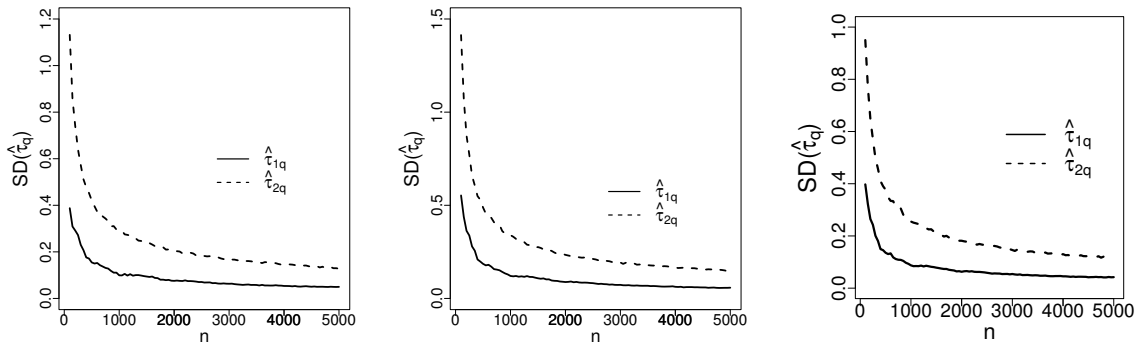

(g) $q = 0.1$ (h) $q = 0.5$ (i) $q = 0.9$

Figure 7 – RMSE on the 3000 estimates of the components $\widehat{\boldsymbol{\beta}}_q$, $\widehat{\boldsymbol{\nu}}_q$ and $\widehat{\boldsymbol{\tau}}_q$ obtained in the RPMON model under different sample sizes.

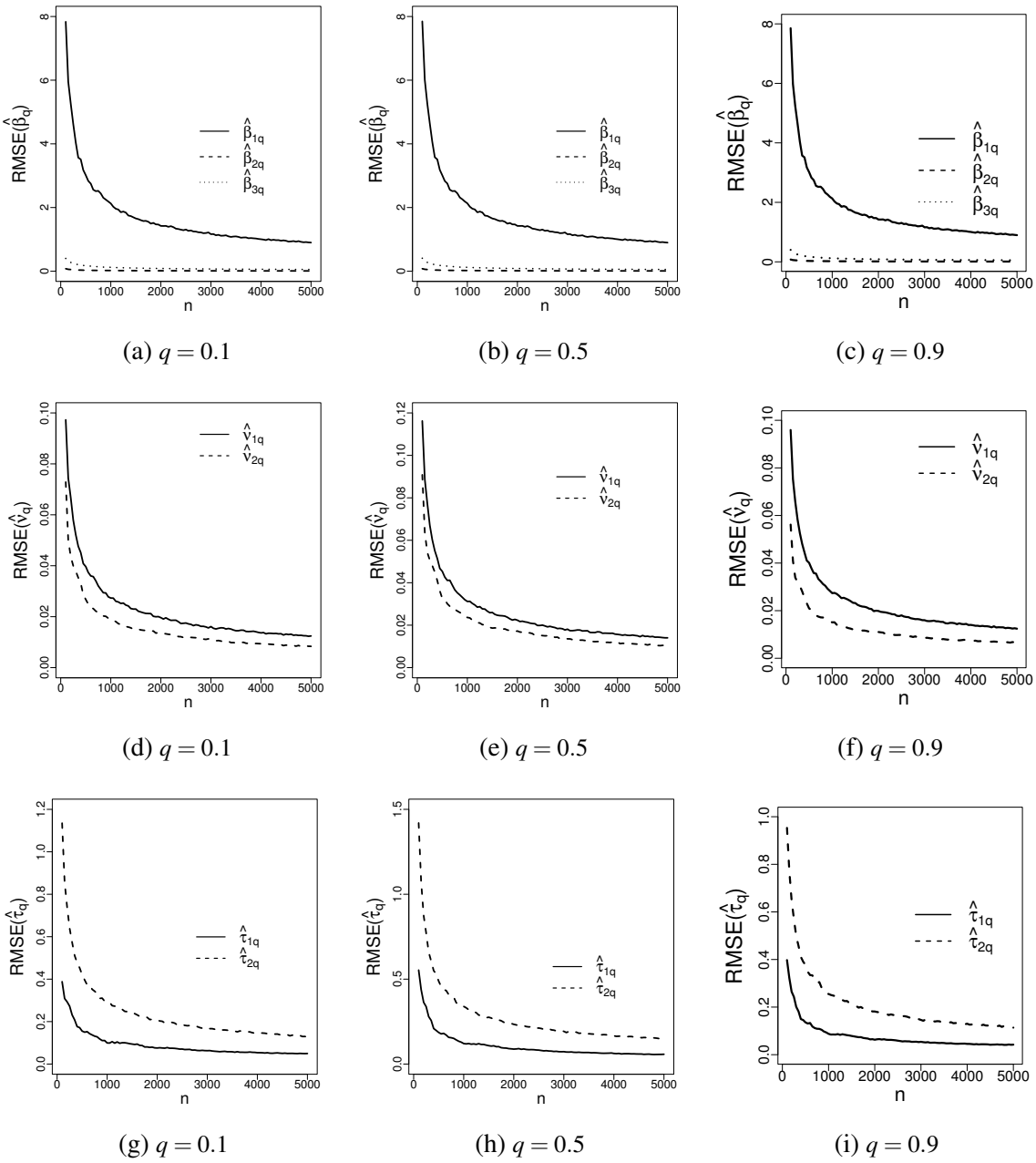

(a) $q = 0.1$ (b) $q = 0.5$ (c) $q = 0.9$

(d) $q = 0.1$ (e) $q = 0.5$ (f) $q = 0.9$

(g) $q = 0.1$ (h) $q = 0.5$ (i) $q = 0.9$

Figure 8 – Mean of the asymptotic SE on the 3000 estimates of the components $\widehat{\boldsymbol{\beta}}_q$, $\widehat{\boldsymbol{\nu}}_q$ and $\widehat{\boldsymbol{\tau}}_q$ obtained in the RPMON model under different sample sizes.

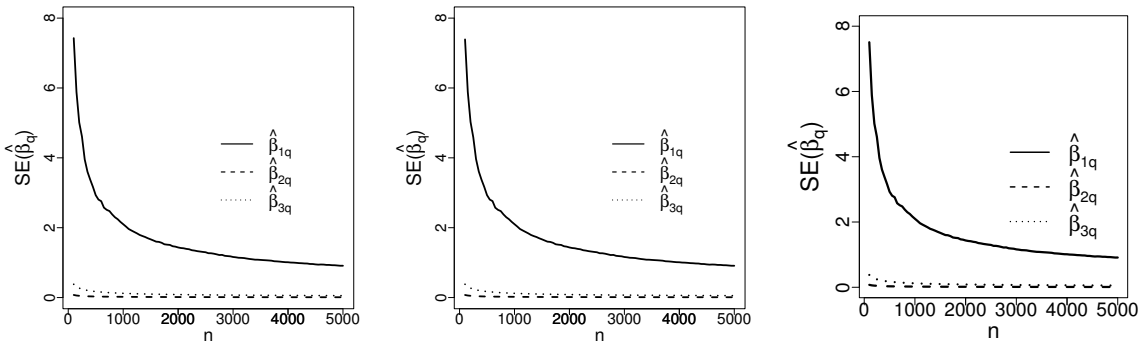

(a) $q = 0.1$ (b) $q = 0.5$ (c) $q = 0.9$

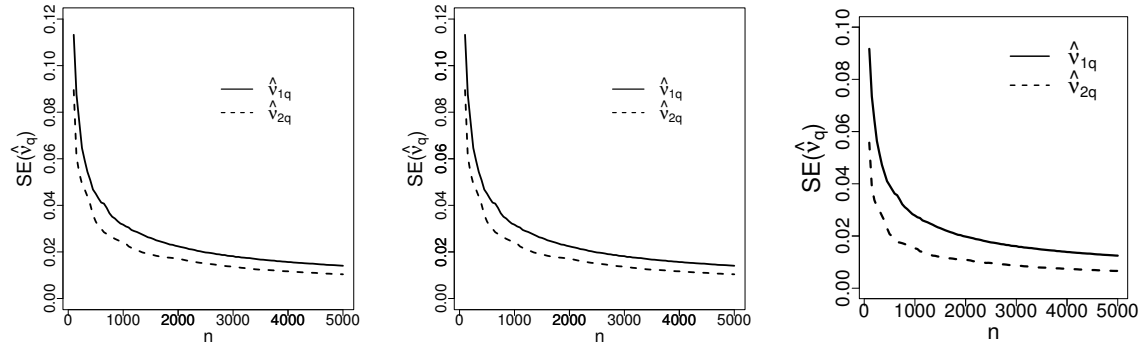

(d) $q = 0.1$ (e) $q = 0.5$ (f) $q = 0.9$

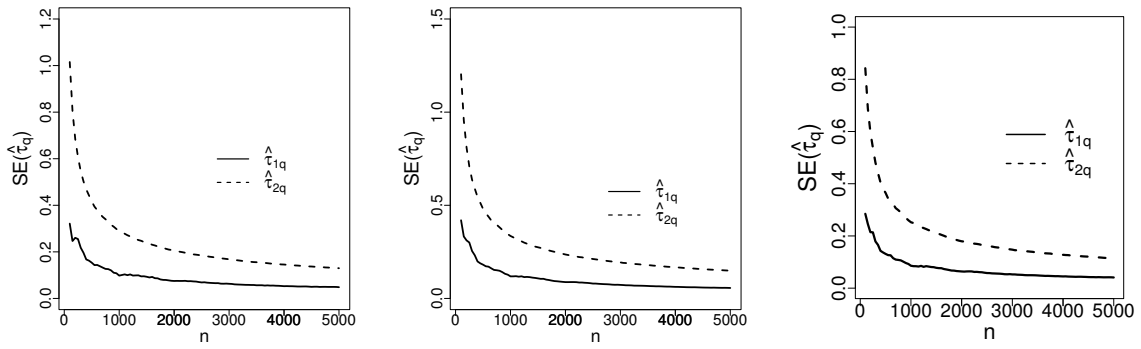

(g) $q = 0.1$ (h) $q = 0.5$ (i) $q = 0.9$

Figure 9 – 95% CP of the components $\widehat{\boldsymbol{\beta}}_q$, $\widehat{\boldsymbol{\nu}}_q$ and $\widehat{\boldsymbol{\tau}}_q$ obtained in the RPMON model under different sample sizes.

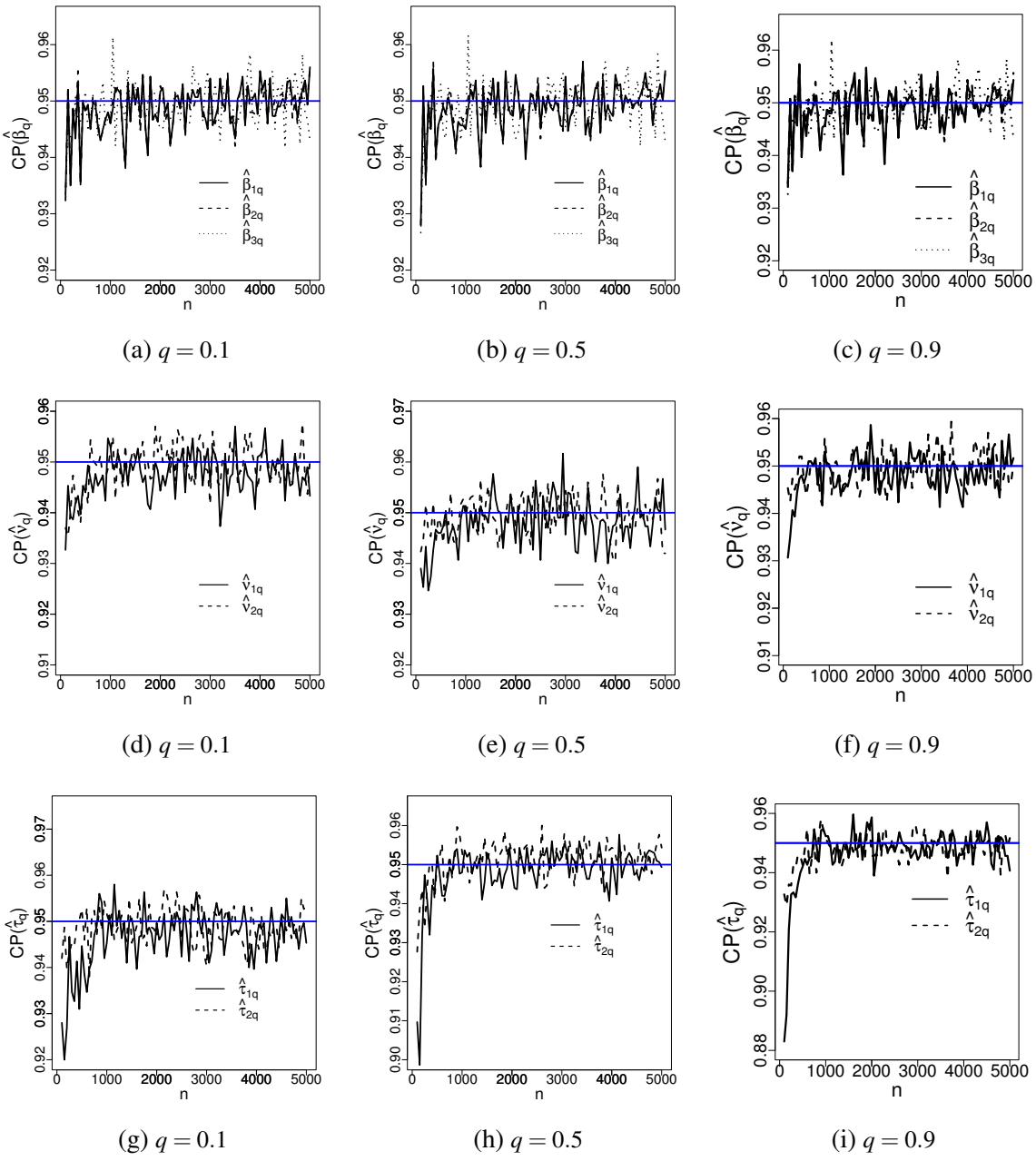

(a) $q = 0.1$ (b) $q = 0.5$ (c) $q = 0.9$

(d) $q = 0.1$ (e) $q = 0.5$ (f) $q = 0.9$

(g) $q = 0.1$ (h) $q = 0.5$ (i) $q = 0.9$

3.2 Data analysis

In this section, we analyze a subset of the data from NHANES (2017-2018) to illustrate potential applications of the RPMO family. Specifically, we focused on 1743 people who self-identified as American-Mexican. Repository <https://github.com/isaaccortes1989/Data-Chapter-3> contains the data file in CSV format. The purpose of this analysis is to investigate the relationship between body mass index (BMI), expressed in kg/m^2 and other covariates using QR models under RPMO distributions. So, we consider waist circumference (Waist) in centimeters, gender (Gender) and age (Age) in years as covariates.

3.2.1 Descriptive analysis

First, we conducted a descriptive analysis of the BMI variable. The sample skewness coefficient, kurtosis coefficient, mean and median are respectively 0.68, 3.85, 25.15 and 24.80. Furthermore, the minimum and maximum values are 12.71 and 71.72, respectively. Then, we expect the RPMO family to present a good performance in the fit of these data.

Figure 10 shows the histogram of BMI and the scatter plots of BMI and each one of the covariates, where we observe the following aspects. First, from Figure 10(a), the BMI has a unimodal empirical distribution with positive skewness and light tails. Second, in Figures 10(b) and 10(c), we can assume that the relationships between BMI and the covariates are linear. Additionally, observations #264, #1267 and #1425 have an atypical behavior in the population. In addition, we calculate Spearman's correlation coefficient between Waist and Age, which is equal to 0.77. The result indicates a strong linear relationship between Waist and Age.

3.2.2 Fitting of the quantile regression models

To study in detail BMI, we fit the QR model from RPMO family. Then, the *q-th* quantile ξ_{iq}, scale σ_{iq} and skewness α_{iq} have the following systematic components

$$\begin{aligned} \xi_{iq} &= \eta_{1iq} = \beta_{1q} + \beta_{2q}\text{Waist}_i + \beta_{3q}\text{Gender}_i, \\ \log(\sigma_{iq}) &= \eta_{2iq} = \nu_{1q} + \nu_{2q}\text{Gender}_i + \nu_{3q}\text{Age}_i \text{ and} \\ \log(\alpha_{iq}) &= \eta_{3iq} = \tau_{1q}\text{Waist} + \tau_{2q}\text{Gender}_i, \end{aligned} \tag{3.1}$$

where Waist_i, Gender_i and Age_i denote the waist circumference, gender and age of the *i-th* observation for $i = 1, \ldots, 1743$. Also, $\boldsymbol{\theta}_q = (\beta_{1q}, \beta_{2q}, \beta_{3q}, \nu_{1q}, \nu_{2q}, \nu_{3q}, \tau_{1q}, \tau_{2q})^\top$ is the vector of unknown parameters for $q \in \{0.1, 0.25, 0.5, 0.75, 0.9\}$. The Waist and Gender variables were selected based on a classification from the National Heart, Lung, and Blood Institute (<https://www.nhlbi.nih.gov/health/educational/lose_wt/BMI/bmi_dis.htm>). On the other hand, the Age variable was selected for exploratory purposes. In order to avoid collinearity problems, the variables Age and Waist do not interact together.

Figure 10 – Histogram of BMI (a), scatter plot for BMI and Waist (b) and scatter plot for BMI and Age (c).

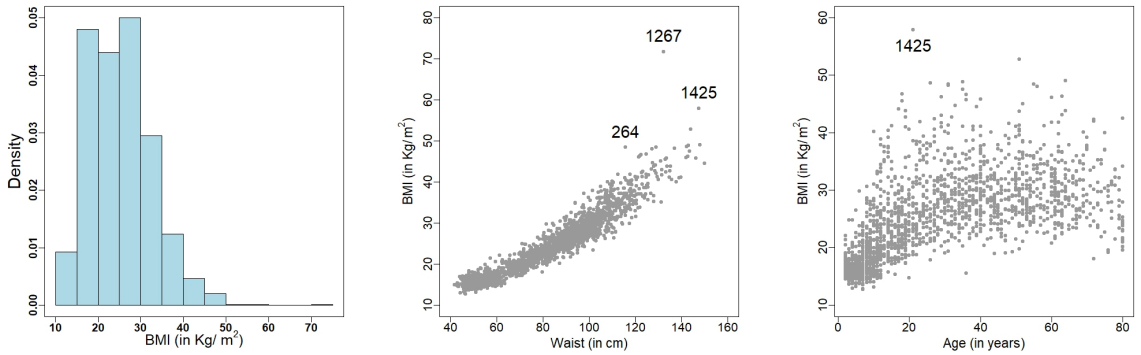

(a) (b) (c)

We have also included the fits of a generalized class of skew densities (SKD) (MORALES *et al.*, 2017) to compare its results with those of the RPMO family. In addition, the particular cases of the RPMO family are added, such as when $\alpha_{iq} = 1$ and when $\sigma_{iq} = \sigma$ (homogeneity of variance) and $\alpha_{iq} = 1$ for all $i = 1, \ldots, 1743$. The codes of the fits of the SKD class and RPMO family were developed using the *lqr* (GALARZA *et al.*, 2022) and *gamlss* packages in the *R* language (<https://github.com/isaaccortes1989/Fits-Chapter-3>). Specifically, in the lqr package, we use the *best.lqr* function that indicates which distribution best fits in the class SKD: the Normal, Student-t, Laplace, Slash and Contaminated Normal distributions.

Table 4 displays the values of the Akaike information criterion (AIC) (AKAIKE, 1974) and Bayesian information criterion (BIC) (SCHWARZ, 1978) for all fitted models. From this table, we note that the Slash distribution has a better fit in the SKD class. Also, this distribution generally has a better fit compared to the RPMOC distribution and, some cases, better than the RPMON distribution (when $\alpha_{iq} = 1$ and $\sigma_{iq} = \sigma$). Furthermore, we highlight that the values from both criteria are smaller in the RPMOG distribution when modeling scale and skewness, especially in the extreme quantiles. To summarize, the RPMOG is the best distribution for explaining the quantiles, scale and skewness of BMI.

From now on, the study will focus on the 90-*th* percentile because it is interesting to study which variables affect obese people, i.e., people whose BMI is greater than or equal to thirty (<https://www.nhlbi.nih.gov/health/educational/lose_wt/risk.htm>). Then, after using the backward elimination method in Equation (3.1), the RPMOG model is reduced as follows:

$$\begin{aligned} \xi_{iq} = \eta_{1iq} &= \beta_{1q} + \beta_{2q}\,\text{Waist}_i + \beta_{3q}\,\text{Gender}_i, \\ \log(\sigma_{iq}) = \eta_{2iq} &= \nu_{1q} + \nu_{3q}\,\text{Age}_i \quad \text{and} \\ \log(\alpha_{iq}) = \eta_{3iq} &= \tau_{1q}\,\text{Waist} + \tau_{2q}\,\text{Gender}_i, \end{aligned} \tag{3.2}$$

for $i = 1, \ldots, 1743$ and $q = 0.9$. In this model, $\boldsymbol{\theta}_q = (\beta_{1q}, \beta_{2q}, \beta_{3q}, \nu_{1q}, \nu_{3q}, \tau_{1q}, \tau_{2q})^\top$ is the vector of unknown parameters and its ML estimates, SEs with their respective z-values and p-values,

can be seen in Table 5. From there, we note that all p-values are less than 0.05, indicating that all coefficients are significant at a 5% level.

Table 4 – AIC and BIC criteria for different QR models.

AIC criterion													
		RPMO family considering $\alpha_{iq}=1$				RPMO family considering $\sigma_{iq}=\sigma$ and $\alpha_{iq}=1$				RPMO family considering σ_{iq} and α_{iq}			
q	Slash	RPMON	RPMOC	RPMOG	RPMOT ($\vartheta=15$)	RPMON	RPMOC	RPMOG	RPMOT ($\vartheta=15$)	RPMON	RPMOC	RPMOG	RPMOT ($\vartheta=15$)
0.10	8,064.9	7,986.5	8,207.1	7,788.3	7,818.3	8,013.3	8,252.9	7,841.8	7,826.8	7,787.5	8,148.6	**7,582.6**	7,668.0
0.25	7,815.2	7,964.7	8,248.9	7,730.0	7,801.1	8,013.3	8,252.9	7,841.8	7,826.8	7,759.7	8,220.5	**7,670.8**	7,773.1
0.50	7,790.6	7,906.8	8,226.9	7,667.0	7,752.4	8,013.3	8,252.9	7,841.8	7,826.8	7,698.9	8,195.5	**7,637.1**	7,717.4
0.75	8,153.5	7,855.1	8,185.5	7,629.7	7,706.6	8,013.3	8,252.9	7,841.8	7,826.8	7,642.7	8,148.2	**7,598.8**	7,663.9
0.90	8,663.3	7,829.3	8,152.2	7,618.1	7,681.5	8,013.3	8,252.9	7,841.8	7,826.8	7,603.8	8,106.9	**7,577.1**	7,631.8
BIC criterion													
		RPMO family considering $\alpha_{iq}=1$				RPMO family considering $\sigma_{iq}=\sigma$ and $\alpha_{iq}=1$				RPMO family considering σ_{iq} and α_{iq}			
q	Slash	RPMON	RPMOC	RPMOG	RPMOT ($\vartheta=15$)	RPMON	RPMOC	RPMOG	RPMOT ($\vartheta=15$)	RPMON	RPMOC	RPMOG	RPMOT ($\vartheta=15$)
0.10	8,086.8	8,019.3	8,239.9	7,821.0	7,851.0	8,035.2	8,274.7	7,863.6	7,848.6	7,831.2	8,192.3	**7,626.3**	7,711.7
0.25	7,837.1	7,997.5	8,281.7	7,762.8	7,833.9	8,035.2	8,274.7	7,863.6	7,848.6	7,803.5	8,264.2	**7,714.5**	7,816.8
0.50	7,812.5	7,939.6	8,259.7	7,699.8	7,785.2	8,035.2	8,274.7	7,863.6	7,848.6	7,742.6	8,239.2	**7,680.8**	7,761.1
0.75	8,175.4	7,887.9	8,218.3	7,662.5	7,739.4	8,035.2	8,274.7	7,863.6	7,848.6	7,686.4	8,191.9	**7,642.5**	7,707.6
0.90	8,685.2	7,862.1	8,184.9	7,650.9	7,714.3	8,035.2	8,274.7	7,863.6	7,848.6	7,647.5	8,150.6	**7,620.8**	7,675.5

Table 5 – ML estimate, SE, z-value and p-value for the indicated parameter fitted with the QR model under RPMOG distribution, considering $q = 0.9$.

	$\widehat{\beta}_{1q}$	$\widehat{\beta}_{2q}$	$\widehat{\beta}_{3q}$	$\widehat{\nu}_{1q}$	$\widehat{\nu}_{3q}$	$\widehat{\tau}_{1q}$	$\widehat{\tau}_{2q}$
Estimate	0.592	0.319	0.817	0.179	0.007	0.012	0.869
SE	0.235	0.003	0.120	0.037	0.001	0.002	0.227
z-value	2.524	119.106	6.817	4.821	13.056	5.232	3.822
p-value	0.012	< 0.001	< 0.001	< 0.001	< 0.001	< 0.001	< 0.001

3.2.3 Identifying outliers and studying model adequacy

Here, we investigate the behavior of the residuals with their corresponding envelopes (see Sections 2.5.1, 2.5.2 and 2.5.3) to detect outlier observations. These residuals are presented graphically in Figure 11, where observations #264, #1267, and #1425 are detected as outliers because they are outside the envelopes. Additionally, we use the Kolmogorov-Smirnov test to verify that the residuals follow a standard normal, exponential and standard normal distribution, respectively. The results in Table 6 show that the null hypotheses are not rejected at a 5% significance level. Furthermore, these results confirm the fact that the response variable follows an RPMOG distribution.

Table 6 – Results of the Kolmogorov-Smirnov tests on the NQRs, GCSRs and MTRs.

	NQRs	GCSRs	MTRs
Statistic	0.017	0.020	0.018
p-value	0.687	0.493	0.625

Figure 11 – QQ-plot with envelopes for NQRs (a), GCSRs (b) and MTRs (c) under the RPMOG model considering $q = 0.9$.

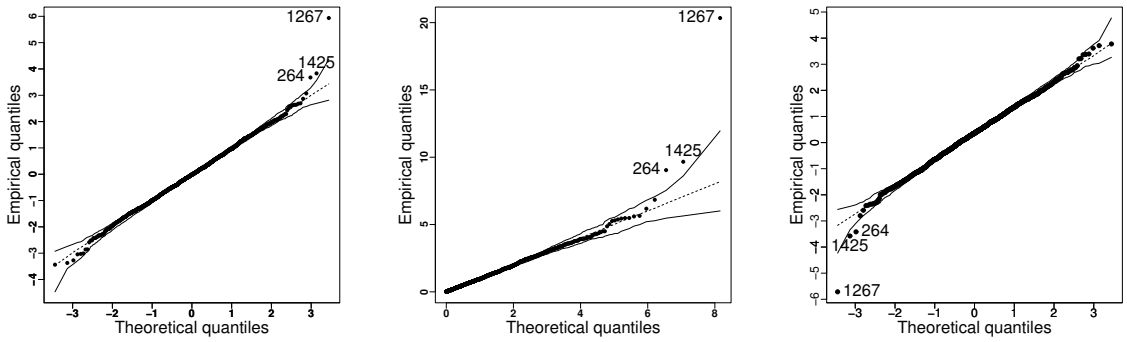

(a) (b) (c)

3.2.4 Identifying influential observations

The likelihood displacement and generalized Cook's distance from Sections 2.6.1 and 2.6.2, respectively, are used to detect potentially influential observations on the vector $\widehat{\boldsymbol{\theta}}_q$. Figure 12 displays these two measures and indicates that observations #1267, #1297 and #1348 exert the greatest influence on $\widehat{\boldsymbol{\theta}}_q$. In addition, the observations that exert a moderate influence are #78, #264 and #1425.

Figure 12 – GCD (a) and LD (b) in the RPMOG model, considering $q = 0.9$

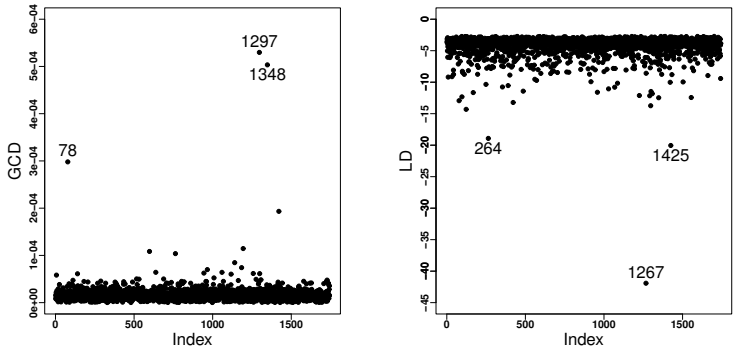

(a) (b)

Now, we present the index plots of C_i for the schemes: case-weight, response variable perturbation and skewness parameter perturbation described in Sections 2.7.1, 2.7.2 and 2.7.3, respectively. These plots will be used to detect potentially influential observations and assess the sensitivity of the ML estimates of $\boldsymbol{\theta}_q$, $\boldsymbol{\beta}_q$, $\boldsymbol{\nu}_q$, and $\boldsymbol{\tau}_q$.

Figure 13 shows the index plots of $C_i(\widehat{\boldsymbol{\theta}}_q)$, $C_i(\widehat{\boldsymbol{\beta}}_q)$, $C_i(\widehat{\boldsymbol{\nu}}_q)$ and $C_i(\widehat{\boldsymbol{\tau}}_q)$ for the RPMOG model under the case-weight perturbation scheme. In Figure 13(a), observations #78, #1267 and #1297 are indicated to have a strong influence on $\widehat{\boldsymbol{\theta}}_q$. Furthermore, Figures 13(b), 13(c), 13(d) indicate that there is a strong influence on $\widehat{\boldsymbol{\beta}}_q$, $\widehat{\boldsymbol{\nu}}_q$ and $\widehat{\boldsymbol{\tau}}_q$ by observations #78, #1297 and #1348. Note that observation #78 is also detected as atypical according to the residual analysis.

Figure 13 – Index plots of C_i for $\boldsymbol{\theta}_q$ (a), $\boldsymbol{\beta}_q$ (b), $\boldsymbol{\nu}_q$ (c) and $\boldsymbol{\tau}_q$ (d) under case-weight perturbation, using NHANES dataset with the RPMOG model and $q = 0.9$.

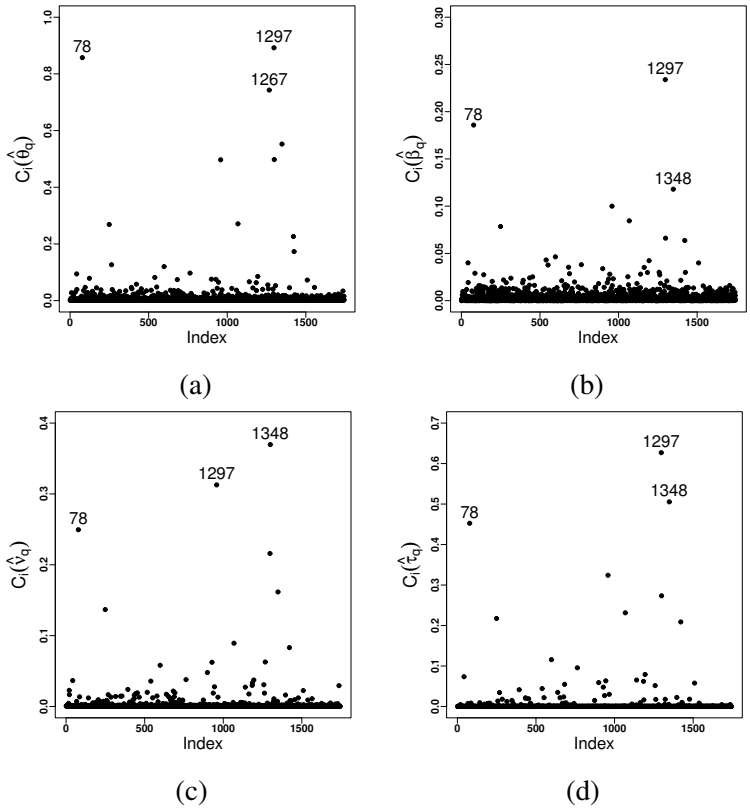

The index plots $C_i(\widehat{\boldsymbol{\theta}}_q)$, $C_i(\widehat{\boldsymbol{\beta}}_q)$, $C_i(\widehat{\boldsymbol{\nu}}_q)$ and $C_i(\widehat{\boldsymbol{\tau}}_q)$ of the RPMOG model under the perturbation scheme of the response variable (Section 2.7.2) are shown in Figure 14. From there, Figures 14(a), 14(b) and 14(d) highlight observations #78, #1297 and #1348 with more influence on $\widehat{\boldsymbol{\theta}}_q$, $\widehat{\boldsymbol{\beta}}_q$ and $\widehat{\boldsymbol{\tau}}_q$. On the other hand, the observations more influential on $\widehat{\boldsymbol{\nu}}_q$ are the following: #78, #1297 and #1299. Finally, note that observations #78, #1297 and #1348 are also detected as more influential in the case-weight scheme.

Finally, Figure 15 presents the index plots C_i for $\boldsymbol{\tau}_q$ under the skewness parameter perturbation scheme. From there, observations #78, #1297 and #1348 are detected as potentially influential. Note that the same observations are potentially influential in the case-weight and response perturbation schemes on $\boldsymbol{\tau}_q$.

In summary, observations #78, #264, #1267, #1297, #1299, #1348 and #1425 are potentially influential. Table 7 provides a classification of overweight, obesity class and risk of diseases such as type 2 diabetes, hypertension and heart disease based on those observations. From the table, we note that observations #78, #1299 and #1348 do not have a disease risk and a normal weight but a large waist circumference. Furthermore, observation #1297 is classified as a person who is overweight and has a high risk of disease. Finally, observations #264, #1267 and #1425 show an extremely high risk of disease and extreme obesity.

Figure 14 – Index plots of C_i for $\boldsymbol{\theta}_q$ (a), $\boldsymbol{\beta}_q$ (b), $\boldsymbol{\nu}_q$ (c) and $\boldsymbol{\tau}_q$ (d) under response perturbation, using NHANES dataset with the RPMOG model and $q = 0.9$.

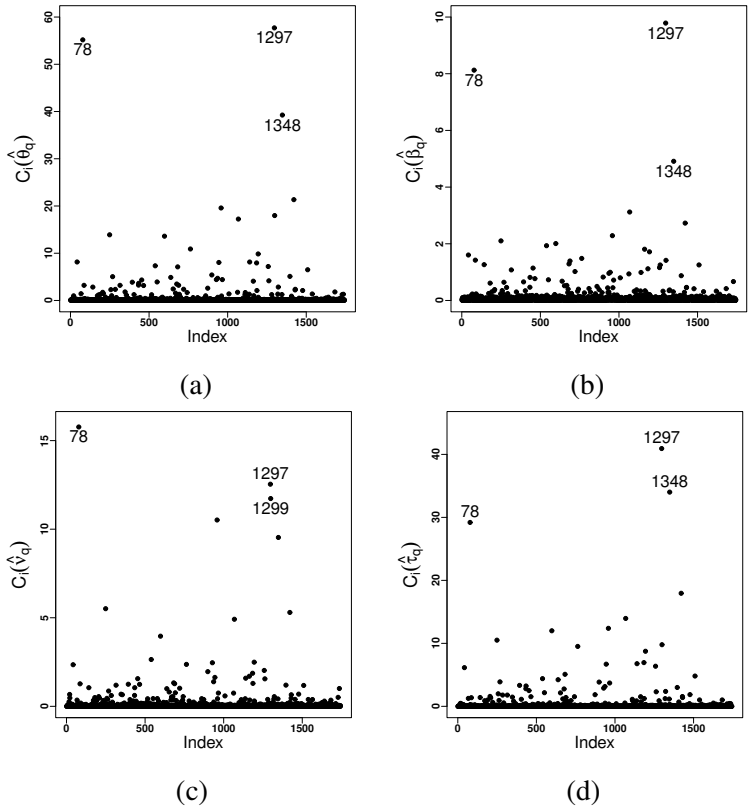

Figure 15 – Index plots of C_i for $\boldsymbol{\tau}_q$ under skewness parameter perturbation, using NHANES dataset with the RPMOG model and $q = 0.9$.

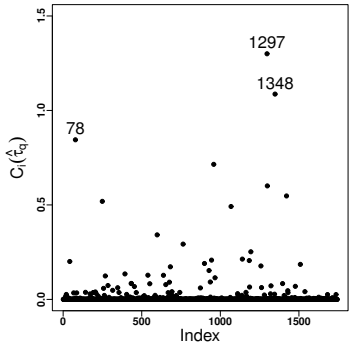

Table 7 – Classification of overweight, obesity class, and associated diseases risk according to BMI, waist circumference, and gender for the potential influential observations.

Observation	Gender	BMI (in kg/m^2)	Waist (in cm)	Classification of overweight	Obesity class	Disease risk
78	Male	24.09	95.2	Normal	-	-
264	Female	48.45	115.8	Extreme obesity	III	Extremely high
1267	Female	71.72	132.3	Extreme obesity	III	Extremely high
1297	Female	25.87	102.3	Overweight	-	High
1299	Male	23.33	101.8	Normal	-	-
1348	Female	19.69	81.8	Normal	-	-
1425	Male	57.93	147.5	Extreme obesity	III	Extremely high

3.2.5 Confirmatory analysis

Now, a confirmatory analysis is realized by refitting the model (3.2) without the potentially influential observations to assess the impact on the estimates of parameters β_{1q}, β_{2q}, β_{3q}, ν_{1q}, ν_{3q}, τ_{1q} and τ_{2q}. The values presented in Table 8 correspond to the changes relative percentages in the estimates, asymptotic standard errors and p-values when we eliminate an observation or the set of all observations, denoted by I. From the results, we observe that the largest percentage variations in the estimates and standard errors occur when we eliminate observations #1297, #1348 and all simultaneously. However, those variations produce no change in inferences.

Table 8 – Percentage relative changes in the estimates and standard errors of the RPMOG model considering $q = 0.9$.

I		β_{1q}	β_{2q}	β_{3q}	ν_{1q}	ν_{3q}	τ_{1q}	τ_{2q}
78	Estimate	5.523	0.155	0.776	0.117	3.609	8.869	7.003
	SE	0.188	0.167	0.572	1.207	1.577	1.742	0.168
	p-value	0.017	< 0.001	< 0.001	< 0.001	< 0.001	< 0.001	< 0.001
264	Estimate	0.938	0.057	0.764	2.324	0.124	1.726	0.003
	SE	0.303	0.269	0.407	0.331	0.067	0.106	0.242
	p-value	0.011	< 0.001	< 0.001	< 0.001	< 0.001	< 0.001	< 0.001
1267	Estimate	1.465	0.098	0.999	8.673	0.496	7.210	1.999
	SE	1.081	0.873	1.504	2.026	0.378	0.179	1.826
	p-value	0.012	< 0.001	< 0.001	< 0.001	< 0.001	< 0.001	< 0.001
1297	Estimate	6.530	0.233	0.103	6.821	0.783	7.492	11.336
	SE	0.732	1.145	1.185	2.435	1.411	0.675	5.458
	p-value	0.019	< 0.001	< 0.001	< 0.001	< 0.001	< 0.001	< 0.001
1299	Estimate	6.173	0.101	1.367	8.244	3.110	7.213	0.031
	SE	0.771	0.555	1.029	1.127	0.251	1.234	2.251
	p-value	0.008	< 0.001	< 0.001	< 0.001	< 0.001	< 0.001	< 0.001
1348	Estimate	1.583	0.043	0.811	5.668	0.260	4.264	11.100
	SE	0.260	0.205	0.983	1.450	1.177	0.287	4.031
	p-value	0.010	< 0.001	< 0.001	< 0.001	< 0.001	< 0.001	< 0.001
1425	Estimate	1.894	0.106	0.511	2.821	0.013	1.278	1.820
	SE	0.366	0.330	0.455	0.335	0.119	0.096	0.419
	p-value	0.010	< 0.001	< 0.001	< 0.001	< 0.001	< 0.001	< 0.001
All	Estimate	13.992	0.110	0.190	8.288	1.473	6.997	6.254
	SE	1.489	0.583	0.940	0.422	0.629	1.848	5.532
	p-value	0.027	< 0.001	< 0.001	< 0.001	< 0.001	< 0.001	< 0.001

3.3 Final comments

This chapter presents simulation studies to assess the behavior of the ML estimators in the RPMON, RPMOG and RPMOT models in small, medium and large samples. In the R language, we use the RS algorithm from the *gamlss* package to obtain the estimates and asymptotic standard errors of the parameters. The studies show that the behavior of the parameters is consistent in the three models. Nonetheless, it has been observed that there exists a significant variance in the estimates (in small and medium samples) of the parameters associated with the intercept of quantile and scale, as well as the parameters associated with the discrete variable of skewness. Also, the estimators present a reasonable asymptotic convergence to normality in the three models. However, the RPMOT model requires the largest sample size for this convergence compared to other models.

Also in this chapter, we illustrate the applicability of RPMO models to a dataset in the area of health and nutrition. For this reason, the fits of the RPMO family and the SKD class were compared. The results indicated that the RPMOG model has a better fit to explain the quantiles, scale and skewness of the BMI. Then, the outliers and influential observations were detected by using the residuals and measures of global and local influence. In practical terms, these analyses allow us to identify those people who are at extremely high risk of dangerous diseases such as cardiovascular diseases. Finally, we note that the RPMOG model shows robustness to outliers and influential observations in a dataset that presents positive skewness and high kurtosis.

CHAPTER

4

PARTIALLY LINEAR QUANTILE REGRESSION MODEL

This chapter extends the QR model formulated in Chapter 2. This extension involves incorporating a nonparametric function in an additive form into the systematic component of the parameter associated with the quantile. The purpose is to enhance the model's flexibility in capturing the nonlinear effects of a covariate on the quantiles of the response variable. We then derive the expressions for the penalized score vector and the penalized observed information matrix. Additionally, we determine the effective degrees of freedom required for model selection.

Furthermore, we introduce the following measures for global diagnostic: generalized Cook's distance and penalized likelihood displacement. Subsequently, we present the expressions for normalized quantile residuals, generalized Cox-Snell residuals and martingale-type residuals. Finally, three different schemes of perturbation are developed for the models.

4.1 Partially linear quantile regression model

This section presents the partially linear QR (PLQR) model for the RPMO family of distributions.

Let $Y_1,\ldots,Y_n$ be independent random variables such that $Y_i \sim \text{RPMO}(\xi_{iq},\sigma_{iq},\alpha_{iq},f_0)$ for $i=1,\ldots,n$, $q\in(0,1)$ fixed and $\boldsymbol{y}=(y_1,\ldots,y_n)^\top$ be a vector of observed responses of dimension $(n\times 1)$. Then, the q-quantile ξ_{iq}, scale σ_{iq} and skewness α_{iq} for the PLQR model under the RPMO distributions satisfy the following functional relations

$$\xi_{iq}=\eta_{1iq}=\mathbf{x}_{1i}^\top\boldsymbol{\beta}_q+s_q(z_i),\quad \log(\sigma_{iq})=\eta_{2iq}=\mathbf{x}_{2i}^\top\boldsymbol{\nu}_q\quad\text{and}\quad \log(\alpha_{iq})=\eta_{3iq}=\mathbf{x}_{3i}^\top\boldsymbol{\tau}_q,\quad (4.1)$$

where $\boldsymbol{\beta}_q=(\beta_{1q},\ldots,\beta_{t_1q})^\top$, $\boldsymbol{\nu}_q=(\nu_{1q},\ldots,\nu_{rq})^\top$ and $\boldsymbol{\tau}_q=(\tau_{1q},\ldots,\tau_{mq})^\top$ are vectors of unknown regression coefficients assumed functionally independent, $s_q(z_i)$ is a continuous smooth function of the observed values z_i; η_{1iq}, η_{2iq} and η_{3iq} are the linear predictors; and $\mathbf{x}_{1i}=$

$(\mathbf{x}_{1i1},\ldots,\mathbf{x}_{1it_1})^\top$, $\mathbf{x}_{2i}=(\mathbf{x}_{2i1},\ldots,\mathbf{x}_{2ir})^\top$ and $\mathbf{x}_{3i}=(\mathbf{x}_{3i1},\ldots,\mathbf{x}_{3im})^\top$ are observations on t_1, r and m known regressors. In model (4.1), we consider the $\boldsymbol{\beta}_q$ vector without an intercept coefficient. Note that when $s_q(z_i)=0$, the model (4.1) is reduced to the linear QR model presented in Chapter 2. Finally, if $\boldsymbol{\beta}_q=\mathbf{0}$, model (4.1) will be referred to as the nonparametric QR model, where $\mathbf{0}$ is a vector of zeros with dimension $(t_1\times 1)$.

Similarly to Cardozo, Paula and Vanegas (2022), we will assume that the smooth function can be approximated by B-splines (BOOR, 1978), i.e. $s_q(z)=\sum_{j=1}^{t_2}N_{j,k}(z)\gamma_j$, where

$$N_{j,0}(z)=\begin{cases}1 & z_j^0\leq z<z_{(j+1)}^0\\ 0 & \text{otherwise}\end{cases}$$

and

$$N_{j,k}(z)=\varpi_{j,k}(z)N_{j,(k-1)}(z)+[1-\varpi_{(j+1),k}(z)]N_{(j+1),(k-1)}(z)$$

$\varpi_{j,k}(z)=(z-z_j^0)/(z_{(j+k)}^0-z_j^0)$, with $N_{j,k}(z)$ denotes the B-spline basis functions of degree k and γ_j are coefficients to be estimated, while $m_1=t_2+k+1$ denotes the number of internal knots, namely $a<z_1^0<\ldots<z_{m_1}^0<b$, for $j=1,\ldots,t_2$ and $k=1,2,3\ldots$. So, following the notation of Cardozo, Paula and Vanegas (2022), we consider $k=3$ (cubic B-splines) and simplify the notation $s_q(z)=\sum_{j=1}^{t_2}N_j(z)\gamma_j$ with $N_j(z)=N_{j,3}(z)$.

Consequently, the model (4.1) can be written in matrix form as follows:

$$\boldsymbol{\xi}_q=\boldsymbol{\eta}_{1q}=\mathbf{X}_1\boldsymbol{\beta}_q+\mathbf{N}\boldsymbol{\gamma}_q,\quad \log(\boldsymbol{\sigma}_q)=\boldsymbol{\eta}_{2q}=\mathbf{X}_2\boldsymbol{\nu}_q \text{ and } \quad \log(\boldsymbol{\alpha}_q)=\boldsymbol{\eta}_{3q}=\mathbf{X}_3\boldsymbol{\tau}_q, \tag{4.2}$$

where $\mathbf{X}_1=(\mathbf{x}_{11}^\top,\ldots,\mathbf{x}_{1n}^\top)^\top$, $\mathbf{X}_2=(\mathbf{x}_{21}^\top,\ldots,\mathbf{x}_{2n}^\top)^\top$ and $\mathbf{X}_3=(\mathbf{x}_{31}^\top,\ldots,\mathbf{x}_{3n}^\top)^\top$ are the design matrices that incorporate the linear additive terms in the model, $\mathbf{N}$ is a B-spline basis matrix of dimension $(n\times t_2)$ and $\boldsymbol{\gamma}_q$ is an $(t_2\times 1)$ vector of B-spline parameters; $\boldsymbol{\eta}_{1q}=(\eta_{11q},\ldots,\eta_{1nq})^\top$, $\boldsymbol{\eta}_{2q}=(\eta_{21q},\ldots,\eta_{2nq})^\top$ and $\boldsymbol{\eta}_{3q}=(\eta_{31q},\ldots,\eta_{3nq})^\top$ are the predictors of the vectors $\boldsymbol{\xi}_q$, $\boldsymbol{\sigma}_q$ and $\boldsymbol{\alpha}_q$ of dimension $(n\times 1)$.

4.2 Inference

This section is devoted to inferences on the parameters of the PLQR models. Specifically, we derive the penalized score vector to describe the RS algorithm. Next, we calculate the expression of the penalized observed information matrix to obtain confidence intervals and confidence bands. Finally, we present the selection criteria of the models, including total effective degrees of freedom.

4.2.1 Penalized score vector

Let $\boldsymbol{\theta}_q=(\boldsymbol{\beta}_q^\top,\boldsymbol{\gamma}_q^\top,\boldsymbol{\nu}_q^\top,\boldsymbol{\tau}_q^\top)^\top$ be the vector of parameters to be estimated. Then, the log-likelihood function that satisfies the functional relations given in Equation (4.1) can be

expressed as

$$\ell(\boldsymbol{\theta}_q) = \sum_{i=1}^{n} \ell_i(\xi_{iq}, \sigma_{iq}, \alpha_{iq}), \text{ where} \tag{4.3}$$
$$\ell_i(\xi_{iq}, \sigma_{iq}, \alpha_{iq}) = \log(\alpha_{iq}) + \log(f_0(u_{iq})) - \log(\sigma_{iq}) - 2\log(\alpha_{iq} + (1-\alpha_{iq})F_0(u_{iq})),$$
$$u_{iq} = (y_{iq} - \xi_{iq})/\sigma_{iq} + F_0^{-1}(\alpha_{iq} q/(1 + q\alpha_{iq} - q)),$$

for $i = 1, \ldots, n$ and $q \in (0,1)$ fixed. The direct maximization of $\ell(\boldsymbol{\theta}_q)$ may cause overfitting and non identification of $\boldsymbol{\gamma}_q$. To solve this problem, we consider as a penalty the integral of square of the second derivative of $s_q(z)$ (CARDOZO; PAULA; VANEGAS, 2022), which leads to the following penalized log-likelihood function

$$\ell_p(\boldsymbol{\theta}_q, \lambda_q) = \ell(\boldsymbol{\theta}_q) - 0.5\lambda_q \int_a^b [s_q''(z)]^2 dz, \tag{4.4}$$

where $\lambda_q > 0$ is the smoothing parameter. If λ_q tends to 0, it implies data interpolation, while if λ_q tends to infinity, it leads to a linear approximation of $s_q(z)$.

According to Wood (2017) the penalization in Equation (4.4) can be written as

$$\int_a^b [s_q''(z)]^2 dz = \boldsymbol{\gamma}_q^\top \mathbf{K}_q \boldsymbol{\gamma}_q,$$

where $\mathbf{K}_q$ is a positive semidefinite penalty matrix of dimension $(t_2 \times t_2)$. Eilers and Marx (1996) showed that the integrated of the square of the k_1-th derivative of $s_q(z)$ can be well approximated by a penalty on finite differences of the coefficients $\boldsymbol{\gamma}_q$ with less computational effort, that is,

$$\int_a^b [s_q''(z)]^{k_1} dz \cong \sum_{j=k_1+1}^{t_2} \left[\nabla^{k_1} \gamma_j\right]^2 = \boldsymbol{\gamma}_q^\top (\boldsymbol{\nabla}^{k_1})^\top \boldsymbol{\nabla}^{k_1} \boldsymbol{\gamma}_q,$$

where $\boldsymbol{\nabla}^{k_1}$ is a $(t_2 - k_1) \times t_2$ difference matrix of order k_1. This approach is named P-spline smoothing (CARDOZO; PAULA; VANEGAS, 2022). Consequently, the penalized log-likelihood has the form

$$\ell_p(\boldsymbol{\theta}_q, \lambda_q) = \ell(\boldsymbol{\theta}_q) - 0.5\lambda_q \boldsymbol{\gamma}_q^\top \mathbf{K}_q \boldsymbol{\gamma}_q. \tag{4.5}$$

Considering $q \in (0,1)$ fixed, the $(t_1 + t_2 + r + m) \times 1$ penalized score vector is expressed as

$$\mathbf{U}_p(\boldsymbol{\theta}_q) = \frac{\partial \ell_p(\boldsymbol{\theta}_q, \lambda_q)}{\partial \boldsymbol{\theta}_q} = (\mathbf{U}_{\boldsymbol{\beta}_q}^\top, \mathbf{U}_{\boldsymbol{\gamma}_q}^\top, \mathbf{U}_{\boldsymbol{\nu}_q}^\top, \mathbf{U}_{\boldsymbol{\tau}_q}^\top)^\top,$$

where $\partial \ell_p(\boldsymbol{\theta}_q, \lambda_q)/\partial \boldsymbol{\theta}_q$ represents the first partial derivative of the penalized log-likelihood function associated with the vector $\boldsymbol{\theta}_q$. In particular, the components of the penalized score

vector are given by the following equations

$$\mathbf{U}_{\boldsymbol{\beta}_q}(\boldsymbol{\theta}_q) = \frac{\partial \ell_p(\boldsymbol{\theta}_q, \lambda_q)}{\partial \boldsymbol{\beta}_q} = \mathbf{X}_1^\top \mathbf{W}_1 \mathbf{A}_1, \tag{4.6}$$

$$\mathbf{U}_{\boldsymbol{\gamma}_q}(\boldsymbol{\theta}_q) = \frac{\partial \ell_p(\boldsymbol{\theta}_q, \lambda_q)}{\partial \boldsymbol{\gamma}_q} = \mathbf{N}^\top \mathbf{W}_1 \mathbf{A}_1 - \lambda_q \mathbf{K}_q \boldsymbol{\gamma}_q, \tag{4.7}$$

$$\mathbf{U}_{\boldsymbol{\nu}_q}(\boldsymbol{\theta}_q) = \frac{\partial \ell_p(\boldsymbol{\theta}_q, \lambda_q)}{\partial \boldsymbol{\nu}_q} = \mathbf{X}_2^\top \mathbf{W}_2 \mathbf{A}_2 \text{ and} \tag{4.8}$$

$$\mathbf{U}_{\boldsymbol{\tau}_q}(\boldsymbol{\theta}_q) = \frac{\partial \ell_p(\boldsymbol{\theta}_q, \lambda_q)}{\partial \boldsymbol{\tau}_q} = \mathbf{X}_3^\top \mathbf{W}_3 \mathbf{A}_3, \tag{4.9}$$

with

$$\mathbf{W}_1 = \left[b_{iq}\, \delta_{ij}\right], \qquad \mathbf{W}_2 = \left[e_{iq}\, \delta_{ij}\right], \qquad \mathbf{W}_3 = \left[d_{iq}\, \delta_{ij}\right],$$
$$\mathbf{A}_1 = (\dot{\ell}_{\xi_{1q}}, \ldots, \dot{\ell}_{\xi_{nq}})^\top, \qquad \mathbf{A}_2 = (\dot{\ell}_{\sigma_{1q}}, \ldots, \dot{\ell}_{\sigma_{nq}})^\top \text{ and } \qquad \mathbf{A}_3 = (\dot{\ell}_{\alpha_{1q}}, \ldots, \dot{\ell}_{\alpha_{nq}})^\top,$$

where

$$b_{iq} = \frac{\partial \xi_{iq}}{\partial \eta_{1iq}} = 1, \qquad e_{iq} = \frac{\partial \sigma_{iq}}{\partial \eta_{2iq}} = \exp\left(\eta_{2iq}\right), \qquad d_{iq} = \frac{\partial \alpha_{iq}}{\partial \eta_{3iq}} = \exp\left(\eta_{3iq}\right),$$

δ_{ij} is the Kronecker delta with $i, j = 1, \ldots, n$. Finally, the elements of vectors $\mathbf{A}_1$, $\mathbf{A}_2$ and $\mathbf{A}_3$ are as follows

$$\begin{aligned}
\dot{\ell}_{\xi_{iq}} &= \frac{\partial \ell_i(\xi_{iq}, \sigma_{iq}, \alpha_{iq})}{\partial \xi_{iq}} \\
&= 2\psi_{1iq}\left[\frac{f_0(u_{iq})(1-\alpha_{iq})}{\alpha_{iq} + (1-\alpha_{iq})F_0(u_{iq})}\right] - \psi_{1iq}\left[\frac{f_0'(u_{iq})}{f_0(u_{iq})}\right], \qquad (4.10) \\
\dot{\ell}_{\sigma_{iq}} &= \frac{\partial \ell_i(\xi_{iq}, \sigma_{iq}, \alpha_{iq})}{\partial \sigma_{iq}} \\
&= 2\psi_{1iq}\psi_{2iq}\left[\frac{f_0(u_{iq})(1-\alpha_{iq})}{\alpha_{iq} + (1-\alpha_{iq})F_0(u_{iq})}\right] - \psi_{1iq} - \psi_{1iq}\psi_{2iq}\left[\frac{f_0'(u_{iq})}{f_0(u_{iq})}\right] \qquad (4.11)
\end{aligned}$$

and

$$\begin{aligned}
\dot{\ell}_{\alpha_{iq}} &= \frac{\partial \ell_i(\xi_{iq}, \sigma_{iq}, \alpha_{iq})}{\partial \alpha_{iq}} \\
&= \psi_{3iq} + u_{\alpha_{iq}}\left[\frac{f_0'(u_{iq})}{f_0(u_{iq})}\right] - 2\left[\frac{1 - F_0(u_{iq}) + (1-\alpha_{iq})f_0(u_{iq})u_{\alpha_{iq}}}{\alpha_{iq} + (1-\alpha_{iq})F_0(u_{iq})}\right], \qquad (4.12)
\end{aligned}$$

where

$$\psi_{1iq} = \frac{1}{\sigma_{iq}}, \qquad \psi_{2iq} = \frac{(y_i - \xi_{iq})}{\sigma_{iq}}, \qquad \psi_{3iq} = \frac{1}{\alpha_{iq}}, \qquad u_{\alpha_{iq}} = \frac{\Psi_0 q(1-q)}{(1 + q\alpha_{iq} - q)^2}$$

and

$$\Psi_0 \;=\; 1/f_0(F_0^{-1}(\alpha_{iq}q/(1+q\alpha_{iq}-q))) \text{ for } i = 1, \ldots, n.$$

The expressions $f_0(u_{iq})$ and $f_0'(u_{iq})$ presented in Equations (4.10)-(4.12) are the same as those shown in Table 2 of Chapter 2.

Note that in Equations (4.6)-(4.9), the penalized ML estimators $\boldsymbol{\beta}_q$, $\boldsymbol{\gamma}_q$, $\boldsymbol{\nu}_q$ and $\boldsymbol{\tau}_q$ do not have a closed form. Therefore, the penalized ML estimates denoted by $\widehat{\boldsymbol{\beta}}_q$, $\widehat{\boldsymbol{\gamma}}_q$, $\widehat{\boldsymbol{\nu}}_q$ and $\widehat{\boldsymbol{\tau}}_q$ can be obtained by numerical maximization of the penalized log-likelihood function. Thus, we adopt the RS algorithm presented by Rigby and Stasinopoulos (2014) in the R (R Core Team, 2022) programming language. It is important to highlight that the algorithm also deals with the problem of estimating the smoothing parameter λ_q at a low computational cost.

4.2.2 RS algorithm

In this section, we present an automatic method for obtaining the penalized ML estimate of $\boldsymbol{\theta}_q$ and addressing the problem of estimating the smoothing parameter λ_q. The RS algorithm fits $\boldsymbol{\xi}_q$, $\boldsymbol{\sigma}_q$ and $\boldsymbol{\tau}_q$ in one cycle, also known as an outer cycle, until convergence. Within the $\boldsymbol{\xi}_q$ parameter fitting, there is a fitting of the linear terms, followed by a fitting of the smoothing terms. When this refit converges the iterative working variable and iterative weights are updated. This process is referred to as the backfitting algorithm. Then, within the remaining two parameters, the linear terms are fitted, and when they converge, the iterative working variable and iterative weights are updated.

Similar to Section 2.4.1, we will describe the quantities needed to develop the RS algorithm for PLQR models under RPMO distributions. These quantities are as follows:

- the score functions

$$\boldsymbol{\Gamma}_{1q} = (\dot{\ell}_{\xi_{1q}} b_{1q}, \ldots, \dot{\ell}_{\xi_{nq}} b_{nq})^\top, \; \boldsymbol{\Gamma}_{2q} = (\dot{\ell}_{\sigma_{1q}} e_{1q}, \ldots, \dot{\ell}_{\sigma_{nq}} e_{nq})^\top \text{ and } \boldsymbol{\Gamma}_{3q} = (\dot{\ell}_{\alpha_{1q}} d_{1q}, \ldots, \dot{\ell}_{\alpha_{nq}} d_{nq})^\top;$$

- the diagonal matrices of iterative weights

$$\mathbf{W}_{11} = \text{diag}(\boldsymbol{\Gamma}_{1q} \circ \boldsymbol{\Gamma}_{1q}), \quad \mathbf{W}_{22} = \text{diag}(\boldsymbol{\Gamma}_{2q} \circ \boldsymbol{\Gamma}_{2q}) \quad \text{and} \quad \mathbf{W}_{33} = \text{diag}(\boldsymbol{\Gamma}_{3q} \circ \boldsymbol{\Gamma}_{3q});$$

- and the adjusted dependent variables

$$\boldsymbol{\rho}_{1q} = \boldsymbol{\eta}_{1q} + \mathbf{W}_{11}^{-1} \boldsymbol{\Gamma}_{1q}, \quad \boldsymbol{\rho}_{2q} = \boldsymbol{\eta}_{2q} + \mathbf{W}_{22}^{-1} \boldsymbol{\Gamma}_{2q} \quad \text{and} \quad \boldsymbol{\rho}_{3q} = \boldsymbol{\eta}_{3q} + \mathbf{W}_{33}^{-1} \boldsymbol{\Gamma}_{3q},$$

where

$$\boldsymbol{\eta}_{1q} = \mathbf{X}_1 \boldsymbol{\beta}_q + \mathbf{N} \boldsymbol{\gamma}_q, \qquad \boldsymbol{\eta}_{2q} = \exp\left(\mathbf{X}_2 \boldsymbol{\nu}_q\right) \quad \text{and} \qquad \boldsymbol{\eta}_{3q} = \exp\left(\mathbf{X}_3 \boldsymbol{\tau}_q\right).$$

In the backfitting algorithm, specifically when fitting $\boldsymbol{\gamma}_q$, we assume the following internal random effects model: $\mathbf{e} \sim \text{N}_n(\mathbf{0}, \sigma_{\mathbf{e}}^2 \mathbf{W}_{11}^{-1})$, $\mathbf{b}_1 = \nabla^{k_1} \boldsymbol{\gamma}_q \sim \text{N}_{t_2 - k_1}(\mathbf{0}, \mathbf{D}_1)$ where $\mathbf{D}_1 = \sigma_{\mathbf{b}_1}^2 \mathbf{I}_{t_2 - k_1}$ and $\nabla^{k_1} \boldsymbol{\gamma}_q$ is a difference matrix of order k_1. The objective is to represent the smoothing term in the quantiles as a random effects term and then estimate the parameters using a penalized

quasi-likelihood (PQL) estimation. This procedure is studied in theoretical and computational aspects by Rigby and Stasinopoulos (2014) in the context of GAMLSS models.

Let j represent the iteration index of the outer cycle and i represent the iteration index of the inner cycle. The algorithm is described as follows:

Step 1: Initialize fitted values for distributional parameter vectors of length n: $\boldsymbol{\xi}_q^{(1,1)}$, $\boldsymbol{\sigma}_q^{(1,1)}$ and $\boldsymbol{\tau}_q^{(1,1)}$, respectively. In this context, consider the outputs of the RPMON, RPMOT and RPMOG PLQR models using the *gamlss* function, taking into account the *pb* function. Then, evaluate the initial linear predictors $\boldsymbol{\eta}_{1q}^{(1,1)} = \boldsymbol{\xi}_q^{(1,1)}$, $\boldsymbol{\eta}_{2q}^{(1,1)} = \exp\left(\boldsymbol{\sigma}_q^{(1,1)}\right)$ and $\boldsymbol{\eta}_{3q}^{(1,1)} = \exp\left(\boldsymbol{\tau}_q^{(1,1)}\right)$.

Step 2: Start the outer cycle $j = 1, 2, \ldots$ until convergence.

(a) Start the inner cycle $i = 1, \ldots, n$ until convergence.

(i) Evaluate the current $\boldsymbol{\Gamma}_{1q}^{(j,i)}$, $\mathbf{W}_{11}^{(j,i)}$ and $\boldsymbol{\rho}_{1q}^{(j,i)}$.

(ii) Compute $\boldsymbol{\varepsilon}^{(j,i)} = \boldsymbol{\rho}_{1q}^{(j,i)} - \mathbf{N}\boldsymbol{\gamma}_q^{(j,i)}$. Then, regress the current $\boldsymbol{\varepsilon}^{(j,i)}$ against design matrix $\mathbf{X}_1$ using iterative weights $\mathbf{W}_{11}^{(j,i)}$ to obtain the updated parameters $\boldsymbol{\beta}_q^{(j,i)}$.

(iii) Compute $\boldsymbol{\varepsilon}^{(j,i)} = \boldsymbol{\rho}_{1q}^{(j,i)} - \mathbf{X}_1\boldsymbol{\beta}_q^{(j,i)}$.

(iv) Perform the following calculations until the convergence of λ_q and $\boldsymbol{\gamma}_q$:

(1) $\boldsymbol{\gamma}^{(j,i)} = (\mathbf{N}^\top \mathbf{W}_{11}^{(j,i)} \mathbf{N} + \lambda_q \mathbf{K}_q)^{-1} \mathbf{N}^\top \mathbf{W}_{11}^{(j,i)} \boldsymbol{\varepsilon}^{(j,i)}$

(2) $\upsilon = \mathrm{tr}((\mathbf{N}^\top \mathbf{W}_{11}^{(j,i)} \mathbf{N} + \lambda_q \mathbf{K}_q)^{-1} \mathbf{N}^\top \mathbf{W}_{11}^{(j,i)} \mathbf{N})$

(3) $\upsilon_1 = \mathrm{tr}((\mathbf{N}^\top \mathbf{W}_{11}^{(j,i)} \mathbf{N} + \lambda_q \mathbf{K}_q)^{-1} \lambda_q \mathbf{K}_q)$

(4) $\widehat{\mathbf{e}} = \boldsymbol{\varepsilon}^{(j,i)} - \mathbf{N}\boldsymbol{\gamma}_q^{(j,i)}$

(5) $\widehat{\sigma}_e^2 = \frac{1}{(n-\upsilon)} \widehat{\mathbf{e}}^\top \mathbf{W}_{11}^{(j,i)} \widehat{\mathbf{e}}$

(6) $\widehat{\sigma}_{b_1}^2 = \frac{1}{(t_2 - \upsilon_1 - k_1)} \widehat{\boldsymbol{\gamma}}_q^\top \mathbf{K}_q \widehat{\boldsymbol{\gamma}}_q$

(7) $\widehat{\lambda}_q = \widehat{\sigma}_e^2 / \widehat{\sigma}_{b_1}^2$

(b) End the inner cycle on convergence of $\boldsymbol{\beta}_q^{(j,\cdot)}$ and $\boldsymbol{\gamma}_q^{(j,\cdot)}$. Set $\boldsymbol{\beta}_q^{(j+1,1)} = \boldsymbol{\beta}_q^{(j,\cdot)}$, $\boldsymbol{\gamma}_q^{(j+1,1)} = \boldsymbol{\gamma}_q^{(j,\cdot)}$, $\boldsymbol{\eta}_{1q}^{(j+1,1)} = \boldsymbol{\eta}_{1q}^{(j,\cdot)}$ and $\boldsymbol{\xi}_q^{(j+1,1)} = \boldsymbol{\xi}_q^{(j,\cdot)}$; otherwise update i and continue the inner cycle.

(a') Start the inner cycle $i = 1, \ldots, n$ until convergence.

(i) Evaluate the current $\boldsymbol{\Gamma}_{2q}^{(j,i)}$, $\mathbf{W}_{22}^{(j,i)}$ and $\boldsymbol{\rho}_{2q}^{(j,i)}$.

(ii) Regress the current $\boldsymbol{\rho}_{2q}^{(j,i)}$ against design matrix $\mathbf{X}_2$ using iterative weights $\mathbf{W}_{22}^{(j,i)}$ to obtain the updated parameters $\boldsymbol{\nu}_q^{(j,i)}$.

(b') End the inner cycle on convergence of $\boldsymbol{\nu}_q^{(j,\cdot)}$ and set $\boldsymbol{\nu}_q^{(j+1,1)} = \boldsymbol{\nu}_q^{(j,\cdot)}$, $\boldsymbol{\eta}_{2q}^{(j+1,1)} = \boldsymbol{\eta}_{2q}^{(j,\cdot)}$ and $\boldsymbol{\sigma}_q^{(j+1,1)} = \boldsymbol{\sigma}_q^{(j,\cdot)}$; otherwise update i and continue inner cycle.

(a") Start the inner cycle $i = 1, \ldots, n$ until convergence.

(i) Evaluate the current $\boldsymbol{\Gamma}_{3q}^{(j,i)}$, $\mathbf{W}_{33}^{(j,i)}$ and $\boldsymbol{\rho}_{3q}^{(j,i)}$.

(ii) Regress the current $\boldsymbol{\rho}_{3q}^{(j,i)}$ against $\mathbf{X}_3$ using iterative weights $\mathbf{W}_{33}^{(j,i)}$ to obtain the updated parameters $\boldsymbol{\tau}_q^{(j,i)}$.

(b") End the inner cycle on convergence of $\boldsymbol{\tau}_q^{(j,\cdot)}$ and set $\boldsymbol{\tau}_q^{(j+1,1)} = \boldsymbol{\tau}_q^{(j,\cdot)}$, $\boldsymbol{\eta}_{3q}^{(j+1,1)} = \boldsymbol{\eta}_{3q}^{(j,\cdot)}$ and $\boldsymbol{\alpha}_q^{(j+1,1)} = \boldsymbol{\alpha}_q^{(j,\cdot)}$; otherwise update i and continue inner cycle.

Step 3: End the outer cycle if the change in the log-likelihood is less than 0.001; otherwise, update j and continue the outer cycle.

4.2.3 Penalized observed information matrix

Let $q \in (0,1)$ fixed, the penalized observed information matrix of dimension $(t_1+t_2+r+m)\times(t_1+t_2+r+m)$ associated with $\widehat{\boldsymbol{\theta}}_q = (\widehat{\boldsymbol{\beta}}_q^\top, \widehat{\boldsymbol{\gamma}}_q^\top, \widehat{\boldsymbol{\nu}}_q^\top, \widehat{\boldsymbol{\tau}}_q^\top)^\top$ is expressed as

$$\ddot{\ell}_p(\widehat{\boldsymbol{\theta}}_q, \widehat{\lambda}_q) = -\frac{\partial^2 \ell_p(\boldsymbol{\theta}_q, \lambda_q)}{\partial \boldsymbol{\theta}_q \partial \boldsymbol{\theta}_q^\top}\Big|_{\boldsymbol{\theta}_q=\widehat{\boldsymbol{\theta}}_q, \lambda_q=\widehat{\lambda}_q} = \begin{bmatrix} -\ddot{\ell}_{\boldsymbol{\beta}_q\boldsymbol{\beta}_q} & -\ddot{\ell}_{\boldsymbol{\beta}_q\boldsymbol{\gamma}_q} & -\ddot{\ell}_{\boldsymbol{\beta}_q\boldsymbol{\nu}_q} & -\ddot{\ell}_{\boldsymbol{\beta}_q\boldsymbol{\tau}_q} \\ & -\ddot{\ell}_{\boldsymbol{\gamma}_q\boldsymbol{\gamma}_q} & -\ddot{\ell}_{\boldsymbol{\gamma}_q\boldsymbol{\nu}_q} & -\ddot{\ell}_{\boldsymbol{\gamma}_q\boldsymbol{\tau}_q} \\ & & -\ddot{\ell}_{\boldsymbol{\nu}_q\boldsymbol{\nu}_q} & -\ddot{\ell}_{\boldsymbol{\nu}_q\boldsymbol{\tau}_q} \\ & & & -\ddot{\ell}_{\boldsymbol{\tau}_q\boldsymbol{\tau}_q} \end{bmatrix}, \quad (4.13)$$

where $\partial^2 \ell_p(\boldsymbol{\theta}_q, \lambda_q)/\partial \boldsymbol{\theta}_q \partial \boldsymbol{\theta}_q^\top$ represents the partial derivatives of the penalized log-likelihood function. The elements of the penalized observed information matrix are the following

$$\begin{aligned}
\ddot{\ell}_{\boldsymbol{\beta}_q\boldsymbol{\beta}_q} &= \frac{\partial^2 \ell_p(\boldsymbol{\theta}_q, \lambda_q)}{\partial \boldsymbol{\beta}_q \partial \boldsymbol{\beta}_q^\top}\Big|_{\boldsymbol{\theta}_q=\widehat{\boldsymbol{\theta}}_q, \lambda_q=\widehat{\lambda}_q} = \mathbf{X}_1^\top \mathbf{W}_4 \mathbf{X}_1, \\
\ddot{\ell}_{\boldsymbol{\beta}_q\boldsymbol{\gamma}_q} &= \frac{\partial^2 \ell_p(\boldsymbol{\theta}_q, \lambda_q)}{\partial \boldsymbol{\beta}_q \partial \boldsymbol{\gamma}_q^\top}\Big|_{\boldsymbol{\theta}_q=\widehat{\boldsymbol{\theta}}_q, \lambda_q=\widehat{\lambda}_q} = \mathbf{X}_1^\top \mathbf{W}_4 \mathbf{N}, \\
\ddot{\ell}_{\boldsymbol{\beta}_q\boldsymbol{\nu}_q} &= \frac{\partial^2 \ell_p(\boldsymbol{\theta}_q, \lambda_q)}{\partial \boldsymbol{\beta}_q \partial \boldsymbol{\nu}_q^\top}\Big|_{\boldsymbol{\theta}_q=\widehat{\boldsymbol{\theta}}_q, \lambda_q=\widehat{\lambda}_q} = \mathbf{X}_1^\top \mathbf{W}_5 \mathbf{X}_2, \\
\ddot{\ell}_{\boldsymbol{\beta}_q\boldsymbol{\tau}_q} &= \frac{\partial^2 \ell_p(\boldsymbol{\theta}_q, \lambda_q)}{\partial \boldsymbol{\beta}_q \partial \boldsymbol{\tau}_q^\top}\Big|_{\boldsymbol{\theta}_q=\widehat{\boldsymbol{\theta}}_q, \lambda_q=\widehat{\lambda}_q} = \mathbf{X}_1^\top \mathbf{W}_6 \mathbf{X}_3, \\
\ddot{\ell}_{\boldsymbol{\gamma}_q\boldsymbol{\gamma}_q} &= \frac{\partial^2 \ell_p(\boldsymbol{\theta}_q, \lambda_q)}{\partial \boldsymbol{\gamma}_q \partial \boldsymbol{\gamma}_q^\top}\Big|_{\boldsymbol{\theta}_q=\widehat{\boldsymbol{\theta}}_q, \lambda_q=\widehat{\lambda}_q} = \mathbf{N}^\top \mathbf{W}_4 \mathbf{N} - \lambda_q \mathbf{K}_q, \\
\ddot{\ell}_{\boldsymbol{\gamma}_q\boldsymbol{\nu}_q} &= \frac{\partial^2 \ell_p(\boldsymbol{\theta}_q, \lambda_q)}{\partial \boldsymbol{\gamma}_q \partial \boldsymbol{\nu}_q^\top}\Big|_{\boldsymbol{\theta}_q=\widehat{\boldsymbol{\theta}}_q, \lambda_q=\widehat{\lambda}_q} = \mathbf{N}^\top \mathbf{W}_5 \mathbf{X}_2,
\end{aligned}$$

$$\ddot{\ell}_{\boldsymbol{\gamma}_q\boldsymbol{\tau}_q} = \frac{\partial^2 \ell_p(\boldsymbol{\theta}_q,\lambda_q)}{\partial \boldsymbol{\gamma}_q \partial \boldsymbol{\tau}_q^\top}\Big|_{\boldsymbol{\theta}_q=\widehat{\boldsymbol{\theta}}_q,\lambda_q=\widehat{\lambda}_q} = \mathbf{N}^\top \mathbf{W}_6 \mathbf{X}_3,$$
$$\ddot{\ell}_{\boldsymbol{\nu}_q\boldsymbol{\nu}_q} = \frac{\partial^2 \ell_p(\boldsymbol{\theta}_q,\lambda_q)}{\partial \boldsymbol{\nu}_q \partial \boldsymbol{\nu}_q^\top}\Big|_{\boldsymbol{\theta}_q=\widehat{\boldsymbol{\theta}}_q,\lambda_q=\widehat{\lambda}_q} = \mathbf{X}_2^\top \mathbf{W}_7 \mathbf{X}_2,$$
$$\ddot{\ell}_{\boldsymbol{\nu}_q\boldsymbol{\tau}_q} = \frac{\partial^2 \ell_p(\boldsymbol{\theta}_q,\lambda_q)}{\partial \boldsymbol{\nu}_q \partial \boldsymbol{\tau}_q^\top}\Big|_{\boldsymbol{\theta}_q=\widehat{\boldsymbol{\theta}}_q,\lambda_q=\widehat{\lambda}_q} = \mathbf{X}_2^\top \mathbf{W}_8 \mathbf{X}_3 \text{ and}$$
$$\ddot{\ell}_{\boldsymbol{\tau}_q\boldsymbol{\tau}_q} = \frac{\partial^2 \ell_p(\boldsymbol{\theta}_q,\lambda_q)}{\partial \boldsymbol{\tau}_q \partial \boldsymbol{\tau}^\top}\Big|_{\boldsymbol{\theta}_q=\widehat{\boldsymbol{\theta}}_q,\lambda_q=\widehat{\lambda}_q} = \mathbf{X}_3^\top \mathbf{W}_9 \mathbf{X}_3,$$

where

$$\mathbf{W}_4 = [(\ddot{\ell}_{\xi_{iq}}\, b_{iq}^2 + \dot{\ell}_{\xi_{iq}}\, b_{iq}\, b'_{iq})\delta_{ij}], \qquad \mathbf{W}_5 = [(\ddot{\ell}_{\xi_{iq}\sigma_{iq}}\, b_{iq}\, e_{iq})\, \delta_{ij}],$$
$$\mathbf{W}_6 = [(\ddot{\ell}_{\xi_{iq}\alpha_{iq}}\, b_{iq}\, d_{iq})\delta_{ij}], \qquad \mathbf{W}_7 = [\big(\ddot{\ell}_{\sigma_{iq}}\, e_{iq}^2 + \dot{\ell}_{\sigma_{iq}}\, e_{iq}\, e'_{iq}\big)\, \delta_{ij}],$$
$$\mathbf{W}_8 = [(\ddot{\ell}_{\sigma_{iq}\alpha_{iq}}\, e_{iq}\, d_{iq})\delta_{ij}], \qquad \mathbf{W}_9 = [(\ddot{\ell}_{\alpha_{iq}}\, d_{iq}^2 + \dot{\ell}_{\alpha_{iq}}\, d_{iq}\, d'_{iq})\delta_{ij}],$$

and

$$b'_{iq} = \frac{\partial b_{iq}}{\partial \xi_{iq}} = 0, \qquad e'_{iq} = \frac{\partial e_{iq}}{\partial \sigma_{iq}} = 1, \qquad d'_{iq} = \frac{\partial d_{iq}}{\partial \alpha_{iq}} = 1,$$

for $i, j = 1, \ldots, n$. Finally, the expressions of the elements $\ddot{\ell}_{\xi_{iq}}$, $\ddot{\ell}_{\xi_{iq}\sigma_{iq}}$, $\ddot{\ell}_{\xi_{iq}\alpha_{iq}}$, $\ddot{\ell}_{\sigma_{iq}}$, $\ddot{\ell}_{\sigma_{iq}\alpha_{iq}}$ and $\ddot{\ell}_{\alpha_{iq}}$ are detailed in Appendix C.

4.2.4 Confidence intervals

Analogously to the parametric case, the variance-covariance matrix of $\widehat{\boldsymbol{\theta}}_q$ can be approximated by the inverse of the penalized Fisher's information matrix (IBACACHE-PULGAR; PAULA; GALEA, 2012). Thus, $\widehat{\text{Var}}_{\text{approx}}(\widehat{\boldsymbol{\theta}}_q) = \mathbb{I}_p^{-1}(\widehat{\boldsymbol{\theta}}_q, \widehat{\lambda}_q)$, where $\mathbb{I}_p(\widehat{\boldsymbol{\theta}}_q, \widehat{\lambda}_q)$ is the penalized Fisher's information matrix.

However, the analytical expression of $\mathbb{I}_p(\widehat{\boldsymbol{\theta}}_q, \widehat{\lambda}_q)$ is not easy to obtain, so we use the penalized observed information matrix for that approximation. In consequence, the asymptotic confidence interval for the j-th element of $\widehat{\boldsymbol{\theta}}_q$, denoted by $\widehat{\theta}_{jq}$, is constructed using the following expression

$$\left(\widehat{\theta}_{jq} - \rho_{\zeta/2}\sqrt{\ddot{\ell}_p^{-1}{}_{jj}(\widehat{\theta}_q, \widehat{\lambda}_q)}, \widehat{\theta}_{jq} + \rho_{\zeta/2}\sqrt{\ddot{\ell}_p^{-1}{}_{jj}(\widehat{\theta}_q, \widehat{\lambda}_q)}\right), \tag{4.14}$$

where $\rho_{\zeta/2}$ represent the quantile of the standard normal distribution leaving, a probability to the right tail with $\zeta/2$ for $0 < \zeta < 1/2$ and $\ddot{\ell}_p^{-1}{}_{jj}(\widehat{\theta}_q, \widehat{\lambda}_q)$ is the j-th element of the main diagonal of $\ddot{\ell}_p^{-1}(\widehat{\boldsymbol{\theta}}_q, \widehat{\lambda}_q)$ for $j = 1, \ldots, (t_1 + t_2 + r + m)$ and $q \in (0,1)$ fixed.

Another interesting statistical inference is the construction of asymptotic confidence bands (CARDOZO; PAULA; VANEGAS, 2022) for the function vector $\mathbf{s}_q(\mathbf{z}) = (s_q(z_1), \ldots, s_q(z_n))^\top$.

These bands, also called pointwise confidence bands (VANEGAS; PAULA, 2016), can be approximated in the following way

$$\left(\mathbf{s}_q(\mathbf{z}) - \rho_{\zeta/2}\ \sqrt{\boldsymbol{\Upsilon}}, \mathbf{s}_q(\mathbf{z}) + \rho_{\zeta/2}\ \sqrt{\boldsymbol{\Upsilon}}\right) \tag{4.15}$$

where $\boldsymbol{\Upsilon}$ is the vector $(n \times 1)$ that contains the elements of the main diagonal of $\mathbf{N}\,\widehat{\text{Var}}_{\text{approx}}(\widehat{\boldsymbol{\gamma}}_q)\,\mathbf{N}^\top$.

4.2.5 Model selection

In this section, we adopt AIC and BIC criteria as well as Rigby and Stasinopoulos (2005) for the selection of PLQR model under RPMO distributions. Therefore, the expressions of the criteria are as follows

$$\text{AIC} = -2\ell(\widehat{\theta}_q) + 2\text{df} \qquad\qquad \text{BIC} = -2\ell(\widehat{\theta}_q) + \log(n)\text{df}$$

where $\ell(\widehat{\boldsymbol{\theta}}_q)$ is described in Equation (4.3), $\text{df} = \text{tr}(\mathbf{A}^{-1}\mathbf{B})$ denotes the total effective degrees of freedom used in the model, and n is the sample size. The matrix $\mathbf{A}$ is defined as

$$\mathbf{A} = \begin{bmatrix} \mathbf{X}_1^\top\mathbf{W}_{11}\mathbf{X}_1 & \mathbf{X}_1^\top\mathbf{W}_{11}\mathbf{N} & \mathbf{X}_1^\top\mathbf{W}_{12}\mathbf{X}_2 & \mathbf{X}_1^\top\mathbf{W}_{13}\mathbf{X}_3 \\ \mathbf{N}^\top\mathbf{W}_{11}\mathbf{X}_1 & \mathbf{N}^\top\mathbf{W}_{11}\mathbf{N} + \lambda_q\mathbf{K}_q & \mathbf{N}^\top\mathbf{W}_{12}\mathbf{X}_2 & \mathbf{N}^\top\mathbf{W}_{13}\mathbf{X}_3 \\ \mathbf{X}_2^\top\mathbf{W}_{12}\mathbf{X}_1 & \mathbf{X}_2^\top\mathbf{W}_{12}\mathbf{N} & \mathbf{X}_2^\top\mathbf{W}_{22}\mathbf{X}_2 & \mathbf{X}_2^\top\mathbf{W}_{23}\mathbf{X}_3 \\ \mathbf{X}_3^\top\mathbf{W}_{13}\mathbf{X}_1 & \mathbf{X}_3^\top\mathbf{W}_{13}\mathbf{N} & \mathbf{X}_3^\top\mathbf{W}_{23}\mathbf{X}_2 & \mathbf{X}_3^\top\mathbf{W}_{33}\mathbf{X}_3 \end{bmatrix},$$

where

$$\begin{aligned} \mathbf{W}_{11} &= [\dot{\ell}_{\xi_{iq}}\ \dot{\ell}_{\xi_{iq}}\ \delta_{ij}], & \mathbf{W}_{12} &= [\dot{\ell}_{\xi_{iq}}\ \dot{\ell}_{\sigma_{iq}}\ \exp(\eta_{2iq})\ \delta_{ij}], \\ \mathbf{W}_{13} &= [\dot{\ell}_{\xi_{iq}}\ \dot{\ell}_{\alpha_{iq}}\ \exp(\eta_{3iq})\ \delta_{ij}], & \mathbf{W}_{22} &= [\dot{\ell}_{\sigma_{iq}}\ \dot{\ell}_{\sigma_{iq}}\ \exp(2\eta_{2iq})\ \delta_{ij}], \\ \mathbf{W}_{23} &= [\dot{\ell}_{\sigma_{iq}}\ \dot{\ell}_{\alpha_{iq}}\ \exp(\eta_{2iq})\ \exp(\eta_{3iq})\ \delta_{ij}], & \mathbf{W}_{33} &= [\dot{\ell}_{\alpha_{iq}}\ \dot{\ell}_{\alpha_{iq}}\ \exp(2\eta_{3iq})\ \delta_{ij}], \end{aligned}$$

with $\dot{\ell}_{\xi_{iq}}$, $\dot{\ell}_{\sigma_{iq}}$ and $\dot{\ell}_{\alpha_{iq}}$ described in Section 4.2, for $i, j = 1, \ldots, n$ and $q \in (0,1)$ fixed. Finally, matrix $\mathbf{B}$ is similar to matrix $\mathbf{A}$, only the set of elements $\mathbf{N}^\top\mathbf{W}_{11}\mathbf{N} + \lambda_q\mathbf{K}_q$ must be replaced by $\mathbf{N}^\top\mathbf{W}_{11}\mathbf{N}$.

4.3 Residual analysis

To detect atypical observations and study the adequacy of the model, the residuals described in Sections 2.5.1, 2.5.2 and 2.5.3 are considered. For this reason, we only present the expressions of the residuals that are as follows:

$$\widehat{r}_{iq}^{(1)} = \Phi^{-1}\big(\widehat{G}(y_i; \widehat{\xi}_{iq}, \widehat{\sigma}_{iq}, \widehat{\alpha}_{iq})\big), \tag{4.16}$$

$$\widehat{r}_{iq}^{(2)} = -\log\big(1 - \widehat{G}(y_i; \widehat{\xi}_{iq}, \widehat{\sigma}_{iq}, \widehat{\alpha}_{iq})\big), \tag{4.17}$$

$$\widehat{r}_{iq}^{(3)} = \text{sign}(1 - \widehat{r}_{iq}^{(2)})\left\{-2\big[1 - \widehat{r}_{iq}^{(2)} + \log\big(\widehat{r}_{iq}^{(2)}\big)\big]\right\}^{0.5}, \tag{4.18}$$

where Φ^{-1} is the inverse cdf of the standard normal distribution, $\widehat{G}$ is the estimated cdf of G defined in Section 2.2, sign$(\cdot)$ denotes the sign function, for $i = 1,\ldots,n$ and $q \in (0,1)$ fixed. Recently, the NQRs have been studied by Ramires *et al.* (2019) and Prataviera *et al.* (2022) in the context of semiparametric models.

4.4 Global influence

Following the idea of Vasconcelos, Cordeiro and Ortega (2022) in the context of semiparametric regression models, we identify possible influential cases through a global influence analysis. Thus, two measures from case deletion are proposed.

The first proposed measure is the generalized Cook's distance, which can be written as

$$\mathrm{GCD}_i = (\widehat{\boldsymbol{\theta}}_{(i)q} - \widehat{\boldsymbol{\theta}}_q)^\top \ddot{\ell}_p^{-1}(\widehat{\boldsymbol{\theta}}_q, \widehat{\lambda}_q)(\widehat{\boldsymbol{\theta}}_{(i)q} - \widehat{\boldsymbol{\theta}}_q) \tag{4.19}$$

where $\widehat{\boldsymbol{\theta}}_{(i)q}$ denotes the penalized ML estimate of $\boldsymbol{\theta}_q$ without the i-th observation and $\ddot{\ell}_p^{-1}(\widehat{\boldsymbol{\theta}}_q, \widehat{\lambda}_q)$ is the inverse of the penalized observed information matrix defined in Section 4.2.3.

On the other hand, the second proposed measure is the penalized likelihood displacement, defined as

$$\mathrm{LD}_i = 2[\ell_p(\widehat{\boldsymbol{\theta}}_q, \widehat{\lambda}_q) - \ell_p(\widehat{\boldsymbol{\theta}}_{(i)q}, \widehat{\lambda}_{(i)q})], \tag{4.20}$$

where $\ell_p(\widehat{\boldsymbol{\theta}}_q, \widehat{\lambda}_q)$ and $\ell_p(\widehat{\boldsymbol{\theta}}_{(i)q}, \widehat{\lambda}_{(i)q})$ are the penalized log-likelihood functions of the complete dataset and without the i-th observation, respectively.

4.5 Local Influence

Similarly to Section 2.7, the model is perturbed by a vector $\boldsymbol{\omega}$ of dimension $(n \times 1)$ restricted to some open subset of $\Omega \subset \mathbb{R}^n$. In addition, the perturbed penalized log-likelihood function is denoted by $\ell_p(\boldsymbol{\theta}_q, \lambda_q|\boldsymbol{\omega})$ and assumes that there is a non-perturbation vector $\boldsymbol{\omega}_0 \in \Omega$ such that $\ell_p(\boldsymbol{\theta}_q, \lambda_q|\boldsymbol{\omega}_0) = \ell_p(\boldsymbol{\theta}_q, \lambda_q)$. In this way, the influence of the perturbation $\boldsymbol{\omega}$ on the penalized ML estimator $\widehat{\boldsymbol{\theta}}_q$ is evaluated.

Here, the normal curvature for $\boldsymbol{\theta}_q$ in the direction of $\mathbf{d}$ is given by

$$\mathbf{C}_\mathbf{d}(\boldsymbol{\theta}_q) = 2|\mathbf{d}^\top \boldsymbol{\Delta}_p^\top \ddot{\ell}_p^{-1}(\boldsymbol{\theta}_q, \lambda_q)\, \boldsymbol{\Delta}_p \mathbf{d}|, \tag{4.21}$$

where $\boldsymbol{\Delta}_p$ is the matrix of dimension $(t_1 + t_2 + r + m) \times n$ with elements

$$\Delta_{ji} = \frac{\partial^2 \ell_p(\boldsymbol{\theta}_q, \lambda_q|\boldsymbol{\omega})}{\partial \theta_j \partial \omega_i}\Big|_{\boldsymbol{\theta}_q = \widehat{\boldsymbol{\theta}}_q, \lambda_q = \widehat{\lambda}_q, \boldsymbol{\omega} = \boldsymbol{\omega}_0} \tag{4.22}$$

for $j = 1,\ldots,(t_1 + t_2 + r + m)$, $i = 1,\ldots,n$, and $\ddot{\ell}_p^{-1}(\boldsymbol{\theta}_q, \lambda_q)$ is the inverse of the penalized observed information matrix defined in Section 4.2.3. Consequently, we will study the total local

influence of the case i, calculated by $C_i = C_{\mathbf{d}_i}(\boldsymbol{\theta}_q)$, where $\mathbf{d}_i$ is a vector of zeros with one in the i-th position.

Now, we present three perturbation schemes in the same way as linear QR models, detailing the calculation of derivatives necessary to obtain the matrix $\boldsymbol{\Delta}_p$.

4.5.1 Case-weight

In this scheme, the perturbed penalized log-likelihood function is expressed as

$$\ell_p(\boldsymbol{\theta}_q, \lambda_q|\boldsymbol{\omega}) = \sum_{i=1}^{n} \omega_i\, \ell_i(\xi_{iq}, \sigma_{iq}, \alpha_{iq}) - 0.5\lambda_q \boldsymbol{\gamma}_q^\top \mathbf{K}_q \boldsymbol{\gamma}_q, \text{ with} \tag{4.23}$$
$$\ell_i(\xi_{iq}, \sigma_{iq}, \alpha_{iq}) = \log(\alpha_{iq}) + \log(f_0(u_{iq})) - \log(\sigma_{iq}) - 2\log(\alpha_{iq} + (1-\alpha_{iq})F_0(u_{iq})),$$
$$u_{iq} = (y_i - \xi_{iq})/\sigma_{iq} + F_0^{-1}(\alpha_{iq} q/(1 + q\alpha_{iq} - q)),$$

where $\boldsymbol{\omega} = (\omega_1, \ldots, \omega_n)^\top$ and $\boldsymbol{\omega}_0 = (1, \ldots, 1)^\top$ are vectors of dimension $(n \times 1)$, $0 \leq \omega_i \leq 1$ for $i = 1, \ldots, n$ and $q \in (0,1)$ fixed. Hence, the matrix $\boldsymbol{\Delta}_p$ is given by

$$\boldsymbol{\Delta}_p = \begin{bmatrix} \mathbf{X}_1^\top & \mathbf{W}_1 & \mathbf{M}_1 \\ \mathbf{N}^\top & \mathbf{W}_1 & \mathbf{M}_1 \\ \mathbf{X}_2^\top & \mathbf{W}_2 & \mathbf{M}_2 \\ \mathbf{X}_3^\top & \mathbf{W}_3 & \mathbf{M}_3 \end{bmatrix},$$

where $\mathbf{M}_1 = \left[\ddot{\ell}_{\xi_{iq}\omega_i}\ \delta_{ij}\right]$, $\mathbf{M}_2 = \left[\ddot{\ell}_{\sigma_{iq}\omega_i}\ \delta_{ij}\right]$ and $\mathbf{M}_3 = \left[\ddot{\ell}_{\alpha_{iq}\omega_i}\ \delta_{ij}\right]$, with $\ddot{\ell}_{\xi_{iq}\omega_i} = \dot{\ell}_{\xi_{iq}}$, $\ddot{\ell}_{\sigma_{iq}\omega_i} = \dot{\ell}_{\sigma_{iq}}$ and $\ddot{\ell}_{\alpha_{iq}\omega_i} = \dot{\ell}_{\alpha_{iq}}$, for $i = 1, \ldots, n$ and $j = 1, \ldots, n$. Thus, the matrices $\mathbf{W}_1$, $\mathbf{W}_2$ and $\mathbf{W}_3$ together with the elements $\dot{\ell}_{\xi_{iq}}$, $\dot{\ell}_{\sigma_{iq}}$ and $\dot{\ell}_{\alpha_{iq}}$ are those defined in Section 4.2.

4.5.2 Response variable

Here, we consider $y_i(\omega_i) = y_i + \omega_i \mathrm{s}_y$ to perturb the response variable values, where s_y is the sample standard deviation of $\mathbf{y}$ and $\omega_i \in \mathbb{R}$ for $i = 1, \ldots, n$. Consequently, the perturbed penalized log-likelihood function has the form

$$\ell_p(\boldsymbol{\theta}_q|\boldsymbol{\omega}) = \sum_{i=1}^{n} \ell_i(\xi_{iq}, \sigma_{iq}, \alpha_{iq}, \omega_i) - 0.5\lambda_q \boldsymbol{\gamma}_q^\top \mathbf{K}_q \boldsymbol{\gamma}_q, \text{ where} \tag{4.24}$$
$$\ell_i(\xi_{iq}, \sigma_{iq}, \alpha_{iq}, \omega_i) = \log(\alpha_{iq}) + \log(f_0(u_{iq}^*)) - \log(\sigma_{iq}) - 2\log(\alpha_{iq} + (1-\alpha_{iq})F_0(u_{iq}^*)),$$
$$u_{iq}^* = (y_i(\omega_i) - \xi_{iq})/\sigma_{iq} + F_0^{-1}(\alpha_{iq} q/(1 + q\alpha_{iq} - q)),$$

for $i = 1, \ldots, n$ and $q \in (0,1)$ fixed. In this case, $\boldsymbol{\omega} = (\omega_1, \ldots, \omega_n)^\top$ and $\boldsymbol{\omega}_0 = (0, \ldots, 0)^\top$ are, respectively, the vectors of perturbation and no perturbation, both of dimension $(n \times 1)$. Then,

differentiating Equation (4.24) with respect to $\boldsymbol{\theta}_q$ and $\boldsymbol{\omega}$ leads to the following matrix

$$\boldsymbol{\Delta}_p = \begin{bmatrix} \mathbf{X}_1^\top & \mathbf{W}_1 & \mathbf{M}_4 \\ \mathbf{N}^\top & \mathbf{W}_1 & \mathbf{M}_4 \\ \mathbf{X}_2^\top & \mathbf{W}_2 & \mathbf{M}_5 \\ \mathbf{X}_3^\top & \mathbf{W}_3 & \mathbf{M}_6 \end{bmatrix},$$

where $\mathbf{M}_4 = \left[\ddot{\ell}_{\xi_{iq}\omega_i}\ \delta_{ij}\right]$, $\mathbf{M}_5 = \left[\ddot{\ell}_{\sigma_{iq}\omega_i}\ \delta_{ij}\right]$ and $\mathbf{M}_6 = \left[\ddot{\ell}_{\alpha_{iq}\omega_i}\ \delta_{ij}\right]$ for $i, j = 1, \ldots, n$. The elements of those matrices are as follows:

$$\begin{aligned}
\ddot{\ell}_{\xi_{iq}\omega_i} &= \frac{\partial^2 \ell_i(\xi_{iq}, \sigma_{iq}, \alpha_{iq}, \omega_i)}{\partial \xi_{iq} \partial \omega_i} \\
&= 2\psi_{8iq}\left[\frac{f_0'(u_{iq}^*)(1-\alpha_{iq})}{\alpha_{iq}+(1-\alpha_{iq})F_0(u_{iq}^*)}\right] - 2\psi_{8iq}\left[\frac{f_0(u_{iq}^*)(1-\alpha_{iq})}{\alpha_{iq}+(1-\alpha_{iq})F_0(u_{iq}^*)}\right]^2 \\
&\quad - \psi_{8iq}\left[\frac{f_0''(u_{iq}^*)}{f_0(u_{iq}^*)} - \frac{f_0'^2(u_{iq}^*)}{f_0^2(u_{iq}^*)}\right], \\
\ddot{\ell}_{\sigma_{iq}\omega_i} &= \frac{\partial^2 \ell_i(\xi_{iq}, \sigma_{iq}, \alpha_{iq}, \omega_i)}{\partial \sigma_{iq} \partial \omega_i} \\
&= 2\psi_{8iq}\left[\frac{f_0(u_{iq}^*)(1-\alpha_{iq})}{\alpha_{iq}+(1-\alpha_{iq})F_0(u_{iq}^*)}\right] - \psi_{8iq}\left[\frac{f_0'(u_{iq}^*)}{f_0(u_{iq}^*)}\right] - 2\psi_{9iq}\left[\frac{f_0(u_{iq}^*)(1-\alpha_{iq})}{\alpha_{iq}+(1-\alpha_{iq})F_0(u_{iq}^*)}\right]^2 \\
&\quad - \psi_{9iq}\left[\frac{f_0''(u_{iq}^*)}{f_0(u_{iq}^*)} - \frac{f_0'^2(u_{iq}^*)}{f_0^2(u_{iq}^*)}\right] + 2\psi_{9iq}\left[\frac{f_0'(u_{iq}^*)(1-\alpha_{iq})}{\alpha_{iq}+(1-\alpha_{iq})F_0(u_{iq}^*)}\right],
\end{aligned}$$

$$\begin{aligned}
\ddot{\ell}_{\alpha_{iq}\omega_i} &= \frac{\partial^2 \ell_i(\xi_{iq}, \sigma_{iq}, \alpha_{iq}, \omega_i)}{\partial \alpha_{iq} \partial \omega_i} \\
&= 2\psi_{7iq}\left[\frac{f_0(u_{iq}^*)}{\alpha_{iq}+(1-\alpha_{iq})F_0(u_{iq}^*)}\right] - 2\psi_{7iq}u_{\alpha_{iq}}^*\left[\frac{f_0'(u_{iq}^*)(1-\alpha_{iq})}{\alpha_{iq}+(1-\alpha_{iq})F_0(u_{iq}^*)}\right] \\
&\quad + 2\psi_{7iq}\left[\frac{f_0(u_{iq}^*)(1-\alpha_{iq})}{\alpha_{iq}+(1-\alpha_{iq})F_0(u_{iq}^*)}\right]\left[\frac{1-F_0(u_{iq}^*)+(1-\alpha_{iq})f_0(u_{iq}^*)u_{\alpha_{iq}}^*}{\alpha_{iq}+(1-\alpha_{iq})F_0(u_{iq}^*)}\right] \\
&\quad + \psi_{7iq}u_{\alpha_{iq}}^*\left[\frac{f_0''(u_{iq}^*)}{f_0(u_{iq}^*)} - \frac{f_0'^2(u_{iq}^*)}{f_0^2(u_{iq}^*)}\right],
\end{aligned}$$

where

$$\psi_{7iq} = \frac{s_y}{\sigma_{iq}}, \qquad \psi_{8iq} = \frac{s_y}{\sigma_{iq}^2}, \qquad \psi_{9iq} = \frac{(y_i(\omega_i) - \xi_{iq})s_y}{\sigma_{iq}^3}, \qquad u_{\alpha_{iq}}^* = \frac{\Psi_0 q(1-q)}{(1+q\alpha_{iq}-q)^2}$$

and $\Psi_0 = 1/f_0(F_0^{-1}(\alpha_{iq}q/(1+q\alpha_{iq}-q)))$ for $i = 1, \ldots, n$ and $q \in (0,1)$ fixed.

4.5.3 Perturbation of the skewness parameter

Consider now perturbing the skewness parameter $\alpha_{iq}(\omega_i) = \alpha_{iq}/\omega_i$ with $\omega_i > 0$ for $i = 1,\ldots,n$ and $q \in (0,1)$ fixed. Then, under this scheme, the perturbed penalized log-likelihood function is given by

$$\ell_p(\boldsymbol{\theta}_q, \lambda_q|\boldsymbol{\omega}) = \sum_{i=1}^{n} \ell_i(\xi_{iq}, \sigma_{iq}, \alpha_{iq}(\omega_i)) - 0.5\lambda_q \boldsymbol{\gamma}_q^\top \mathbf{K}_q \boldsymbol{\gamma}_q, \text{ with} \tag{4.25}$$

$$\ell_i(\xi_{iq}, \sigma_{iq}, \alpha_{iq}(\omega_i)) = \log(\alpha_{iq}) + \log(\omega_i) + \log(f_0(u_{iq})) - \log(\sigma_{iq}) - 2\log(\rho_i(u_{iq})),$$

$$\rho_i(u_{iq}) = \alpha_{iq} + (\omega_i - \alpha_{iq})F_0(u_{iq}),$$

where $u_{iq} = (y_i - \xi_{iq})/\sigma_{iq} + F_0^{-1}(\alpha_{iq}q/(\omega_i + q\alpha_{iq} - q\omega_i))$. Consequently, taking derivatives of Equation (4.25) with respect to $\boldsymbol{\theta}_q$ and $\boldsymbol{\omega}$, the matrix $\boldsymbol{\Delta}_p$ is expressed as

$$\boldsymbol{\Delta}_p = \begin{bmatrix} \mathbf{X}_3^\top & \mathbf{W}_3 & \mathbf{M}_7 \end{bmatrix},$$

where $\mathbf{M}_7 = \begin{bmatrix} \ddot{\ell}_{\alpha_{iq}\omega_i} & \delta_{ij} \end{bmatrix}$, whose elements are

$$\begin{aligned}
\ddot{\ell}_{\alpha_{iq}\omega_i} = {} & u_{\alpha_{iq}\omega_i}\left[\frac{f_0'(u_{iq})}{f_0(u_{iq})}\right] + u_{\alpha_{iq}}u_{\omega_i}\left[\frac{f_0''(u_{iq})}{f_0(u_{iq})} - \frac{f_0'^2(u_{iq})}{f_0^2(u_{iq})}\right] + 2\left[\frac{f_0(u_{iq})u_{\omega_i} - f_0(u_{iq})u_{\alpha_{iq}}}{\alpha_{iq} + (\omega_i - \alpha_{iq})F_0(u_{iq})}\right] \\
& - 2\left[\frac{(\omega_i - \alpha_{iq})f_0'(u_{iq})u_{\omega_i}u_{\alpha_{iq}}}{\alpha_{iq} + (\omega_i - \alpha_{iq})F_0(u_{iq})}\right] - 2\left[\frac{(\omega_i - \alpha_{iq})f_0(u_{iq})u_{\alpha_{iq}\omega_i}}{\alpha_{iq} + (\omega_i - \alpha_{iq})F_0(u_{iq})}\right] \\
& + 2\left[\frac{1 - F_0(u_{iq}) + (\omega_i - \alpha_{iq})f_0(u_{iq})u_{\alpha_{iq}}}{\alpha_{iq} + (\omega_i - \alpha_{iq})F_0(u_{iq})}\right]\left[\frac{F_0(u_{iq}) + (\omega_i - \alpha_{iq})f_0(u_{iq})u_{\omega_i}}{\alpha_{iq} + (\omega_i - \alpha_{iq})F_0(u_{iq})}\right],
\end{aligned}$$

with

$$u_{\omega_i} = \frac{\Psi_0\alpha_{iq}q(q-1)}{(\omega_i + q\alpha_{iq} - q\omega_i)^2}, \quad u_{\alpha_{iq}} = \frac{\Psi_0\omega_i q(1-q)}{(\omega_i + q\alpha_{iq} - q\omega_i)^2}, \quad \Psi_0 = \frac{1}{f_0(F_0^{-1}(q\alpha_{iq}/(\omega_i + q\alpha_{iq} - q\omega_i)))},$$

and

$$u_{\omega_i\alpha_{iq}} = \left[\frac{\omega_i\alpha_{iq}q^2(q-1)^2}{(\omega_i + q\alpha_{iq} - q\omega_i)^4}\right]\Psi_0^3 f_0'(F_0^{-1}(q\alpha_{iq}/(\omega_i + q\alpha_{iq} - q\omega_i))) + \Psi_0(q-1)q\left[\frac{(\omega_i - q\omega_i - q\alpha_{iq})}{(\omega_i + q\alpha_{iq} - q\omega_i)^3}\right],$$

for $i = 1,\ldots,n$ and $q \in (0,1)$ fixed. Note that for this scheme, $\boldsymbol{\omega} = (\omega_1,\ldots,\omega_n)^\top$ and $\boldsymbol{\omega}_0 = (1,\ldots,1)^\top$ are the vectors of perturbation and no perturbation, respectively.

4.6 Final comments

The main contribution of this chapter is to present the PLQR models that extend the QR models in the RPMO family of distributions. Its great advantage is that it can be used to model the quantiles with nonparametric effects of one covariate and parametric effects of another set of covariates. From the penalized log-likelihood function, we calculate the penalized score functions and the penalized observed information matrix to perform statistical inference. The RS algorithm is proposed to simultaneously obtain the penalized ML estimates and the smoothing parameter estimate. Moreover, the AIC and BIC criteria are suggested for the selection of models.

This chapter also provides expressions for NQR, GCSR and MTR to study outlier observations and the adequacy of PLQR models under RPMO distributions. The generalized Cook's distance and the penalized likelihood displacement are presented as measures of global influence to identify the influential observations on the parameter vector estimated in the models. Thus, the perturbation schemes addressed are case-weight, response variable and skewness parameter. All the resulting expressions and matrices have a closed form that allows them to be implemented in any statistical-mathematical software at a low computational cost.

CHAPTER

5

SIMULATION STUDIES AND DATA ANALYSIS FOR PARTIALLY LINEAR REGRESSION MODELS

This chapter presents simulation studies to assess the statistical properties of penalized ML estimators in nonparametric QR models under RPMON and RPMOG distributions. Subsequently, we illustrate the process of estimation, statistical inference, residual analysis, global and local influence methods on another dataset belonging to NHANES.

5.1 Simulation studies

In order to carry out the simulation studies, a total of 500 random samples were generated by utilizing the qf function of Equation (2.3) with sample size $n \in \{200, 400, \ldots, 4000\}$ and probabilities $q \in \{0.1, 0.5, 0.9\}$. Penalized ML estimates were obtained using the RS algorithm described in Section 4.2.2 with the R programming language. The initial values for ξ_{iq}, σ_{iq} and α_{iq} are the outputs of the nonparametric QR models under the RPMON and RPMOG distributions using the *gamlss* package from R.

The statistical properties of the penalized ML estimators are evaluated using two scenarios. The structure of the scenarios is as follows:

$$\begin{aligned} \xi_{iq} &= \eta_{1iq} = s_q(z_i), \\ \log(\sigma_{iq}) &= \eta_{2iq} = -1.2 + 0.15x_{2i2}, \\ \log(\alpha_{iq}) &= \eta_{3iq} = -0.5x_{3i1}; \quad \text{and} \end{aligned} \tag{I}$$

$$\begin{aligned} \xi_{iq} &= \eta_{1iq} = s_q(z_i), \\ \log(\sigma_{iq}) &= \eta_{2iq} = -1.2 + 0.15x_{2i2}, \\ \log(\alpha_{iq}) &= \eta_{3iq} = 2.7x_{3i1}, \end{aligned} \tag{II}$$

where $s_q(z_i) = 0.45\sin(\pi z_i)$ with $z_i \sim \mathrm{U}(0, 2.5)$, $x_{2i2} \sim \mathrm{N}(0,1)$, $x_{3i1} \sim \mathrm{Logis}(0,1)$ for $i = 1,\ldots,n$. Scenario I and Scenario II were developed under the RPMON and RPMOG distributions, respectively. Finally, the function $s_q(z_i)$ is approximated by P-splines with 22 internal knots and a difference penalty term of order 3 ($k_1 = 3$).

Under the nonparametric QR model of the RPMON distribution, Figures 16-19 display the empirical RB, SD, RMSE, and mean of the asymptotic SE for the penalized ML estimates of ν_{1q}, ν_{2q}, and τ_{1q}, respectively. From the figures, we observe that as the sample size n increases, the quantities decrease, as expected in the standard asymptotic theory. Note also from Figure 16 that the estimates of the τ_{1q} parameter have a high bias in medium samples. On the other hand, Figure 20 shows the CPs of the 95% confidence intervals for the nonparametric QR model. Based on this figure, it can be seen that the CPs are close to the nominal values, with an approximate minimum value of 92% when the sample size is larger than 400.

On the other hand, the five measures for the nonparametric QR model under the RPMOG distribution are shown in Figures 51-55 from Appendix B. The results indicate that as the sample size n increases, the first four quantities decrease. However, we highlight that the penalized ML estimates of the τ_{1q} parameter have a high bias in medium samples. Figure 55 displays that the CPs are close to the nominal values used for their construction as n increases. These values are higher than 90% for the three parameters.

The behavior of the mean of the nonparametric function vectors from the nonparametric QR model under the RPMON distribution in different sample sizes is presented graphically in Figures 21-23. Thus, we note that as the sample size n increases, the mean of the nonparametric function vectors captures in a better way the trend of the true function (solid black line). Can be seen the same pattern in the plots of the nonparametric QR model under the RPMOG distribution (Figures 56-58 of Appendix B).

To observe the behavior of the mean SE in $\widehat{\nu}_{1q}$, $\widehat{\nu}_{2q}$ and $\widehat{\tau}_{1q}$ as a function of the sample size, we present the plots of $\mathrm{SE}_i/\mathrm{SE}_{i+1}$ and $\sqrt{n_{i+1}/n_i}$ rates for $i = 1,...,19$ correspondent to $n \in \{200, 400, \ldots, 4000\}$. These plots can be seen in Figures 59-60 from Appendix B. From these plots, we note that the behavior of the mean SE decreases according to $\sqrt{n_{i+1}/n_i}$, as expected in the standard asymptotic theory in both models.

Figure 16 – Mean of the RB on the 500 estimates of the components $\widehat{\boldsymbol{\nu}}_q$ and $\widehat{\boldsymbol{\tau}}_q$ obtained in the RPMON model under different sample sizes.

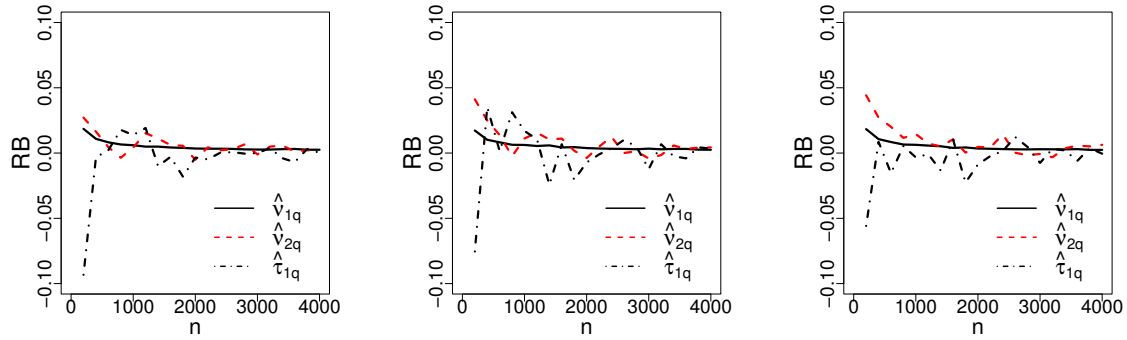

(a) $q = 0.1$ (b) $q = 0.5$ (c) $q = 0.9$

Figure 17 – SD on the 500 estimates of the components $\widehat{\boldsymbol{\nu}}_q$ and $\widehat{\boldsymbol{\tau}}_q$ obtained in the RPMON model under different sample sizes.

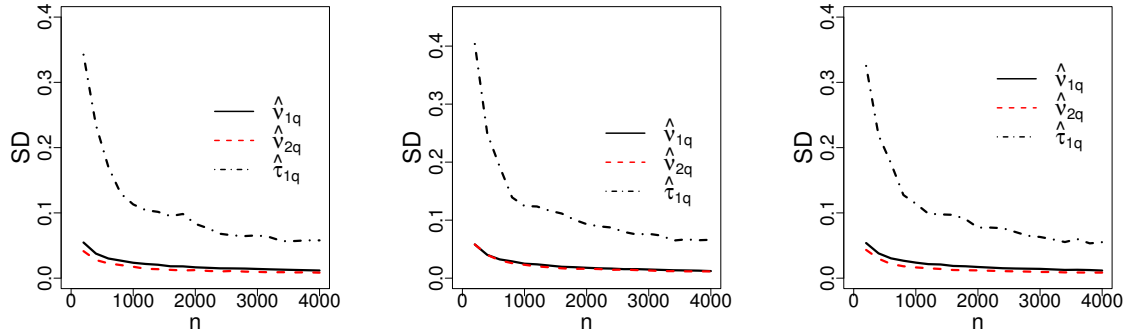

(a) $q = 0.1$ (b) $q = 0.5$ (c) $q = 0.9$

Figure 18 – RMSE on the 500 estimates of the components $\widehat{\boldsymbol{\nu}}_q$ and $\widehat{\boldsymbol{\tau}}_q$ obtained in the RPMON model under different sample sizes.

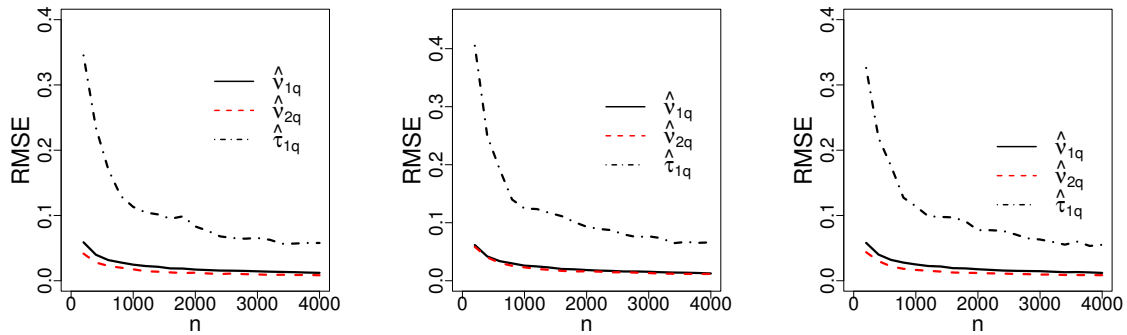

(a) $q = 0.1$ (b) $q = 0.5$ (c) $q = 0.9$

Figure 19 – Mean of the asymptotic SE on the 500 estimates of the components $\widehat{\boldsymbol{\nu}}_q$ and $\widehat{\boldsymbol{\tau}}_q$ obtained in the RPMON model under different sample sizes.

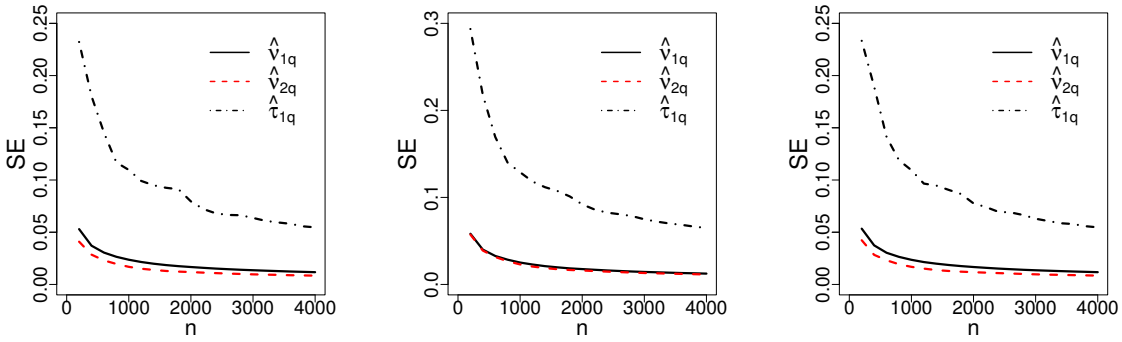

(a) $q = 0.1$ (b) $q = 0.5$ (c) $q = 0.9$

Figure 20 – 95% CP of the components $\widehat{\boldsymbol{\nu}}_q$ and $\widehat{\boldsymbol{\tau}}_q$ obtained in the RPMON model under different sample sizes.

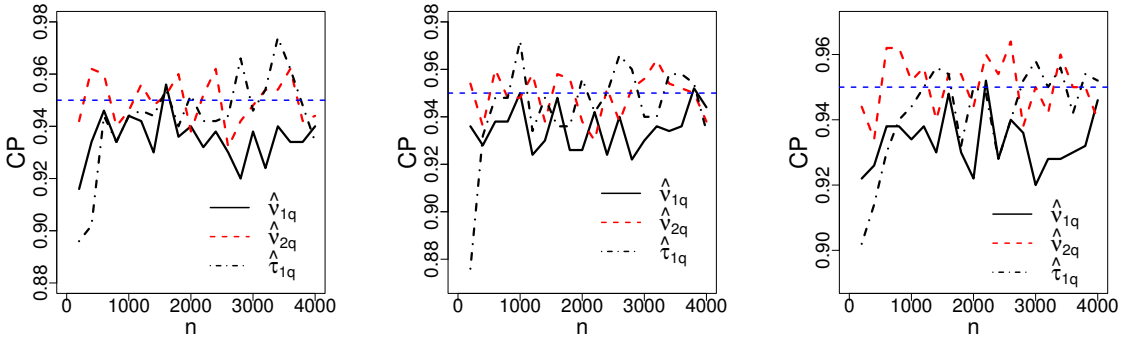

(a) $q = 0.1$ (b) $q = 0.5$ (c) $q = 0.9$

Figure 21 – Smooth function mean on the 500 estimates obtained in the RPMON model under different sample sizes and $q = 0.1$.

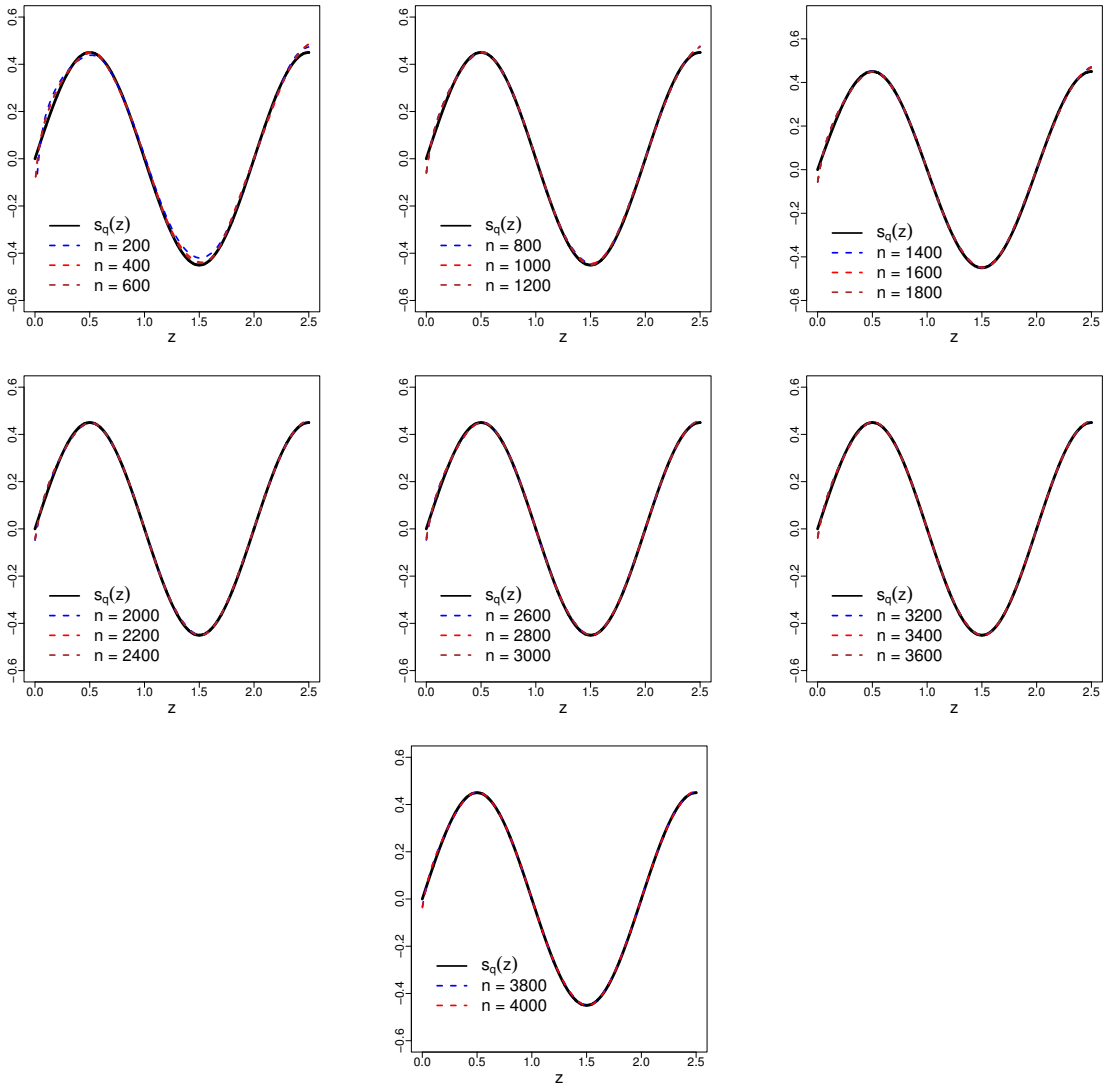

Figure 22 – Smooth function mean on the 500 estimates obtained in the RPMON model under different sample sizes and $q = 0.5$.

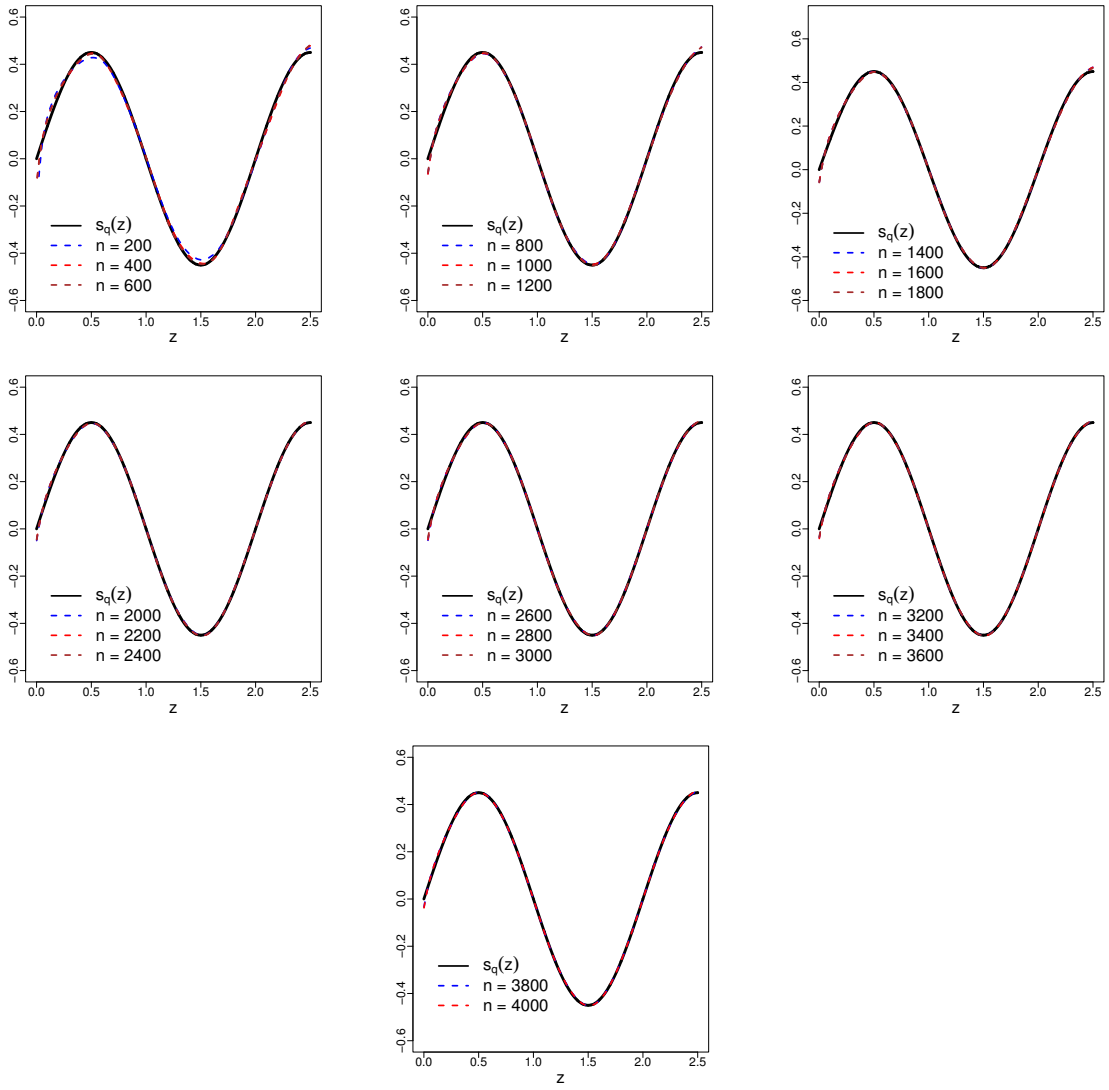

Figure 23 – Smooth function mean on the 500 estimates obtained in the RPMON model under different sample sizes and $q = 0.9$.

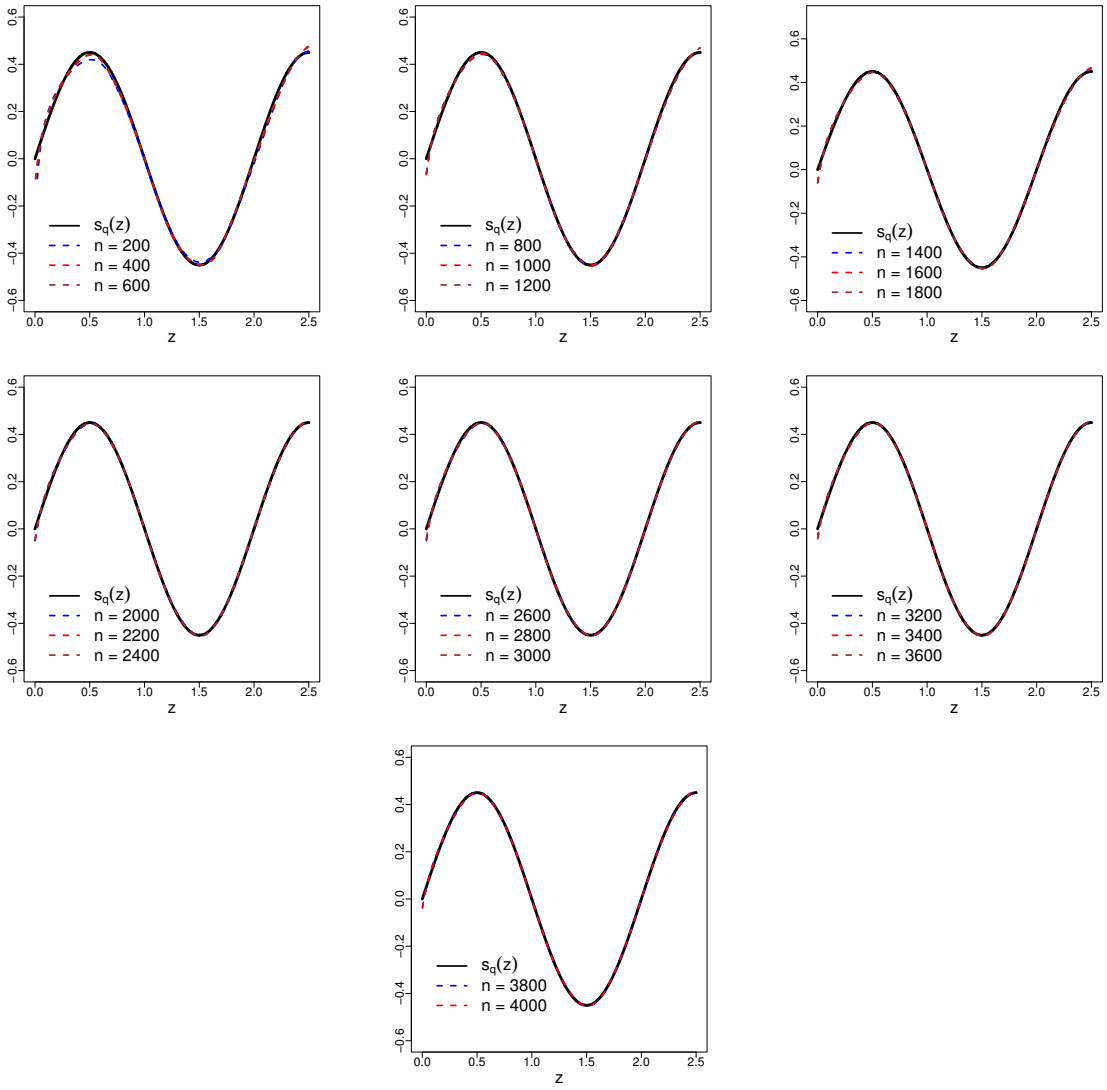

5.2 Data analysis

This section analyzes a dataset from NHANES (1999-2000) that pertains to 4077 individuals. The purpose is to illustrate the methodologies described in Chapter 4. The primary objective of this study is to assess the association between estimated fat-free mass (EFFM) in kilograms and upper arm length (UAL) in centimeters. The first measurement represents the portion of body mass comprising muscles, bones, organs, and other non-fat tissues. Its estimation holds significance in various fields, including nutrition, sports medicine, and health research, as it provides valuable insights into body composition and can be employed to evaluate an individual's health and physical condition, as well as to tailor dietary and training programs. The second measurement pertains to the length of the arm from the shoulder to the elbow. In the medical and health context, upper arm length serves to determine the appropriate sizing of medical devices such as blood pressure monitors or cuffs. The data file in CSV format is available in the repository at <https://github.com/isaaccortes1989/Data-Chapter-5>.

5.2.1 Descriptive analysis

A descriptive summary of EFFM and UAL that includes minimum (Min), maximum (Max), the sample mean, median, standard deviation (SD), coefficient of variation (CV), skewness coefficient (CS), and kurtosis coefficient (CK) is provided in Table 9. Then, we add the histogram of EFFM and the scatter plot between EFFM and UAL in Figure 24.

Based on Table 9 and the histogram of Figure 24(a), we observe that EFFM has an empirical distribution unimodal with positive skewness. In Figure 24(b), it can be seen that the nonlinear relation between EFFM and UAL indicates that the nonparametric QR models are a good alternative to modeling the quantiles, scale and skewness of the EFFM. Additionally, observations #270, #312, #822 and #2787 with atypical behavior in the population are highlighted.

Figure 24 – Histogram of EFFM (a), and scatter plot of EFFM and UAL (b).

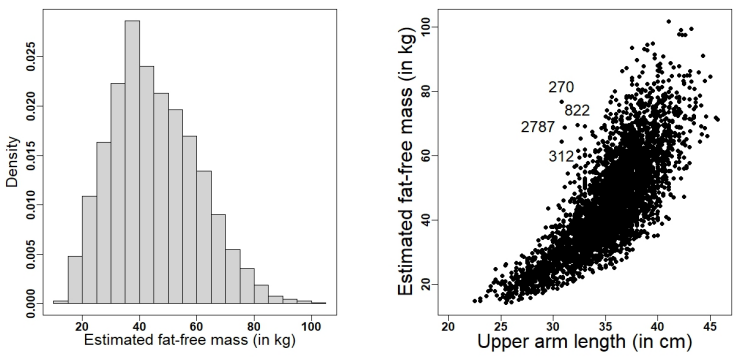

(a) (b)

Table 9 – Descriptive statistics of the variables in the NHANES dataset.

Variable	Mean	Median	SD	CS	CK	CV	Min	Max
EFFM	45.19	43.4	15.11	0.45	2.83	0.33	14.2	101.7
ARML	35.26	35.7	3.58	-0.46	3.16	0.10	22.5	45.7

5.2.2 Fitting of the nonparametric quantile regression models

To analyze the data, we propose using the nonparametric QR model. In this model, the q-th quantile ξ_{iq}, scale σ_{iq} and skewness α_{iq} are given by

$$\xi_{iq} = \eta_{1iq} = s_q(\text{UAL}_i),\ \sigma_{iq} = \eta_{2iq} = \nu_{1q} + \nu_{2q}\text{UAL}_i \text{ and } \log(\alpha_{iq}) = \eta_{3iq} = \tau_{1q}\text{UAL}_i, \quad (5.1)$$

where $s_q(\cdot)$ is a continuous smooth function approximated by using B-splines, and UAL_i denotes the upper arm length in centimeters of the i-th person for $i = 1,\ldots,4077$. The parameters ν_{1q}, ν_{2q} and τ_{1q} are unknown, while q ranges from the set $\{0.10, 0.25, 0.50, 0.75, 0.90\}$. Furthermore, we assume that the response variable EFFM follows an RPMO distribution, i.e., $y_i \sim \text{RPMO}(\xi_{iq}, \sigma_{iq}, \alpha_{iq}, f_0)$. For comparison purposes, we also include the following models: nonparametric QR models considering $\sigma_{iq} = \sigma_q$ and $\alpha_{iq} = 1$, linear QR models with $\xi_{iq} = \eta_{1iq} = \beta_{1q} + \beta_{2q}\text{UAL}_i$ in Equation (5.1), and finally, the class of SKD distributions.

Table 10 reports the values of the AIC and BIC criteria presented in Section 4.2.5. Notably, the following aspects can be observed: linear QR models under the RPMOG, RPMON, and RPMOT (with $\vartheta = 15$) distributions exhibit a better fit than the class of SKD distributions. Additionally, the nonparametric QR models under the RPMO distributions display a better fit than their particular cases, with the RPMOG distribution being the most suitable for analyzing EFFM.

Table 10 – AIC and BIC criteria for different QR models.

AIC criterion													
		Linear QR models				Nonparametric QR models considering $\sigma_{iq} = \sigma$ and $\alpha_{iq} = 1$				Nonparametric QR models			
q	SKD class	RPMOG	RPMON	RPMOC	RPMOT	RPMOG	RPMON	RPMOC	RPMOT	RPMOG	RPMON	RPMOC	RPMOT
0.10	29987.5	28928.8	29040.2	30329.3	29110.4	29440.7	29677.1	30809.5	29686.5	28790.1	28893.9	30235.4	28980.1
0.25	29523.5	28985.3	29093.9	30461.3	29169.7	29440.7	29677.1	30809.5	29686.5	28788.5	28904.2	30191.1	28989.9
0.50	29672.6	29048.3	29145.0	30534.4	29226.6	29440.7	29677.1	30809.5	29686.5	28800.3	28895.8	30191.3	29001.4
0.75	30590.0	29102.9	29190.6	30604.0	29274.8	29440.7	29677.1	30809.5	29686.5	28793.5	28903.8	30214.1	28979.8
0.90	31806.1	29144.9	29231.4	30676.0	29314.8	29440.7	29677.1	30809.5	29686.5	28791.6	28907.9	30361.4	28987.9
BIC criterion													
		Linear QR models				Nonparametric QR models considering $\sigma_{iq} = \sigma$ and $\alpha_{iq} = 1$				Nonparametric QR models			
q	SKD class	RPMOG	RPMON	RPMOC	RPMOT	RPMOG	RPMON	RPMOC	RPMOT	RPMOG	RPMON	RPMOC	RPMOT
0.10	30,006.5	28,960.3	29,071.8	30,360.8	29,141.9	29,474.1	29,724.1	30,828.4	29,705.4	28,881.4	28,971.9	30,304.1	29,055.6
0.25	29,542.4	29,016.8	29,125.4	30,492.9	29,201.2	29,474.1	29,724.1	30,828.4	29,705.4	28,881.0	28,976.8	30,276.2	29,060.2
0.50	29,691.5	29,079.9	29,176.6	30,566.0	29,258.2	29,474.1	29,724.1	30,828.4	29,705.4	28,873.0	28,984.8	30,281.7	29,071.4
0.75	30,609.0	29,134.4	29,222.2	30,635.6	29,306.4	29,474.1	29,724.1	30,828.4	29,705.4	28,877.6	29,000.4	30,307.2	29,068.9
0.90	31,825.1	29,176.5	29,263.0	30,707.6	29,346.4	29,474.1	29,724.1	30,828.4	29,705.4	28,885.6	28,997.2	30,450.3	29,088.0

The penalized ML estimates of ν_{1q}, ν_{2q} and τ_{1q}, along with their respective 95% confidence intervals, can be seen graphically in Figure 25. We observe in the figure that the estimates of the three parameters exhibit an almost linear behavior and are significant for all q values. Additionally, we include the graphs of the nonparametric vector $\boldsymbol{s}_q(\mathbf{z})$ along with their respective confidence bands for different q values in Figure 26. The figure shows that the nonparametric vector $\boldsymbol{s}_q(\mathbf{z})$ captures the nonlinear trend between UAL and the EFFM quantiles very effectively and significantly for all values of q. In practical terms, model 5.1 enables the explanation of the nonlinear relationship between UAL and the EFFM quantiles through a smooth function, as well as the relationship between UAL and the variability of EFFM, and finally, the relationship between UAL and the skewness of EFFM.

Figure 25 – Penalized ML estimates (center line) and their 95% confidence intervals for parameters in the nonparametric QR model with the RPMOG distribution at different probabilities.

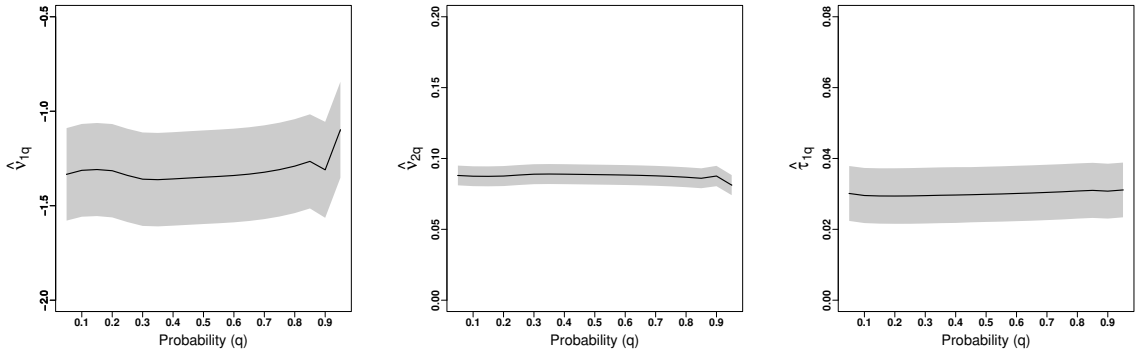

The subsequent analyzes will be carried out using the nonparametric QR model with the RPMOG distribution and $q = 0.1$. As a result, Table 11 displays the penalized ML estimates, approximate standard errors, z-values, and their respective p-values for the fit. From this table, we can observe that all the coefficients are statistically significant at the 5% level.

Table 11 – Penalized ML estimate, approximate standard error, z-value and p-value for the specified parameter fitted in the NHANES dataset under RPMOG distribution with $q = 0.1$.

	$\widehat{\nu}_{1q}$	$\widehat{\nu}_{2q}$	$\widehat{\tau}_{1q}$	$\widehat{\lambda}_q$
Estimate	-1.313	0.087	0.030	0.350
SE	0.125	0.004	0.004	
z-value	-10.482	24.496	7.446	
p-value	< 0.001	< 0.001	< 0.001	

Figure 26 – Estimates of the nonparametric vector $\mathbf{s}_q(\mathbf{z})$ (center line) and their confidence bands fitting the nonparametric QR model with the RPMOG distribution at different probabilities.

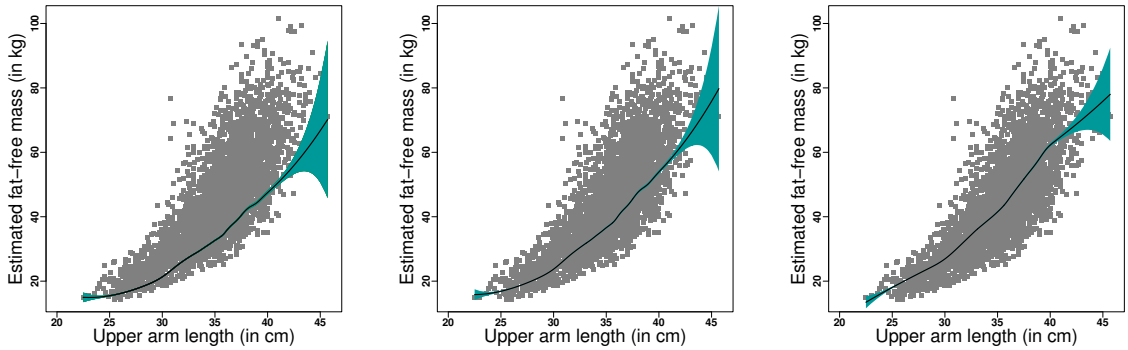

(a) $q = 0.1$ (b) $q = 0.25$ (c) $q = 0.5$

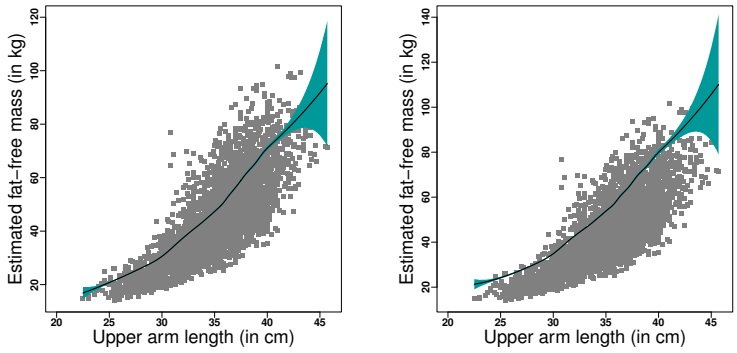

(d) $q = 0.75$ (e) $q = 0.90$

5.2.3 Identifying outliers

Figures 27(a), 27(b) and 27(c) present the plots of the NQR, GCS and MTR residuals with envelopes generated, respectively. It can be seen in 27(a) and 27(b) that observations #312 and #2787 lie outside the envelopes. These observations were identified with atypical behavior in the scatter plot. Figure 27(c) shows that only observation #312 is outside the envelopes. However, it does not appear to be inadequate to assume that the response variable follows an RPMOG distribution.

5.2.4 Identifying influential observations

In Figures 28(a) and 28(b), the generalized Cook's distance and the penalized likelihood displacement are shown graphically to detect potentially influential observations on the vector $\widehat{\boldsymbol{\theta}}_q$. Both measures described in Section 4.4. The first figure indicates that observations #108, #2158 and #2440 are potentially influential. In the second figure, observations #270, #312 and #2787 are identified as more potentially influential.

Figure 27 – QQ-plot with envelopes for NQRs (a), GCSRs (b) and MTRs (c) in the nonparametric QR model, considering RPMOG distribution and $q = 0.1$.

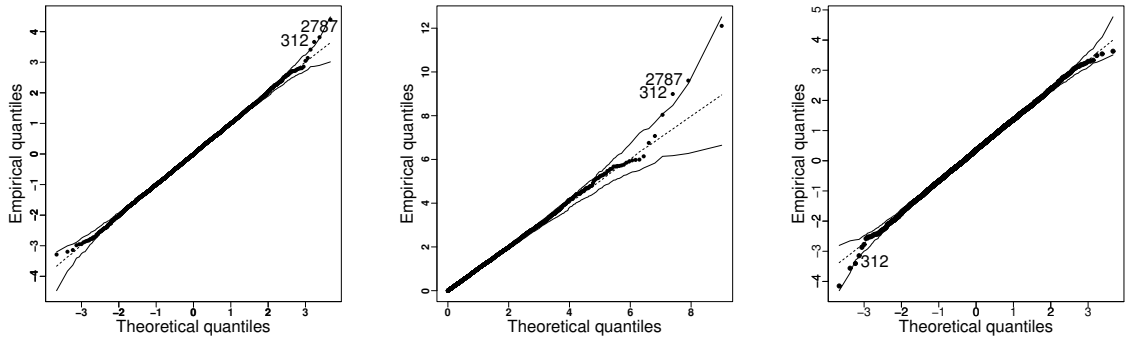

(a) (b) (c)

Figure 28 – Generalized Cook's distance (a) and the penalized likelihood displacement (b) in the nonparametric QR model, considering RPMOG distribution and $q = 0.1$

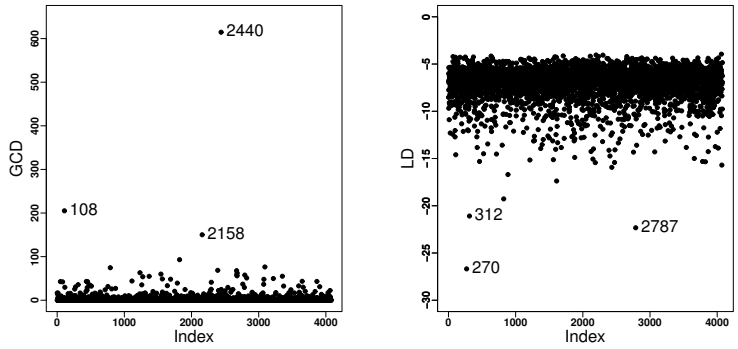

(a) (b)

The index plots of $C_i(\widehat{\boldsymbol{\theta}}_q)$, $C_i(\widehat{\boldsymbol{\gamma}}_q)$, $C_i(\widehat{\boldsymbol{\nu}}_q)$ and $C_i(\widehat{\boldsymbol{\tau}}_q)$ under the case-weight perturbation scheme are presented in Figures 29(a), 29(b), 29(c) and 29(d), respectively. The observations revealed as potentially influential in the figures are #270, #312, #1788, #1879, #2787, #3449, #3782 and #3866. It is important to note that observations #270, #312 and #2787 were identified with atypical behavior in the scatter plot of the descriptive analysis.

Figure 30 displays the index plot of C_i, considering the scheme of perturbation of the response for the fitted model. Observations #114, #1788 and #3449 are detected as potentially influential in Figures 30(a) and 30(b). Furthermore, Figures 30(c) and 30(d) jointly show that observations #997, #1879, #2152, #2530, #3782 and #3866 are potentially influential. In summary, only observations #114, #997, #2152 and #2530 were not identified as potentially influential in the scheme of case-weight perturbation.

Figure 29 – Index plots of C_i for $\boldsymbol{\theta}_q$ (a), $\boldsymbol{\gamma}_q$ (b), $\boldsymbol{\nu}_q$ (c) and $\boldsymbol{\tau}_q$ (d) under case-weight perturbation, fitting the nonparametric QR model under the RPMOG distribution with $q = 0.1$.

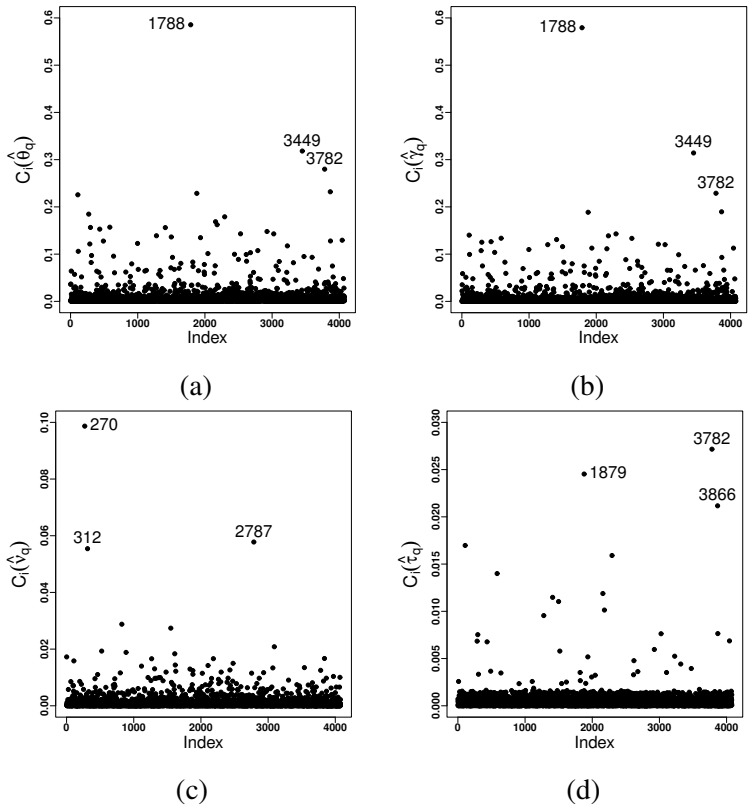

Figure 30 – Index plots of C_i for $\boldsymbol{\theta}_q$ (a), $\boldsymbol{\gamma}_q$ (b), $\boldsymbol{\nu}_q$ (c), and $\boldsymbol{\tau}_q$ under response perturbation, fitting the nonparametric QR model under the RPMOG distribution with $q = 0.1$.

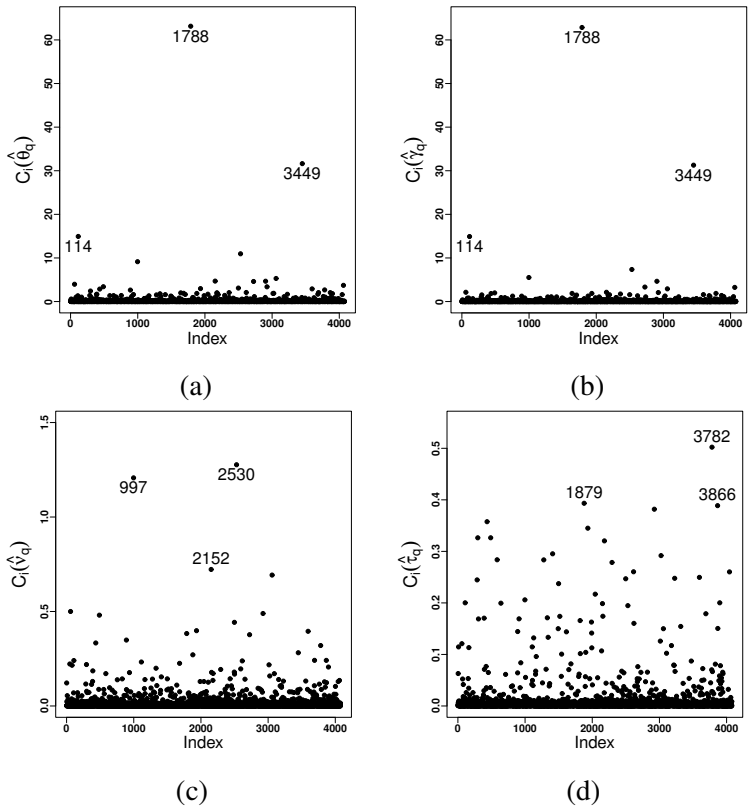

Finally, Figure 31 presents the index plot of C_i for $\boldsymbol{\tau}_q$ under the scheme of the skewness parameter perturbation. From there, observations #108, #1879 and #3782 are indicated as potentially influential. Only observation #108 is not presented in the two previous schemes.

Figure 31 – Index plots of C_i for $\boldsymbol{\tau}_q$ under skewness parameter perturbation, fitting the nonparametric QR model under the RPMOG distribution with $q = 0.1$.

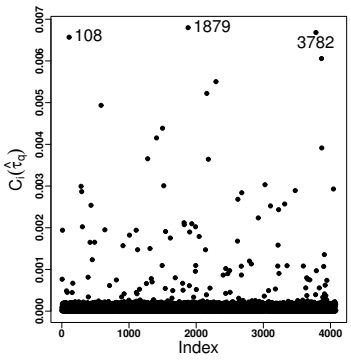

Table 12 provides the EFFM and UAL measures for the observations that are potentially influential. From the table, we can see that observations #114, #997, #1788, #2152, #2530, and #3449 have a low value of EFFM. Additionally, it can be observed that observations #114, #1788, and #2152 have a low value of UAL.

Table 12 – Estimated fat-free mass and upper arm length for potentially influential observations.

Observation	Estimated fat-free mass (in kg)	Upper arm length (in cm)	Observation	Estimated fat-free mass (in kg)	Upper arm length (in cm)
108	35.2	40	2158	35.1	39.6
114	15.6	23	2440	47.2	42.5
270	76.8	30.8	2530	14.2	25.5
312	64.4	30.8	2787	68.8	31.1
997	14.4	26	3449	14.8	23
1788	14.8	22.5	3782	25.1	35.8
1879	28.4	37	3866	27.6	36.5
2152	15.7	27.8			

5.2.5 Confirmatory analysis

We now investigate the impact on model inference when observations identified as potentially influential in the diagnostic analysis are removed. Table 13 reports the percentage RCs of the penalized ML estimates, asymptotic standard errors and p-values of ν_{1q}, ν_{2q} and τ_{1q} when we eliminate an observation or the set of all observations, denoted by I. When all potentially influential observations are removed, the largest relative changes occur, but no change in inferences is observed. Consequently, the nonparametric QR model under the RPMOG distribution showed robustness to outliers and influential observations.

Table 13 – Percentage relative changes in the estimates and standard errors fitting the nonparametric QR model under the RPMOG distribution and $q = 0.1$.

I		ν_{1q}	ν_{2q}	τ_{1q}	I		ν_{1q}	ν_{2q}	τ_{1q}
108	Estimate	0.762	0.276	1.336	2158	Estimate	0.464	0.153	1.164
	SE	0.386	0.353	0.013		SE	0.277	0.252	0.078
	p-value	< 0.001	< 0.001	< 0.001		p-value	< 0.001	< 0.001	< 0.001
114	Estimate	0.351	0.145	0.132	2440	Estimate	1.172	0.519	0.258
	SE	0.051	0.027	0.051		SE	0.231	0.228	0.153
	p-value	< 0.001	< 0.001	< 0.001		p-value	< 0.001	< 0.001	< 0.001
270	Estimate	1.154	0.629	2.370	2530	Estimate	0.569	0.234	0.137
	SE	0.034	0.056	0.638		SE	0.367	0.371	0.028
	p-value	< 0.001	< 0.001	< 0.001		p-value	< 0.001	< 0.001	< 0.001
312	Estimate	1.586	0.547	1.781	2787	Estimate	1.586	0.541	1.840
	SE	0.056	0.151	0.141		SE	0.076	0.175	0.158
	p-value	< 0.001	< 0.001	< 0.001		p-value	< 0.001	< 0.001	< 0.001
997	Estimate	0.887	0.377	0.225	3449	Estimate	0.341	0.139	0.078
	SE	0.338	0.347	0.029		SE	0.098	0.103	0.418
	p-value	< 0.001	< 0.001	< 0.001		p-value	< 0.001	< 0.001	< 0.001
1788	Estimate	0.245	0.100	0.132	3782	Estimate	0.033	0.055	1.523
	SE	0.089	0.061	0.092		SE	0.121	0.081	0.069
	p-value	< 0.001	< 0.001	< 0.001		p-value	< 0.001	< 0.001	< 0.001
1879	Estimate	0.331	0.109	1.254	3866	Estimate	0.553	0.218	1.227
	SE	0.063	0.042	0.325		SE	0.061	0.032	0.412
	p-value	< 0.001	< 0.001	< 0.001		p-value	< 0.001	< 0.001	< 0.001
2152	Estimate	0.676	0.297	0.352	All	Estimate	3.515	1.529	5.554
	SE	0.343	0.374	0.091		SE	2.106	1.890	0.607
	p-value	< 0.001	< 0.001	< 0.001		p-value	< 0.001	< 0.001	< 0.001

5.3 Final comments

This chapter presents simulation studies of the nonparametric QR models under the RPMON and RPMOG distributions in medium and large samples. The results indicate that the estimated nonparametric functions accurately capture the trend of the true function. Furthermore, the expected empirical values of the linear coefficients for the scale and skewness parameters are close to the true values of the parameters. However, for medium sample sizes, the estimates corresponding to the linear coefficients associated with the skewness parameter show a considerable bias. In addition, the coverage probabilities of the 95% confidence intervals are fairly close to the nominal values. Therefore, it is reasonable to assume that the empirical distributions of the estimates are close to the normal distribution.

From the results obtained in the application, we observed that the nonparametric QR models under the RPMOG distribution were a better fit than the other classes of QR models. The outlier observations were identified by utilizing the three distinct residuals proposed. Furthermore, influential observations are exposed by global and local influence tools. Finally, it is shown that the model is robust to the presence of outliers and influential observations through confirmatory analysis.

CHAPTER

6

CONCLUDING REMARKS

This dissertation proposes families of linear and partially linear quantile regression models where the response variable follows a reparameterized Marshall-Olkin (RPMO) distribution.

The RPMO distributions arise from applying the Marshall-Olkin transformation to distributions belonging to the location-scale family and then reparameterizing the location parameter as a function of the quantiles. These distributions presented closed forms of the pdf, cdf and qf. Studies on the skewness and kurtosis coefficients have shown that the distributions are flexible, especially in RPMON and RPMOG models. Based on these results, we formulate regression models that relate the q-th quantile, scale and skewness of the response variable to linear predictors using appropriate link functions.

From the log-likelihood function, were calculated the expressions of the score vector and the observed information matrix. The ML estimators do not have a closed form, which requires numerical maximization of the log-likelihood function. For this reason, the RS algorithm was adapted for obtaining ML estimates. Furthermore, the NQR, GCSR and MTR were used for studying the adequacy of the models and atypical observations. To detect influential observations, we presented measures of case deletion, such as likelihood displacement and generalized Cook's distance. Diagnostic techniques are developed to assess the sensitivity of the estimates in three perturbation schemes: case-weight, response variable and skewness parameter.

Subsequently, we introduce the partially linear QR models that are an extension of linear QR models. In order to approximate the nonparametric function, we use B-splines with the penalty criterion of difference matrices. Then, the penalized log-likelihood function was formulated to obtain the penalized score vector and the penalized observed information matrix. The estimation of the parameters, including the smoothing parameter, was carried out using the RS algorithm. Furthermore, we detail the selection of the models and the total effective degrees of freedom. Similar to linear QR models, the same three types of residuals, two measures of global influence, and three perturbation schemes as local influence techniques are adopted.

Also, the theory discussed during the dissertation is applied to two datasets from the area of health and nutrition. According to the descriptive analysis of both datasets, the relationship between the response variable and the covariates can be studied using linear and partially linear QR models. By means of the model selection criteria, the fits of the proposed QR model families are compared with their respective particular cases and other models. The best fit is observed when the response variable is assumed to follow an RPMOG distribution. In a particular quantile, the adequacy of the models was verified, and outlier observations were identified through residual analysis. Then, potentially influential observations were identified using techniques of global and local influence. The respective confirmatory analyses show that the inferences do not change if potentially influential observations are removed. Therefore, both families of models are robust to the presence of outliers and influential observations.

6.1 Computational aspects

In this dissertation, the expressions of pdf, cdf, qf, generator of random numbers, score vector and observed information matrix of the RPMO distributions were implemented as GAMLSS family distributions in the R language. Thus, the RS algorithm within the *gamlss* function was used to estimate the set of parameters of the family of linear QR models under the RPMO distributions. The great advantage was the optimization in programming, such as a few lines of code. However, one issue was finding good initial values for the RS algorithm to converge, especially for the RPMOG distribution. The reason is the high flexibility, demonstrated by the skewness and kurtosis coefficients, which rule out many outputs of other distributions as initial values.

The RS algorithm for the PLQR models was implemented manually in the R programming language. The initial values for the quantile, scale and skewness are the computational outputs of the gamlss function, specifying the RS algorithm, pb() function and RPMO family as options. This last function has the difficulty of not retrieving the smoothing parameter and the estimate of the vector B-spline, which is the reason for manually implementing the RS algorithm.

On the other hand, the residuals and methods of global and local influence were implemented in the R programming language with few lines of code. The expressions of the residuals and their envelopes require statistical and mathematical calculations such as the inverse cdf of the standard normal distribution, logarithm function and sign function found in any version of the software. The penalized likelihood displacement and the generalized Cook's distance have expressions that are often slow to calculate if the sample size is large because they require cycles. Finally, the three perturbation schemes that depend on the inverse of the penalized observed information matrix require low computational effort because the expressions of vectors and matrices are easy to calculate in the software.

6.2 Future works

A first prospect for future work is related to proposing bias-corrected estimators for the family of linear QR models under RPMO distributions. Recently, Magalhães, Gallardo and Bourguignon (2021) mentioned that efforts to improve the estimators continue to be well-received in the statistical literature. For example, Magalhães *et al.* (2020) presented a method to obtain estimators with a reduced bias for the parameters of extended Marshall-Olkin distributions. Palm, Bayer and Cintra (2020) introduced bias-adjusted estimators tailored for the Rayleigh regression model. Magalhães, Gallardo and Bourguignon (2021) and Barreto-Souza and Vasconcellos (2011) developed bias correction schemes for reparameterized inverse gamma regression model with varying precision and general extreme-value regression model, respectively.

Most of the works mentioned use the general expression given by Cox and Snell (1968), the bias adjustment given by Firth (1993), or bootstrap-based Efron (1992) bias adjustment. The results show that correcting for bias makes the corrected ML estimates better than the ML estimates without correction, even in small samples.

A second perspective of work is to extend the partially linear QR model to the class of semiparametric additive QR models. This class allows modeling the effects of covariates that contribute in a parametric and nonparametric way to the quantiles of the response variable. However, the approximation to the smooth functions would be through by using natural cubic splines (ncs). Some authors, such as Vanegas (2015) and Ibacache-Pulgar, Paula and Cysneiros (2013), have worked with ncs in semiparametric additive models and shown through illustrations its high flexibility.

BIBLIOGRAPHY

AKAIKE, H. A new look at the statistical model identification. **IEEE Transactions on Automatic Control**, IEEE, v. 19, n. 6, p. 716–723, 1974. Citation on page 55.

BARRETO-SOUZA, W.; VASCONCELLOS, K. L. Bias and skewness in a general extreme-value regression model. **Computational Statistics & Data Analysis**, Elsevier, v. 55, n. 3, p. 1379–1393, 2011. Citation on page 95.

BOOR, C. D. **A practical guide to splines**. [S.l.]: Springer-Verlag New York, 1978. Citation on page 64.

CAI, Z. Regression quantiles for time series. **Econometric Theory**, Cambridge University Press, v. 18, n. 1, p. 169–192, 2002. Citation on page 24.

CAI, Z.; GU, J.; LI, Q. Some recent developments on nonparametric econometrics. **Nonparametric Econometric Methods**, Emerald Group Publishing Limited, v. 25, p. 495–549, 2009. Citation on page 24.

CAI, Z.; XIAO, Z. Semiparametric quantile regression estimation in dynamic models with partially varying coefficients. **Journal of Econometrics**, Elsevier, v. 167, n. 2, p. 413–425, 2012. Citation on page 24.

CARDOZO, C. A.; PAULA, G. A.; VANEGAS, L. H. Generalized log–gamma additive partial linear models with p–spline smoothing. **Statistical Papers**, Springer, v. 63, n. 6, p. 1953–1978, 2022. Citations on pages 64, 65, and 70.

COOK, R. D. Assessment of local influence. **Journal of the Royal Statistical Society: Series B (Methodological)**, Wiley Online Library, v. 48, n. 2, p. 133–155, 1986. Citation on page 43.

COOK, R. D.; WEISBERG, S. **Residuals and influence in regression**. [S.l.]: New York: Chapman and Hall, 1982. Citations on pages 42 and 43.

CORTÉS, I. E.; CASTRO, M. de; GALLARDO, D. I. A new family of quantile regression models applied to nutritional data. **Journal of Applied Statistics**, Taylor & Francis, p. 1–21, 2023. Citation on page 24.

COX, D. R.; SNELL, E. J. A general definition of residuals. **Journal of the Royal Statistical Society: Series B (Methodological)**, Wiley Online Library, v. 30, n. 2, p. 248–265, 1968. Citations on pages 41 and 95.

DAVINO, C.; FURNO, M.; VISTOCCO, D. **Quantile regression: theory and applications**. [S.l.]: John Wiley & Sons, 2013. Citation on page 24.

DRAPER, N. R.; SMITH, H. **Applied regression analysis**. [S.l.]: John Wiley & Sons, 1998. Citation on page 23.

DUNN, P. K.; SMYTH, G. K. Randomized quantile residuals. **Journal of Computational and Graphical Statistics**, Taylor & Francis, v. 5, n. 3, p. 236–244, 1996. Citation on page 40.

EFRON, B. **Bootstrap methods: another look at the jackknife**. [S.l.]: Springer, 1992. Citation on page 95.

EILERS, P. H.; MARX, B. D. Flexible smoothing with b–splines and penalties. **Statistical Science**, Institute of Mathematical Statistics, v. 11, n. 2, p. 89–121, 1996. Citation on page 65.

FERREIRA, C. d. S. **Inferência e diagnósticos em modelos assimétricos**. Phd Thesis (PhD Thesis) — Universidade de São Paulo, 2008. Citation on page 43.

FIRTH, D. Bias reduction of maximum likelihood estimates. **Biometrika**, Oxford University Press, v. 80, n. 1, p. 27–38, 1993. Citation on page 95.

GALARZA, C. E.; BENITES, L.; BOURGUIGNON, M.; LACHOS, V. H. **lqr: Robust Linear Quantile Regression**. [S.l.], 2022. R package version 5.0. Available: <https://CRAN.R-project.org/package=lqr>. Citation on page 55.

GALLARDO, D. I.; BOURGUIGNON, M.; GALARZA, C. E.; GÓMEZ, H. W. A parametric quantile regression model for asymmetric response variables on the real line. **Symmetry**, Multidisciplinary Digital Publishing Institute, v. 12, n. 12, p. 1938, 2020. Citation on page 24.

GARCÍA, V. J.; GÓMEZ-DÉNIZ, E.; VÁZQUEZ-POLO, F. J. A new skew generalization of the normal distribution: Properties and applications. **Computational Statistics & Data Analysis**, Elsevier, v. 54, n. 8, p. 2021–2034, 2010. Citation on page 25.

GOOIJER, J. G. D.; ZEROM, D. On additive conditional quantiles with high-dimensional covariates. **Journal of the American Statistical Association**, Taylor & Francis, v. 98, n. 461, p. 135–146, 2003. Citation on page 24.

GORDON, R. A. **Regression analysis for the social sciences**. [S.l.]: Routledge, 2015. Citation on page 23.

HAO, L.; NAIMAN, D. Q. **Quantile regression**. [S.l.]: Sage, 2007. Citation on page 23.

HUNTER, D. R.; LANGE, K. Quantile regression via an mm algorithm. **Journal of Computational and Graphical Statistics**, Taylor & Francis, v. 9, n. 1, p. 60–77, 2000. Citation on page 24.

IBACACHE-PULGAR, G.; PAULA, G. A.; CYSNEIROS, F. J. A. Semiparametric additive models under symmetric distributions. **Test**, Springer, v. 22, p. 103–121, 2013. Citation on page 95.

IBACACHE-PULGAR, G.; PAULA, G. A.; GALEA, M. Influence diagnostics for elliptical semiparametric mixed models. **Statistical Modelling**, Sage Publications Sage India: New Delhi, India, v. 12, n. 2, p. 165–193, 2012. Citation on page 70.

JACOB, E.; JAYAKUMAR, K. Skew cauchy distribution and process. **Journal of Statistics and Applications**, Prints Publications Pvt. Ltd., v. 7, n. 1/2, p. 15, 2012. Citation on page 25.

JODRA, P.; JIMENEZ-GAMERO, M. D. **A quantile regression model for bounded responses based on the exponential-geometric distribution**. [S.l.], 2020. Citation on page 24.

KOENKER, R.; JR, G. B. Regression quantiles. **Econometrica: Journal of the Econometric Society**, JSTOR, p. 33–50, 1978. Citation on page 23.

KORKMAZ, M. Ç.; KORKMAZ, Z. S. The unit log–log distribution: a new unit distribution with alternative quantile regression modeling and educational measurements applications. **Journal of Applied Statistics**, Taylor & Francis, v. 50, n. 4, p. 889–908, 2023. Citation on page 24.

MAGALHÃES, T. M.; GALLARDO, D. I.; BOURGUIGNON, M. Improved point estimation for inverse gamma regression models. **Journal of Statistical Computation and Simulation**, Taylor & Francis, v. 91, n. 12, p. 2444–2456, 2021. Citation on page 95.

MAGALHÃES, T. M.; GÓMEZ, Y. M.; GALLARDO, D. I.; VENEGAS, O. Bias reduction for the marshall-olkin extended family of distributions with application to an airplane's air conditioning system and precipitation data. **Symmetry**, MDPI, v. 12, n. 5, p. 851, 2020. Citation on page 95.

MARSHALL, A. W.; OLKIN, I. A new method for adding a parameter to a family of distributions with application to the exponential and weibull families. **Biometrika**, Oxford University Press, v. 84, n. 3, p. 641–652, 1997. Citations on pages 24 and 25.

MAZUCHELI, J.; MENEZES, A.; FERNANDES, L.; OLIVEIRA, R. D.; GHITANY, M. The unit-weibull distribution as an alternative to the kumaraswamy distribution for the modeling of quantiles conditional on covariates. **Journal of Applied Statistics**, Taylor & Francis, v. 47, n. 6, p. 954–974, 2020. Citation on page 24.

MORALES, C. G.; DAVILA, V. L.; CABRAL, C. B.; CEPERO, L. C. Robust quantile regression using a generalized class of skewed distributions. **Stat**, Wiley Online Library, v. 6, n. 1, p. 113–130, 2017. Citations on pages 24 and 55.

NELDER, J. A.; WEDDERBURN, R. W. Generalized linear models. **Journal of the Royal Statistical Society: Series A (General)**, Wiley Online Library, v. 135, n. 3, p. 370–384, 1972. Citation on page 24.

NOUFAILY, A.; JONES, M. Parametric quantile regression based on the generalized gamma distribution. **Journal of the Royal Statistical Society Series C: Applied Statistics**, Oxford University Press, v. 62, n. 5, p. 723–740, 2013. Citation on page 24.

PALM, B. G.; BAYER, F. M.; CINTRA, R. J. Improved point estimation for the rayleigh regression model. **IEEE Geoscience and Remote Sensing Letters**, IEEE, v. 19, p. 1–4, 2020. Citation on page 95.

PRATAVIERA, F.; ORTEGA, E. M.; CORDEIRO, G. M.; CANCHO, V. G. The exponentiated power exponential semiparametric regression model. **Communications in Statistics-Simulation and Computation**, Taylor & Francis, v. 51, n. 10, p. 5933–5953, 2022. Citation on page 72.

R Core Team. **R: A Language and Environment for Statistical Computing**. Vienna, Austria, 2022. Available: <https://www.R-project.org/>. Citations on pages 35 and 67.

RAMIRES, T. G.; NAKAMURA, L. R.; RIGHETTO, A. J.; PESCIM, R. R.; MAZUCHELI, J.; CORDEIRO, G. M. A new semiparametric weibull cure rate model: fitting different behaviors within gamlss. **Journal of Applied Statistics**, Taylor & Francis, v. 46, n. 15, p. 2744–2760, 2019. Citation on page 72.

RIGBY, R. A.; STASINOPOULOS, D. M. Generalized additive models for location, scale and shape. **Journal of the Royal Statistical Society: Series C (Applied Statistics)**, Wiley Online Library, v. 54, n. 3, p. 507–554, 2005. Citation on page 71.

____. Automatic smoothing parameter selection in gamlss with an application to centile estimation. **Statistical Methods in Medical Research**, Sage Publications Sage UK: London, England, v. 23, n. 4, p. 318–332, 2014. Citations on pages 67 and 68.

RUBIO, F. J.; STEEL, M. F. On the marshall–olkin transformation as a skewing mechanism. **Computational Statistics & Data Analysis**, Elsevier, v. 56, n. 7, p. 2251–2257, 2012. Citations on pages 25 and 28.

SÁNCHEZ, L.; LEIVA, V.; GALEA, M.; SAULO, H. Birnbaum-saunders quantile regression and its diagnostics with application to economic data. **Applied Stochastic Models in Business and Industry**, Wiley Online Library, v. 37, n. 1, p. 53–73, 2021. Citations on pages 24 and 45.

SCHWARZ, G. Estimating the dimension of a model. **The Annals of Statistics**, JSTOR, p. 461–464, 1978. Citation on page 55.

STASINOPOULOS, D. M.; RIGBY, R. A. Generalized additive models for location scale and shape (gamlss) in r. **Journal of Statistical Software**, v. 23, p. 1–46, 2008. Citation on page 36.

STASINOPOULOS, M. D.; RIGBY, R. A.; HELLER, G. Z.; VOUDOURIS, V.; BASTIANI, F. D. **Flexible regression and smoothing: using GAMLSS in R**. [S.l.]: CRC Press, 2017. Citation on page 35.

THERNEAU, T. M.; GRAMBSCH, P. M.; FLEMING, T. R. Martingale-based residuals for survival models. **Biometrika**, Oxford University Press, v. 77, n. 1, p. 147–160, 1990. Citation on page 42.

VANEGAS, L. H. **Log-symmetric Regression Models under the Presence of Uncensored, Left- or Right-censored Observations: A Semiparametric Approach**. Phd Thesis (PhD Thesis) — Universidade de São Paulo, 2015. Citation on page 95.

VANEGAS, L. H.; PAULA, G. A. An extension of log-symmetric regression models: R codes and applications. **Journal of Statistical Computation and Simulation**, Taylor & Francis, v. 86, n. 9, p. 1709–1735, 2016. Citation on page 71.

VASCONCELOS, J. C. S.; CORDEIRO, G. M.; ORTEGA, E. M. M. The semiparametric regression model for bimodal data with different penalized smoothers applied to climatology, ethanol and air quality data. **Journal of Applied Statistics**, Taylor & Francis, v. 49, n. 1, p. 248–267, 2022. Citation on page 72.

WOOD, S. N. **Generalized additive models: an introduction with R**. [S.l.]: CRC press, 2017. Citation on page 65.

APPENDIX

A

COMPLEMENTARY RESULTS OF SIMULATION STUDIES

This appendix shows the plots of the simulation studies on the linear QR models in the RPMO distributions mentioned in Section 3.1.

Figure 32 – Mean of the RB on the 3000 estimates of the components $\widehat{\boldsymbol{\beta}}_q$, $\widehat{\boldsymbol{\nu}}_q$ and $\widehat{\boldsymbol{\tau}}_q$ obtained in the RPMOG model under different sample sizes.

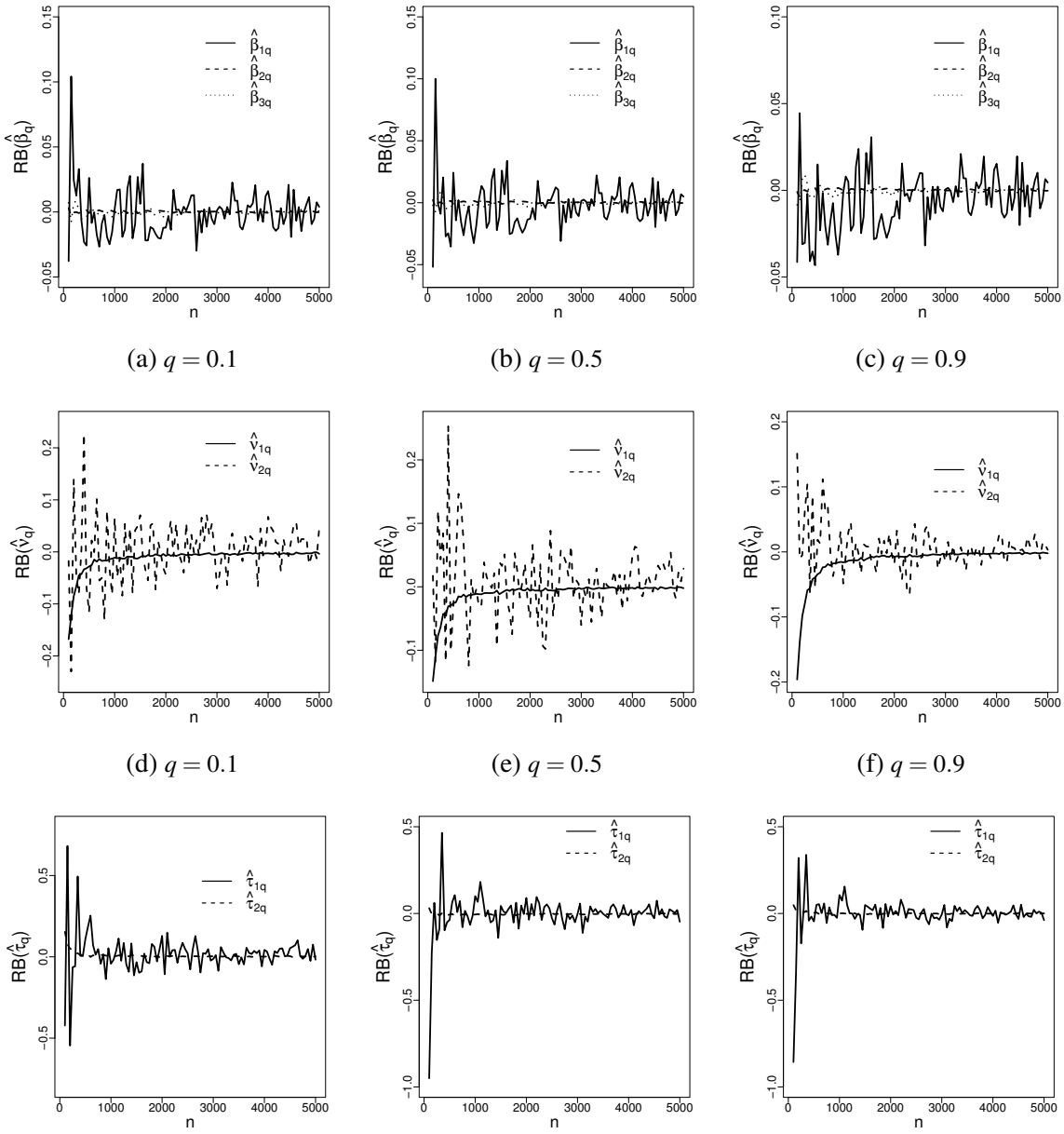

(a) $q = 0.1$ (b) $q = 0.5$ (c) $q = 0.9$

(d) $q = 0.1$ (e) $q = 0.5$ (f) $q = 0.9$

(g) $q = 0.1$ (h) $q = 0.5$ (i) $q = 0.9$

Figure 33 – SD on the 3000 estimates of the components $\widehat{\boldsymbol{\beta}}_q$, $\widehat{\boldsymbol{\nu}}_q$ and $\widehat{\boldsymbol{\tau}}_q$ obtained in the RPMOG model under different sample sizes.

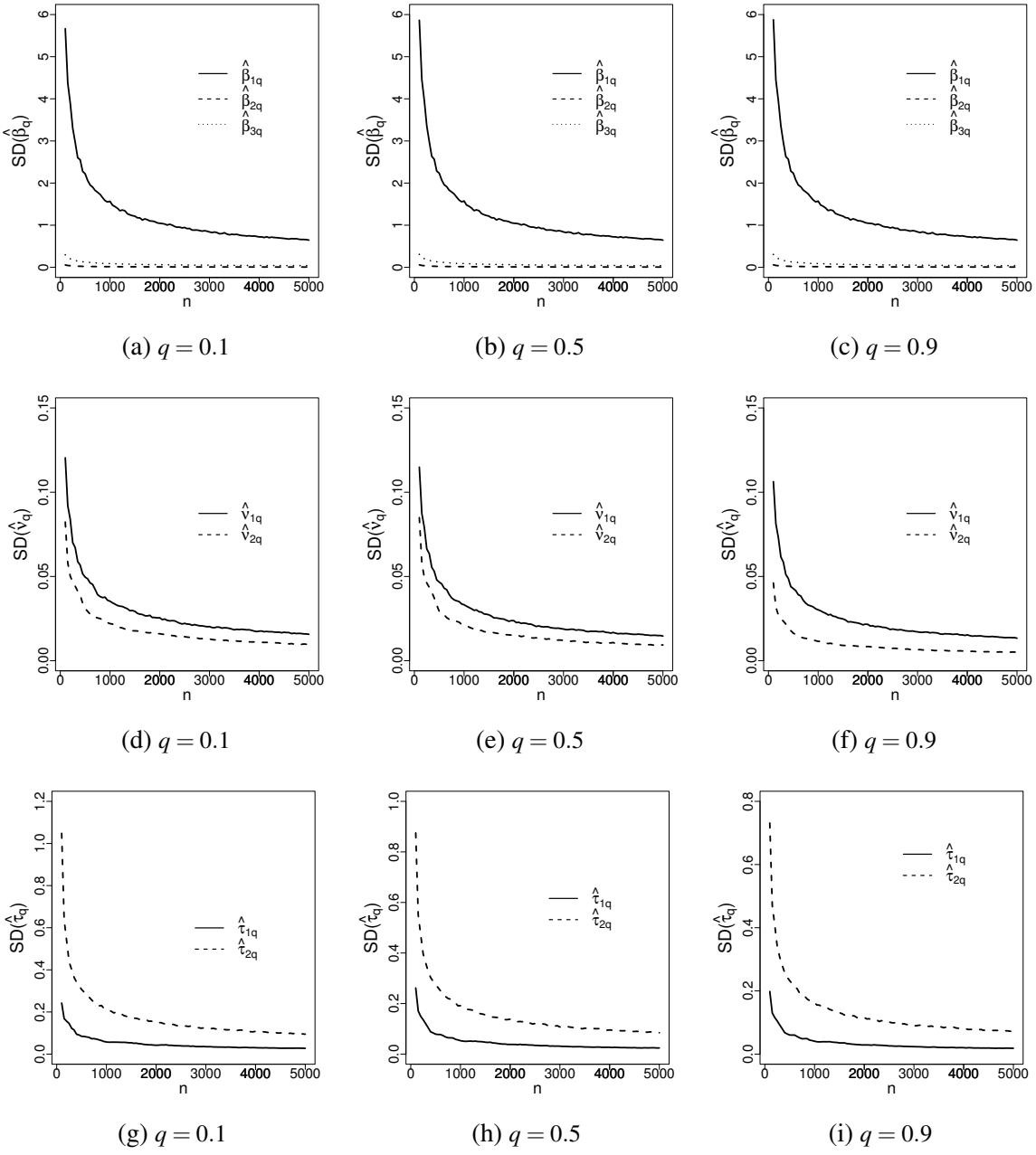

(a) $q = 0.1$ (b) $q = 0.5$ (c) $q = 0.9$

(d) $q = 0.1$ (e) $q = 0.5$ (f) $q = 0.9$

(g) $q = 0.1$ (h) $q = 0.5$ (i) $q = 0.9$

Figure 34 – RMSE on the 3000 estimates of the components $\widehat{\boldsymbol{\beta}}_q$, $\widehat{\boldsymbol{\nu}}_q$ and $\widehat{\boldsymbol{\tau}}_q$ obtained in the RPMOG model under different sample sizes.

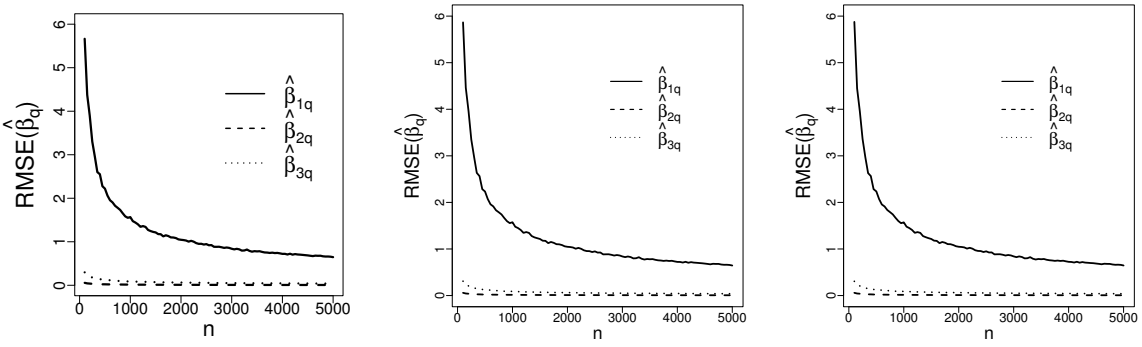

(a) $q = 0.1$ (b) $q = 0.5$ (c) $q = 0.9$

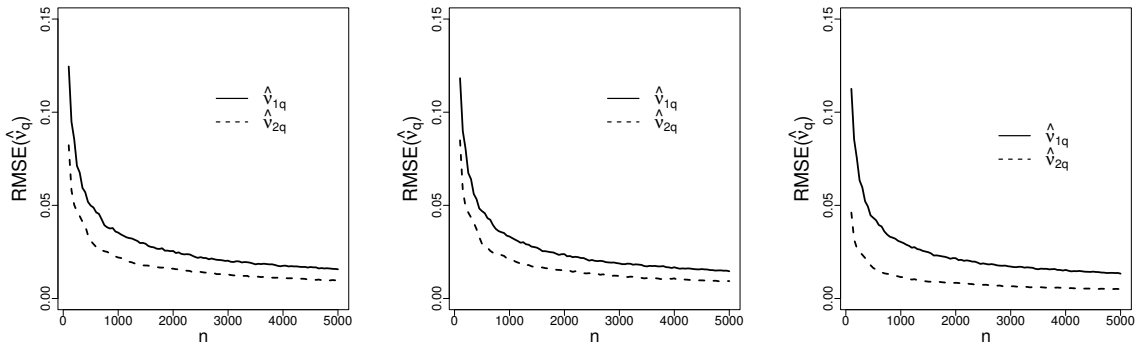

(d) $q = 0.1$ (e) $q = 0.5$ (f) $q = 0.9$

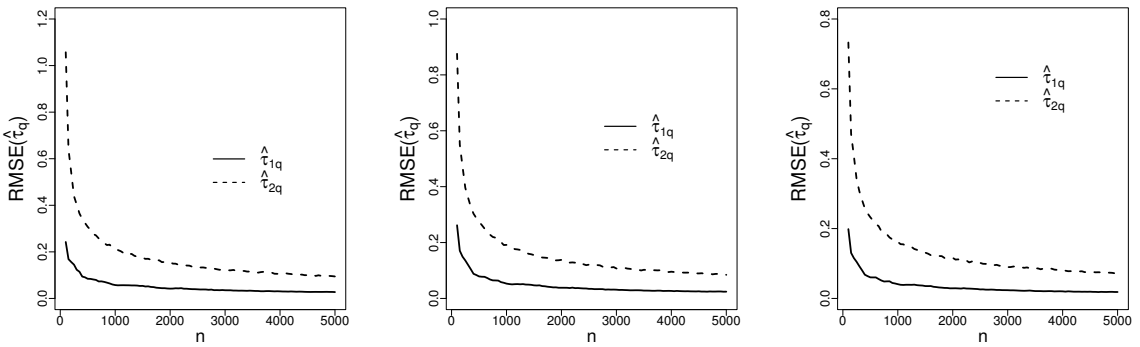

(g) $q = 0.1$ (h) $q = 0.5$ (i) $q = 0.9$

Figure 35 – Mean of the asymptotic SE on the 3000 estimates of the components $\widehat{\boldsymbol{\beta}}_q$, $\widehat{\boldsymbol{\nu}}_q$ and $\widehat{\boldsymbol{\tau}}_q$ obtained in the RPMOG model under different sample sizes.

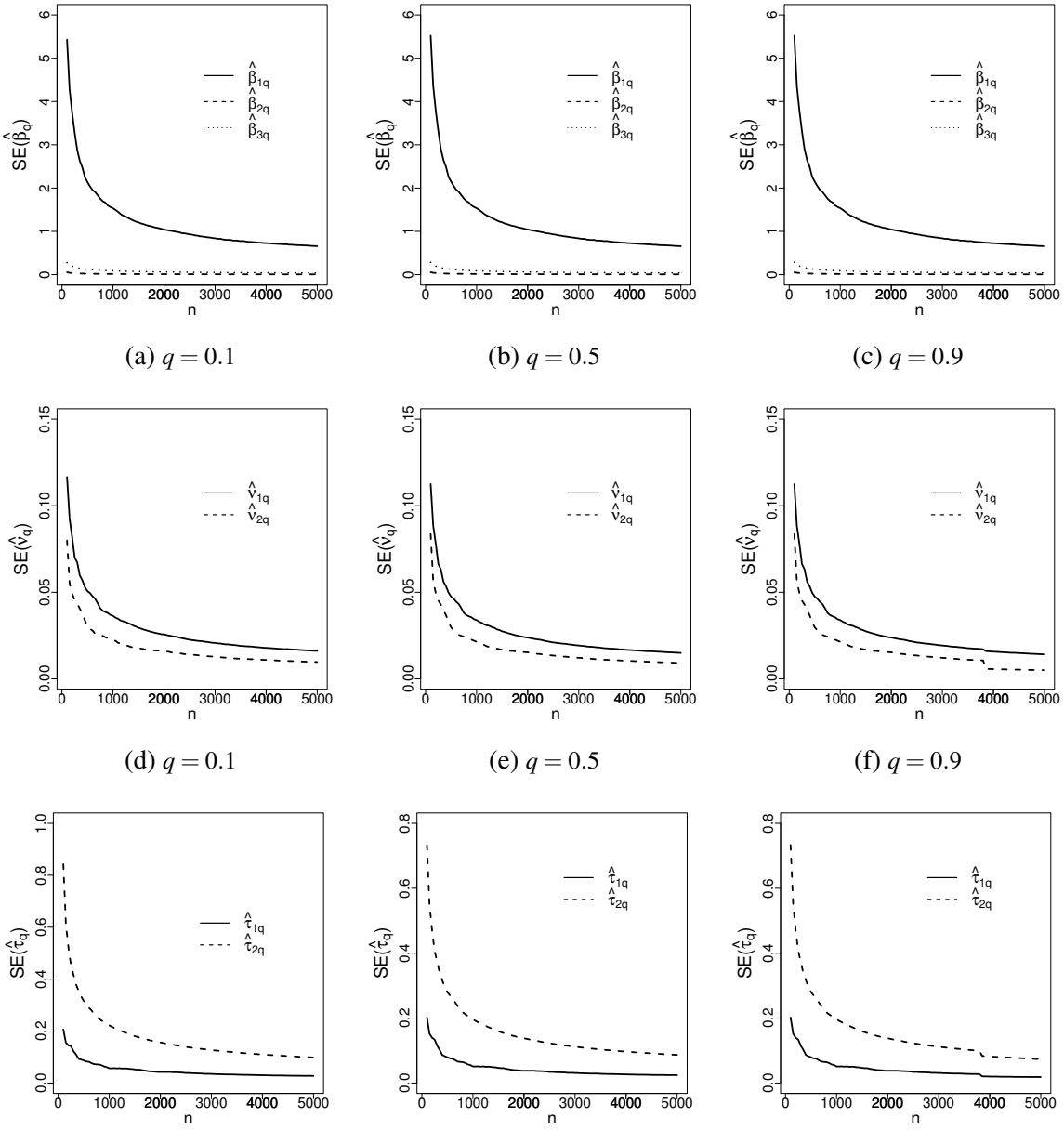

(a) $q = 0.1$ (b) $q = 0.5$ (c) $q = 0.9$

(d) $q = 0.1$ (e) $q = 0.5$ (f) $q = 0.9$

(g) $q = 0.1$ (h) $q = 0.5$ (i) $q = 0.9$

Figure 36 – 95% CP of the components $\widehat{\boldsymbol{\beta}}_q$, $\widehat{\boldsymbol{\nu}}_q$ and $\widehat{\boldsymbol{\tau}}_q$ obtained in the RPMOG model under different sample sizes.

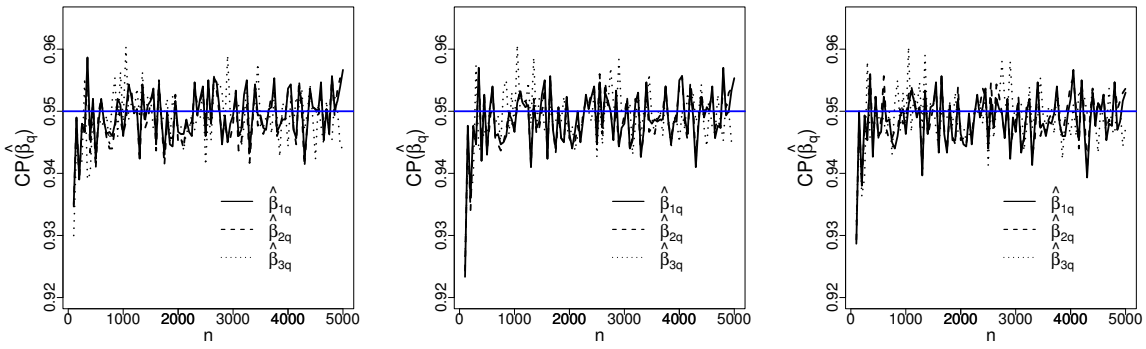

(a) $q = 0.1$ (b) $q = 0.5$ (c) $q = 0.9$

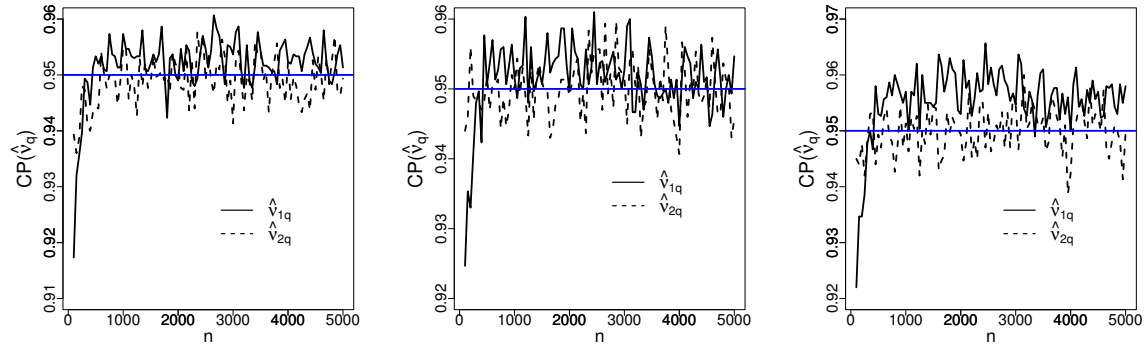

(d) $q = 0.1$ (e) $q = 0.5$ (f) $q = 0.9$

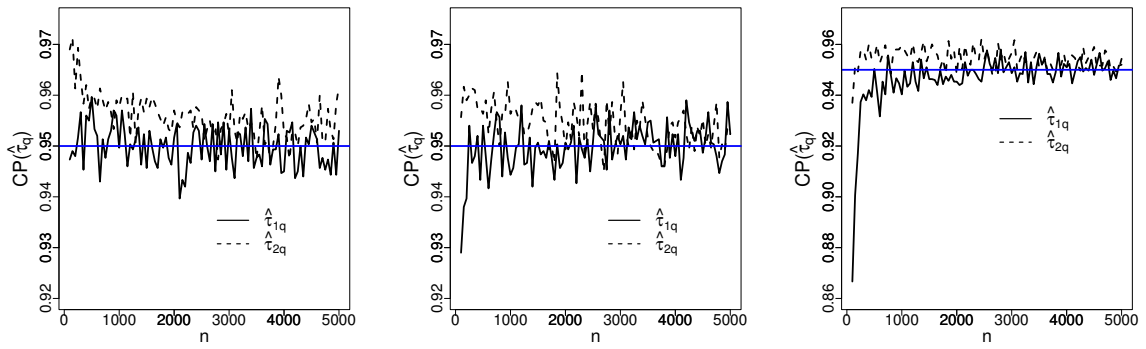

(g) $q = 0.1$ (h) $q = 0.5$ (i) $q = 0.9$

Figure 37 – Mean of the RB on the 3000 estimates of the components $\widehat{\boldsymbol{\beta}}_q$, $\widehat{\boldsymbol{\nu}}_q$ and $\widehat{\boldsymbol{\tau}}_q$ obtained in the RPMOT model under different sample sizes.

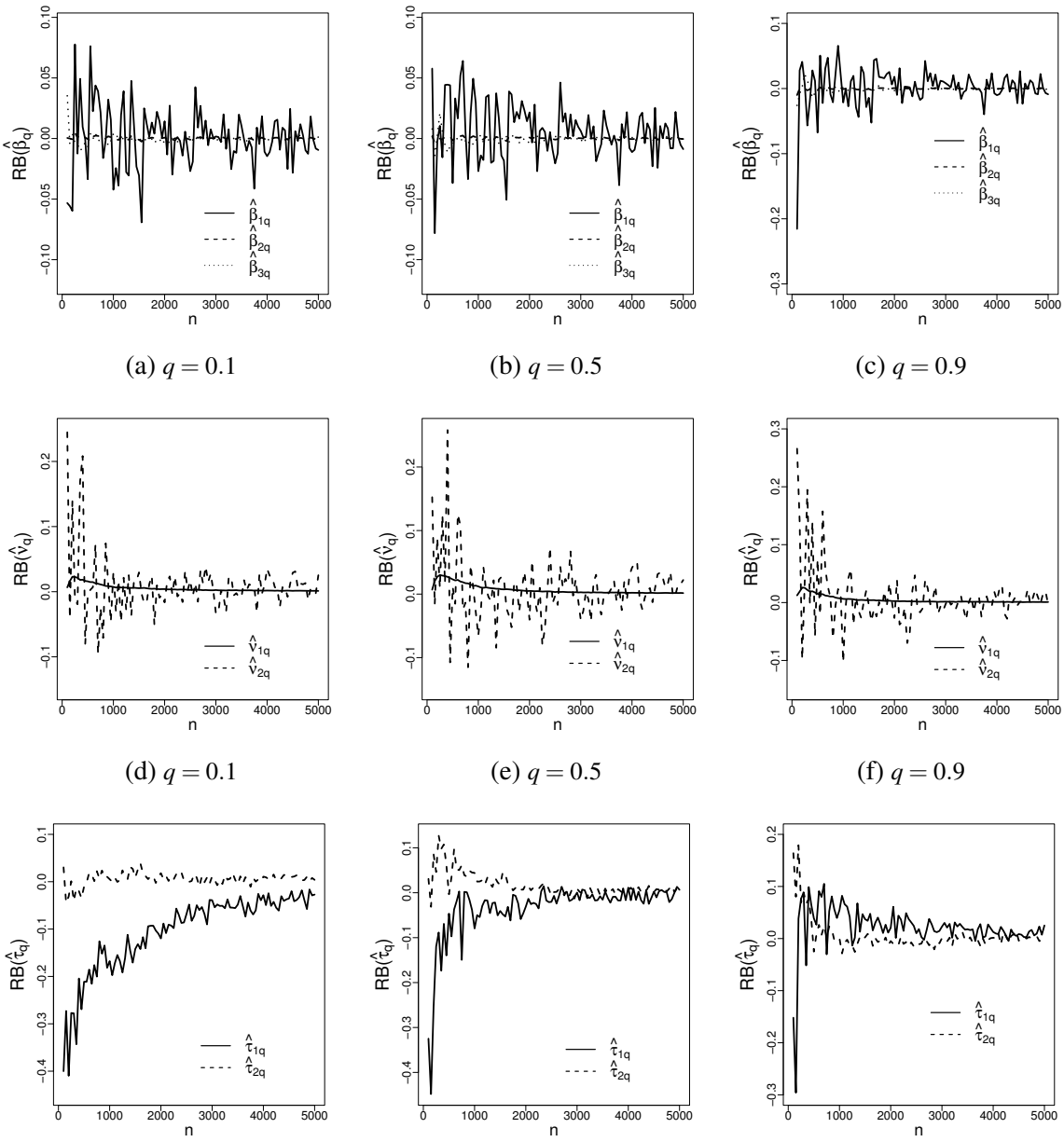

(a) $q = 0.1$ (b) $q = 0.5$ (c) $q = 0.9$

(d) $q = 0.1$ (e) $q = 0.5$ (f) $q = 0.9$

(g) $q = 0.1$ (h) $q = 0.5$ (i) $q = 0.9$

Figure 38 – SD on the 3000 estimates of the components $\widehat{\boldsymbol{\beta}}_q$, $\widehat{\boldsymbol{\nu}}_q$ and $\widehat{\boldsymbol{\tau}}_q$ obtained in the RPMOT model under different sample sizes.

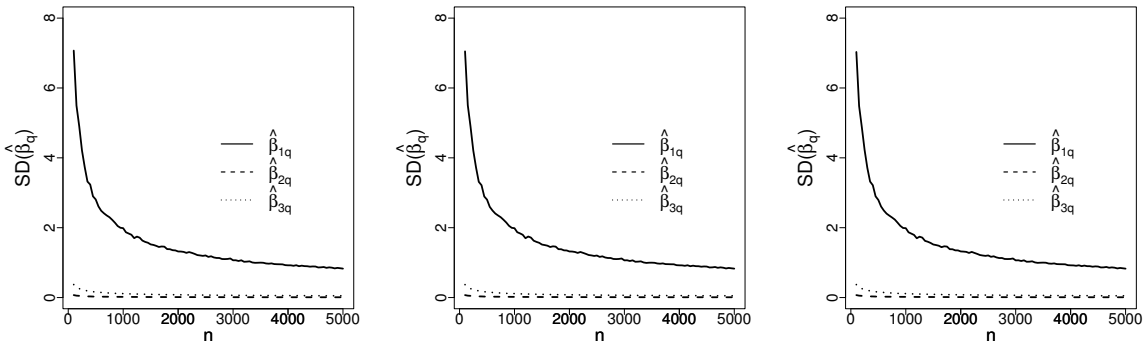

(a) $q = 0.1$ (b) $q = 0.5$ (c) $q = 0.9$

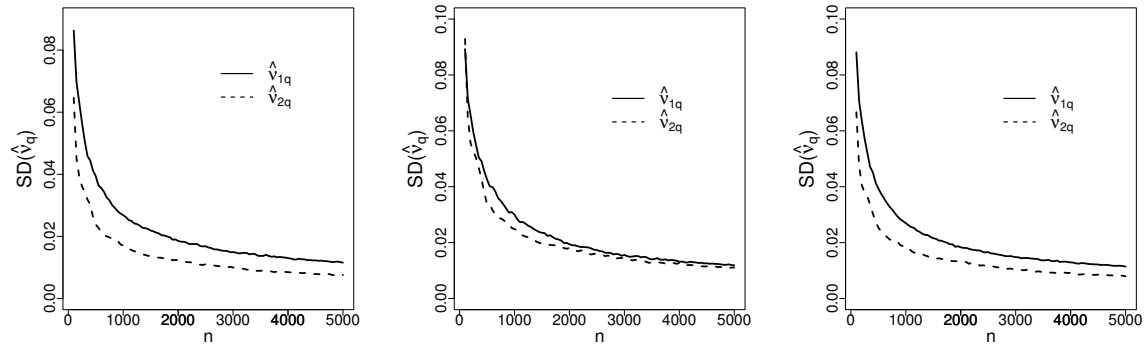

(d) $q = 0.1$ (e) $q = 0.5$ (f) $q = 0.9$

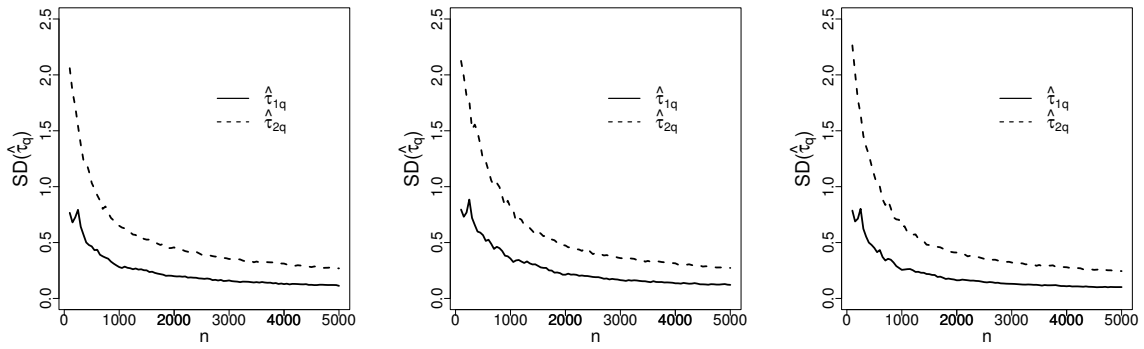

(g) $q = 0.1$ (h) $q = 0.5$ (i) $q = 0.9$

Figure 39 – RMSE on the 3000 estimates of the components $\widehat{\boldsymbol{\beta}}_q$, $\widehat{\boldsymbol{\nu}}_q$ and $\widehat{\boldsymbol{\tau}}_q$ obtained in the RPMOT model under different sample sizes.

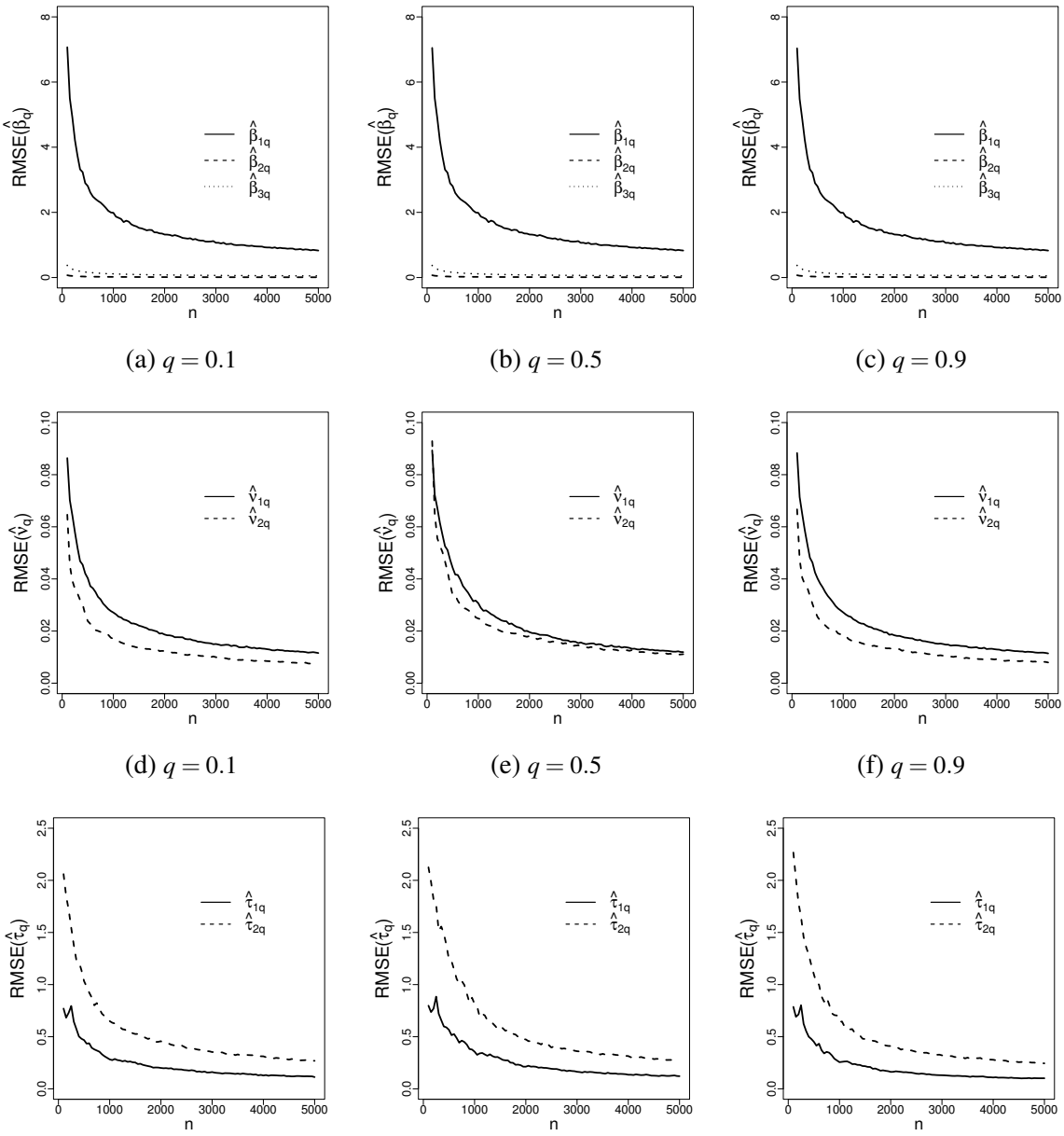

(a) $q = 0.1$ (b) $q = 0.5$ (c) $q = 0.9$

(d) $q = 0.1$ (e) $q = 0.5$ (f) $q = 0.9$

(g) $q = 0.1$ (h) $q = 0.5$ (i) $q = 0.9$

Figure 40 – Mean of the asymptotic SE on the 3000 estimates of the components $\widehat{\boldsymbol{\beta}}_q$, $\widehat{\boldsymbol{\nu}}_q$ and $\widehat{\boldsymbol{\tau}}_q$ obtained in the RPMOT model under different sample sizes.

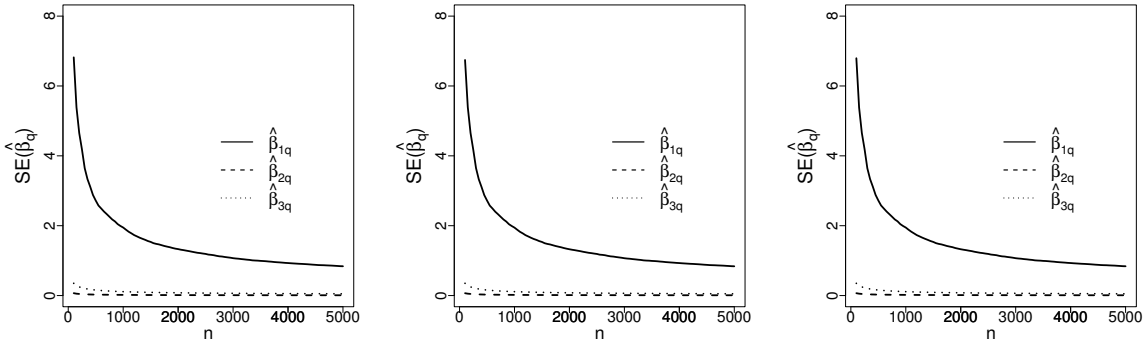

(a) $q = 0.1$ (b) $q = 0.5$ (c) $q = 0.9$

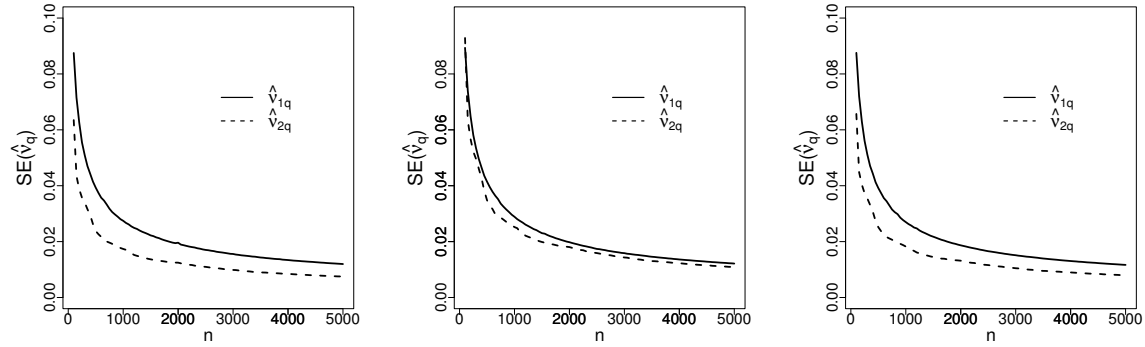

(d) $q = 0.1$ (e) $q = 0.5$ (f) $q = 0.9$

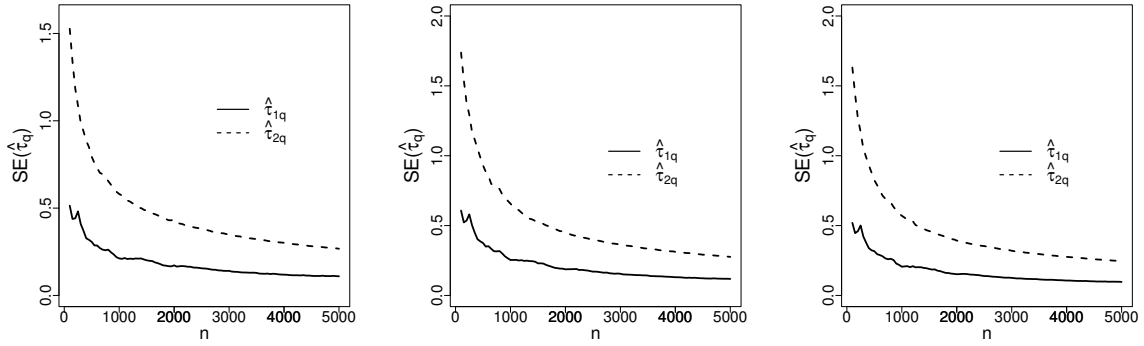

(g) $q = 0.1$ (h) $q = 0.5$ (i) $q = 0.9$

Figure 41 – 95% CP of the components $\widehat{\boldsymbol{\beta}}_q$, $\widehat{\boldsymbol{\nu}}_q$ and $\widehat{\boldsymbol{\tau}}_q$ obtained in the RPMOT model under different sample sizes.

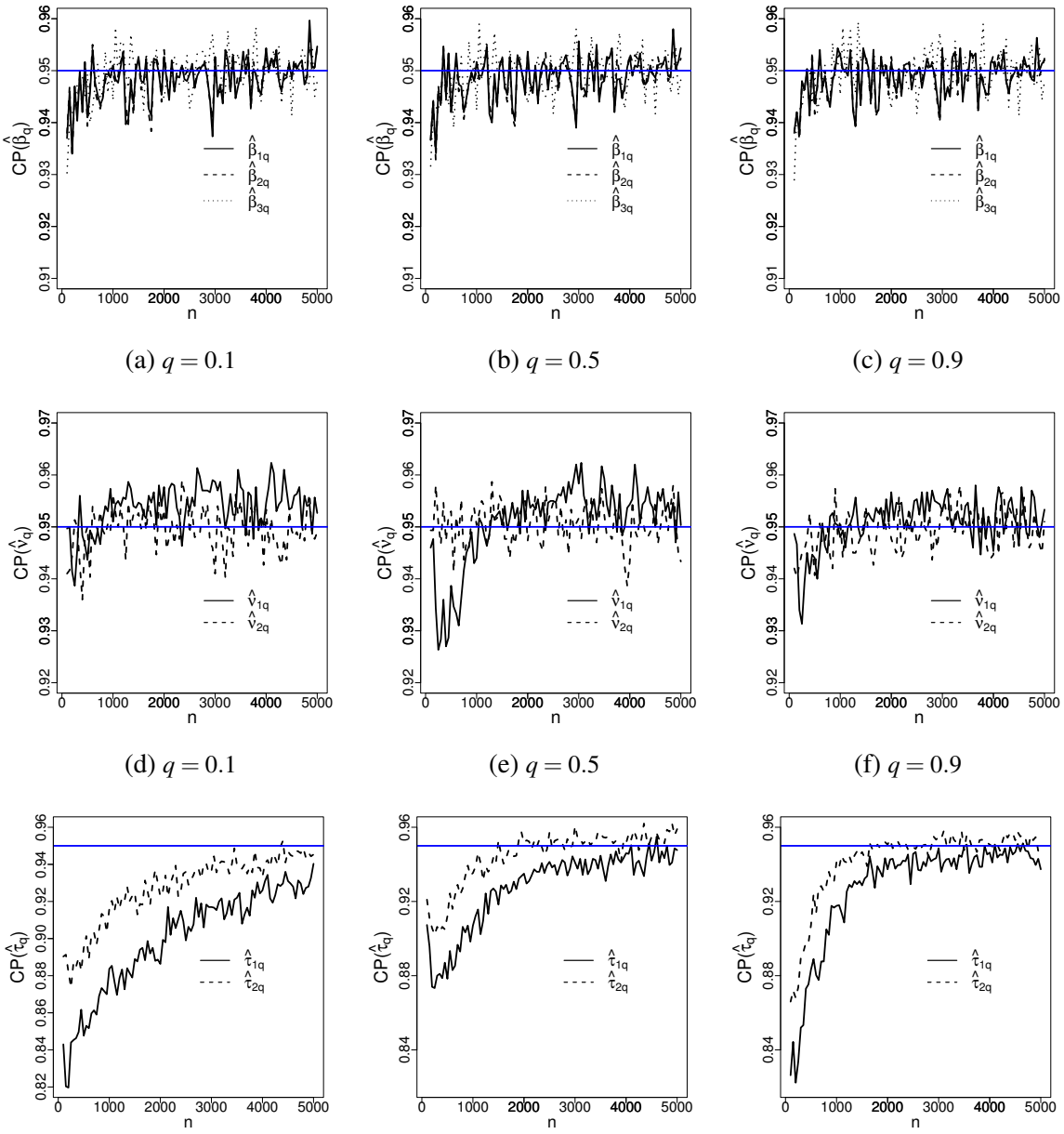

(a) $q = 0.1$ (b) $q = 0.5$ (c) $q = 0.9$

(d) $q = 0.1$ (e) $q = 0.5$ (f) $q = 0.9$

(g) $q = 0.1$ (h) $q = 0.5$ (i) $q = 0.9$

Figure 42 – $\mathrm{SE}_i/\mathrm{SE}_{i+1}$ and $\sqrt{n_{i+1}/n_i}$ rates for the parameters indicated in the linear QR model under RPMON distribution, considering $q = 0.1$.

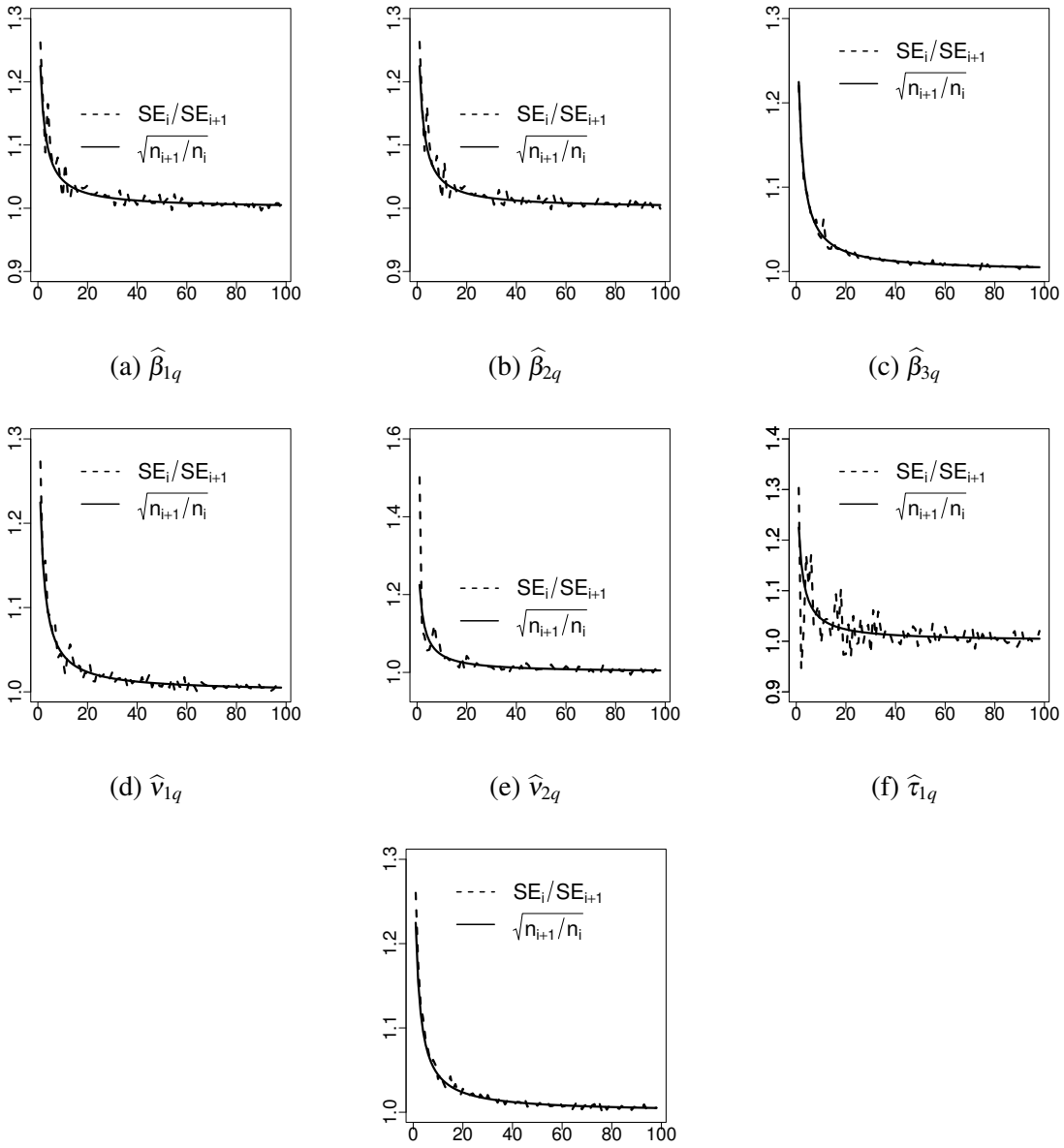

(a) $\widehat{\beta}_{1q}$ (b) $\widehat{\beta}_{2q}$ (c) $\widehat{\beta}_{3q}$

(d) $\widehat{\nu}_{1q}$ (e) $\widehat{\nu}_{2q}$ (f) $\widehat{\tau}_{1q}$

(g) $\widehat{\tau}_{2q}$

Figure 43 – $\mathrm{SE}_i/\mathrm{SE}_{i+1}$ and $\sqrt{n_{i+1}/n_i}$ rates for the parameters indicated in the linear QR model under RPMON distribution, considering $q = 0.5$.

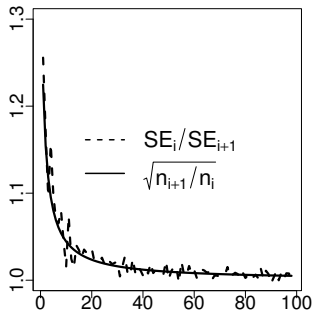

(a) $\widehat{\beta}_{1q}$

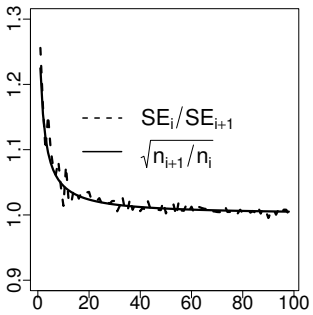

(b) $\widehat{\beta}_{2q}$

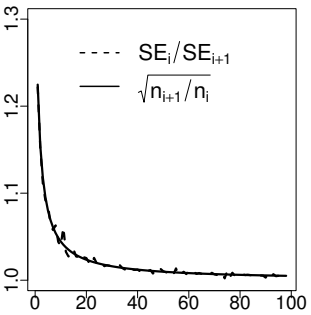

(c) $\widehat{\beta}_{3q}$

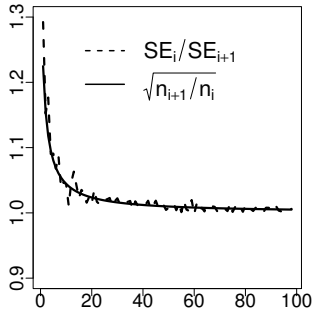

(d) $\widehat{\nu}_{1q}$

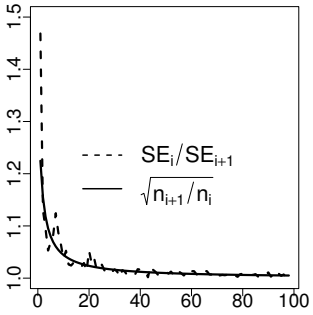

(e) $\widehat{\nu}_{2q}$

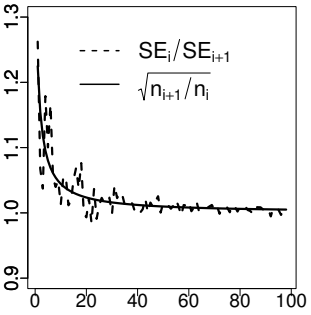

(f) $\widehat{\tau}_{1q}$

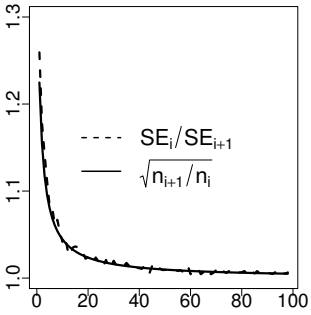

(g) $\widehat{\tau}_{2q}$

Figure 44 – $\mathrm{SE}_i/\mathrm{SE}_{i+1}$ and $\sqrt{n_{i+1}/n_i}$ rates for the parameters indicated in the linear QR model under RPMON distribution, considering $q = 0.9$.

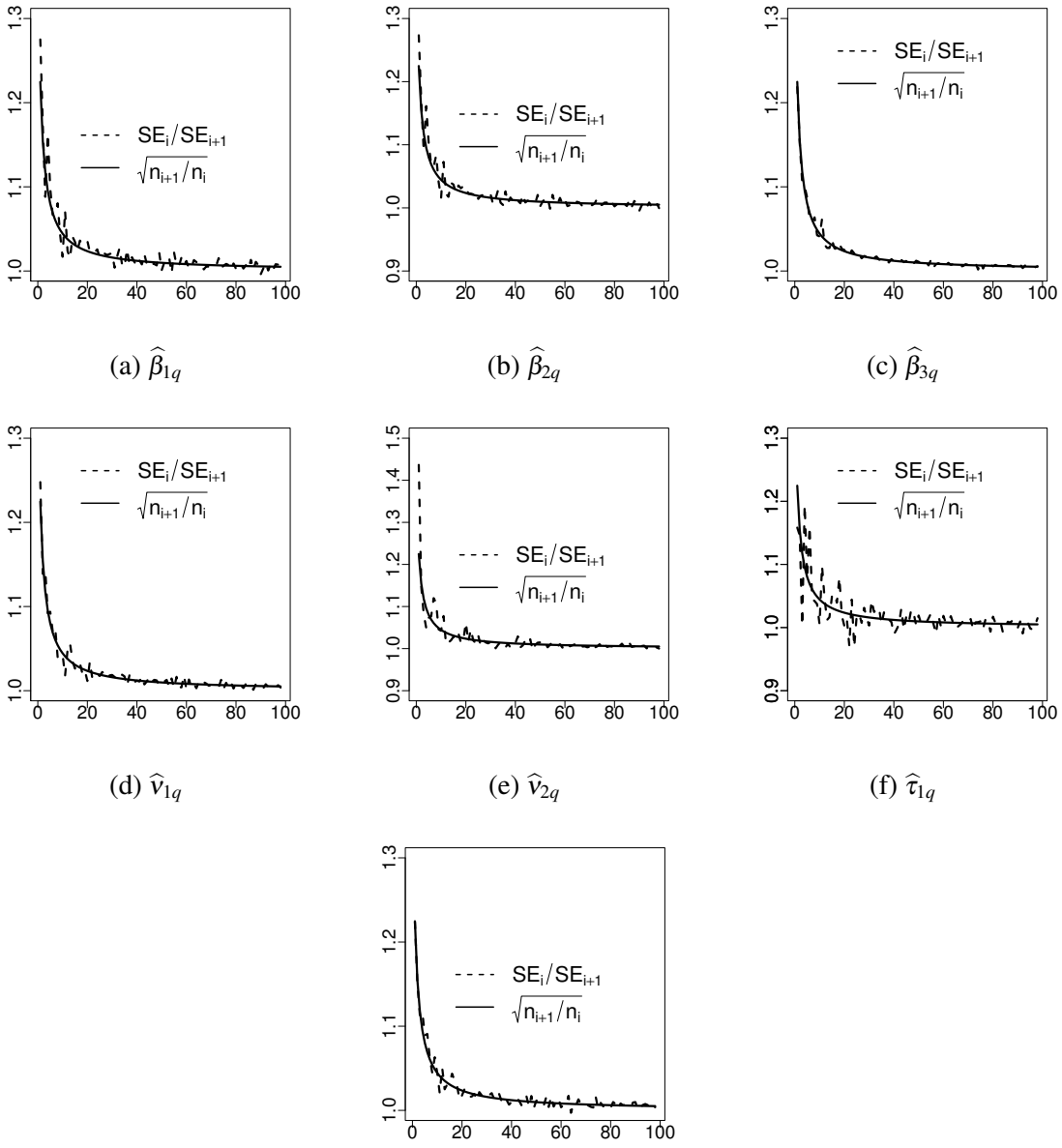

(a) $\widehat{\beta}_{1q}$ (b) $\widehat{\beta}_{2q}$ (c) $\widehat{\beta}_{3q}$

(d) $\widehat{\nu}_{1q}$ (e) $\widehat{\nu}_{2q}$ (f) $\widehat{\tau}_{1q}$

(g) $\widehat{\tau}_{2q}$

Figure 45 – $\mathrm{SE}_i/\mathrm{SE}_{i+1}$ and $\sqrt{n_{i+1}/n_i}$ rates for the parameters indicated in the linear QR model under RPMOG distribution, considering $q = 0.1$.

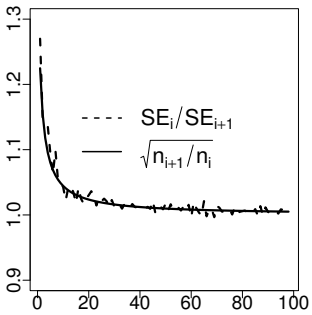

(a) $\widehat{\beta}_{1q}$

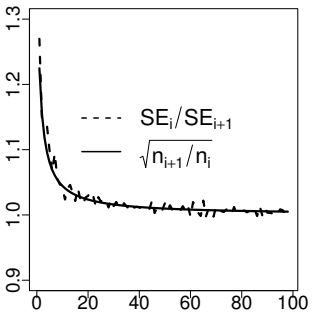

(b) $\widehat{\beta}_{2q}$

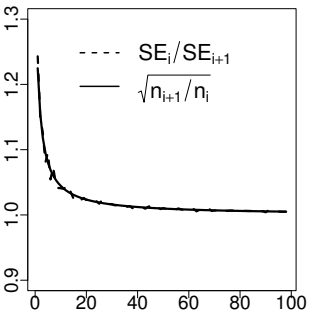

(c) $\widehat{\beta}_{3q}$

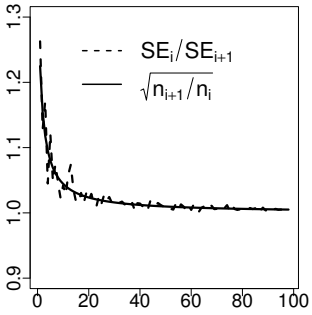

(d) $\widehat{\nu}_{1q}$

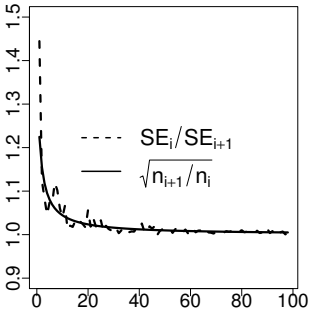

(e) $\widehat{\nu}_{2q}$

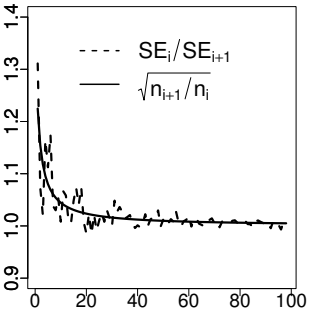

(f) $\widehat{\tau}_{1q}$

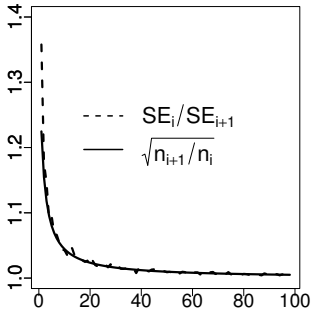

(g) $\widehat{\tau}_{2q}$

Figure 46 – $\mathrm{SE}_i/\mathrm{SE}_{i+1}$ and $\sqrt{n_{i+1}/n_i}$ rates for the parameters indicated in the linear QR model under RPMOG distribution, considering $q = 0.5$.

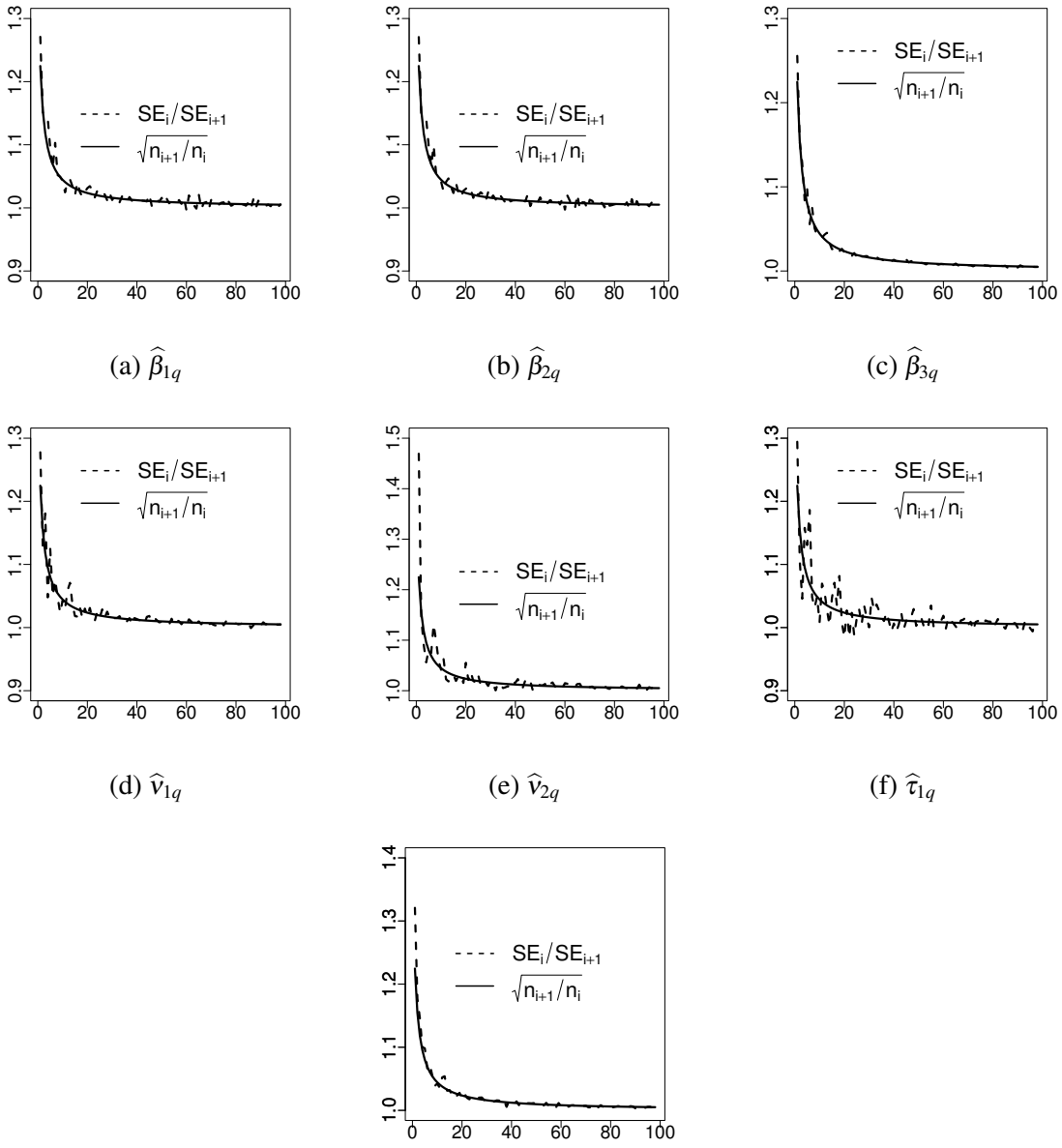

(a) $\widehat{\beta}_{1q}$ (b) $\widehat{\beta}_{2q}$ (c) $\widehat{\beta}_{3q}$

(d) $\widehat{\nu}_{1q}$ (e) $\widehat{\nu}_{2q}$ (f) $\widehat{\tau}_{1q}$

(g) $\widehat{\tau}_{2q}$

Figure 47 – $\mathrm{SE}_i/\mathrm{SE}_{i+1}$ and $\sqrt{n_{i+1}/n_i}$ rates for the parameters indicated in the linear QR model under RPMOG distribution, considering $q = 0.9$.

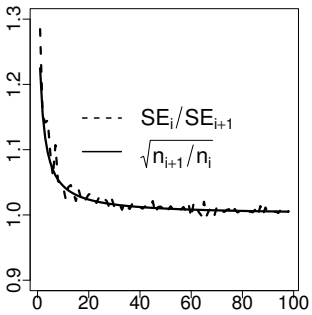

(a) $\widehat{\beta}_{1q}$

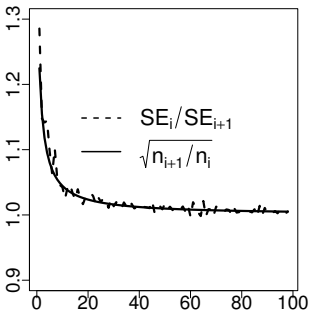

(b) $\widehat{\beta}_{2q}$

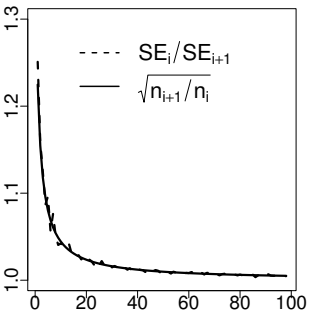

(c) $\widehat{\beta}_{3q}$

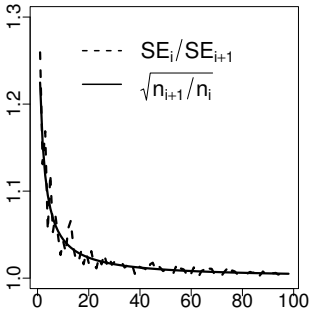

(d) $\widehat{\nu}_{1q}$

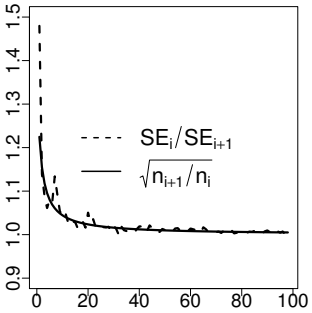

(e) $\widehat{\nu}_{2q}$

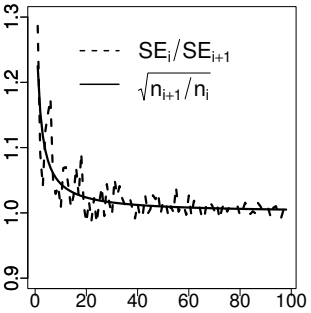

(f) $\widehat{\tau}_{1q}$

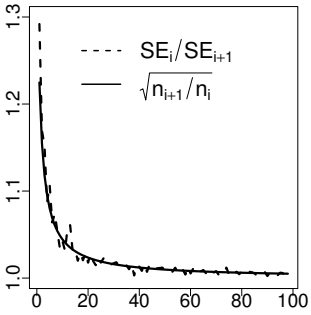

(g) $\widehat{\tau}_{2q}$

Figure 48 – $\mathrm{SE}_i/\mathrm{SE}_{i+1}$ and $\sqrt{n_{i+1}/n_i}$ rates for the parameters indicated in the linear QR model under RPMOT distribution ($\vartheta = 15$), considering $q = 0.1$.

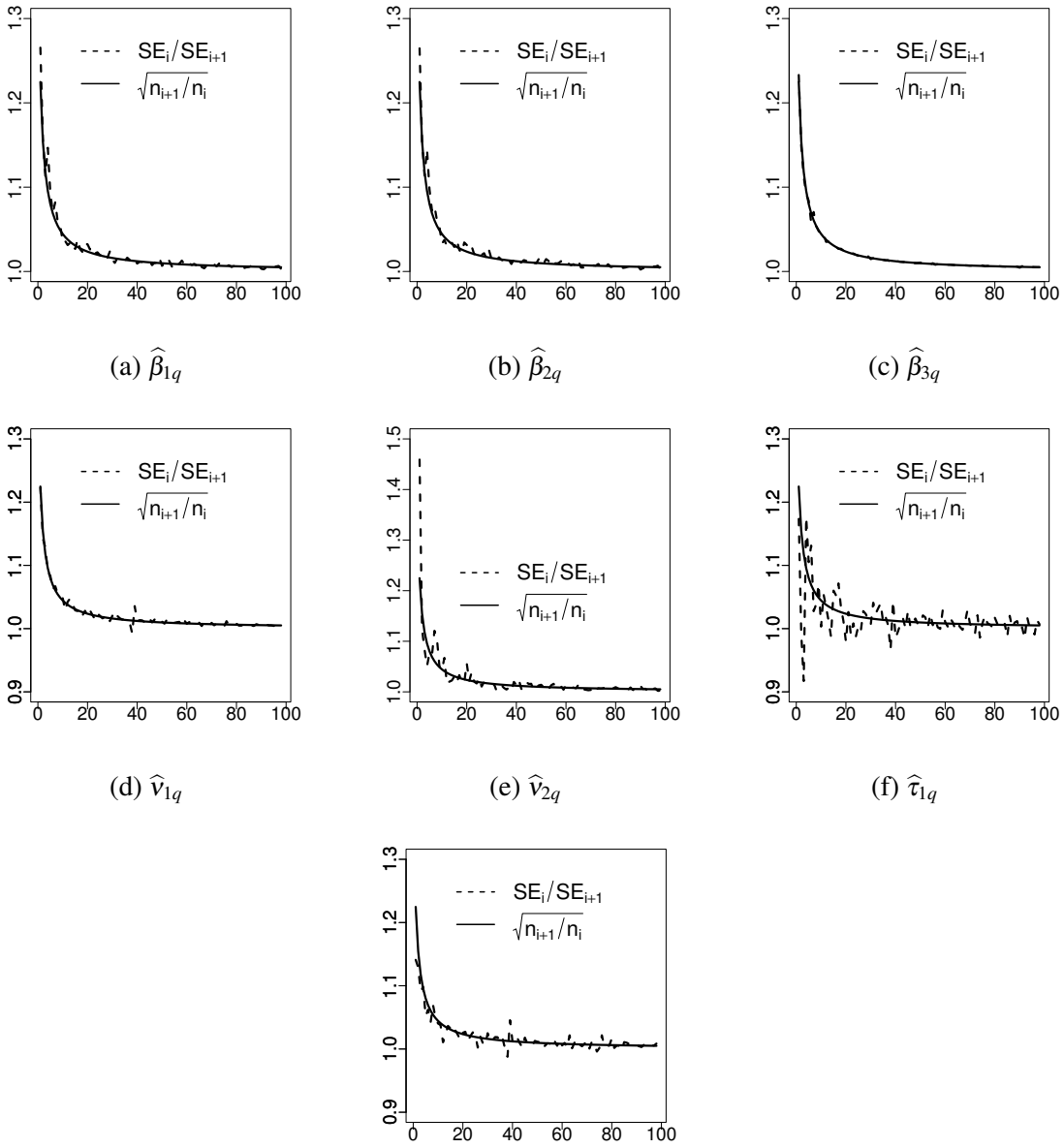

(a) $\widehat{\beta}_{1q}$ (b) $\widehat{\beta}_{2q}$ (c) $\widehat{\beta}_{3q}$

(d) $\widehat{\nu}_{1q}$ (e) $\widehat{\nu}_{2q}$ (f) $\widehat{\tau}_{1q}$

(g) $\widehat{\tau}_{2q}$

Figure 49 – $\mathrm{SE}_i/\mathrm{SE}_{i+1}$ and $\sqrt{n_{i+1}/n_i}$ rates for the parameters indicated in the linear QR model under RPMOT distribution ($\vartheta = 15$), considering $q = 0.5$.

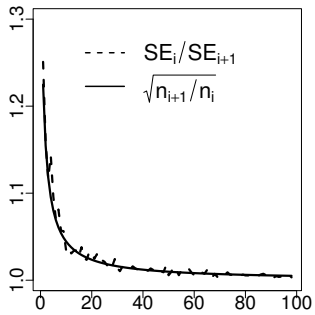

(a) $\widehat{\beta}_{1q}$

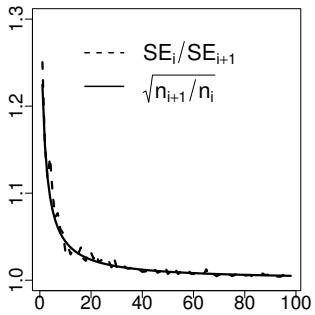

(b) $\widehat{\beta}_{2q}$

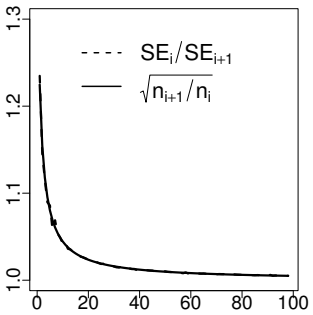

(c) $\widehat{\beta}_{3q}$

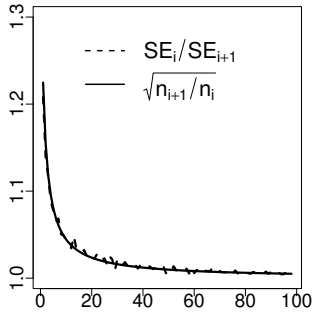

(d) $\widehat{\nu}_{1q}$

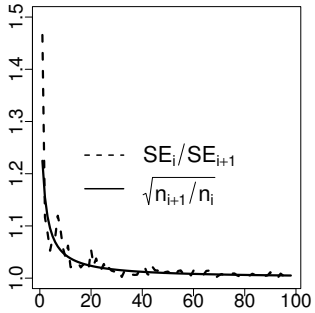

(e) $\widehat{\nu}_{2q}$

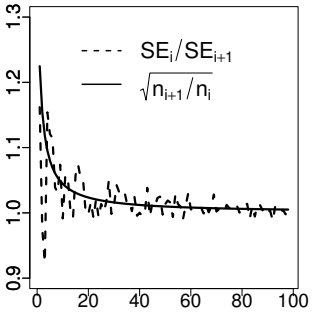

(f) $\widehat{\tau}_{1q}$

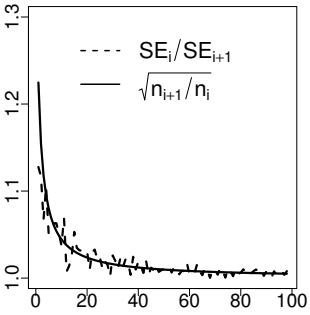

(g) $\widehat{\tau}_{2q}$

Figure 50 – $\mathrm{SE}_i/\mathrm{SE}_{i+1}$ and $\sqrt{n_{i+1}/n_i}$ rates for the parameters indicated in the linear QR model under RPMOT distribution ($\vartheta = 15$), considering $q = 0.9$.

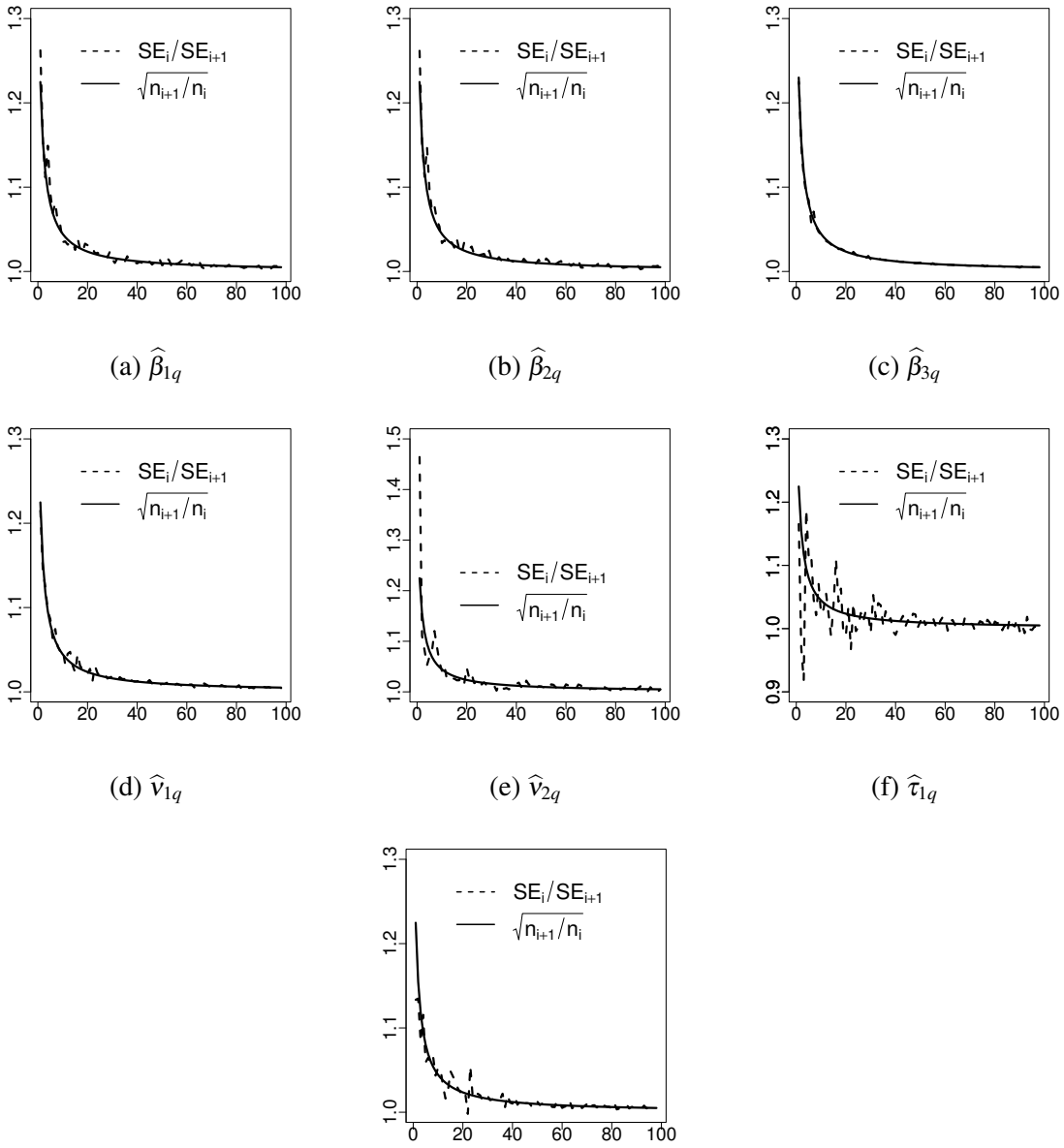

(a) $\widehat{\beta}_{1q}$ (b) $\widehat{\beta}_{2q}$ (c) $\widehat{\beta}_{3q}$

(d) $\widehat{\nu}_{1q}$ (e) $\widehat{\nu}_{2q}$ (f) $\widehat{\tau}_{1q}$

(g) $\widehat{\tau}_{2q}$

APPENDIX

B

COMPLEMENTARY RESULTS OF SIMULATION STUDIES II

This appendix shows the plots of the simulation studies on the nonparametric QR models in the RPMO distributions mentioned in Section 5.1.

Figure 51 – Mean of the RB on the 500 estimates of the components $\widehat{\boldsymbol{\nu}}_q$ and $\widehat{\boldsymbol{\tau}}_q$ obtained in the RPMOG model under different sample sizes.

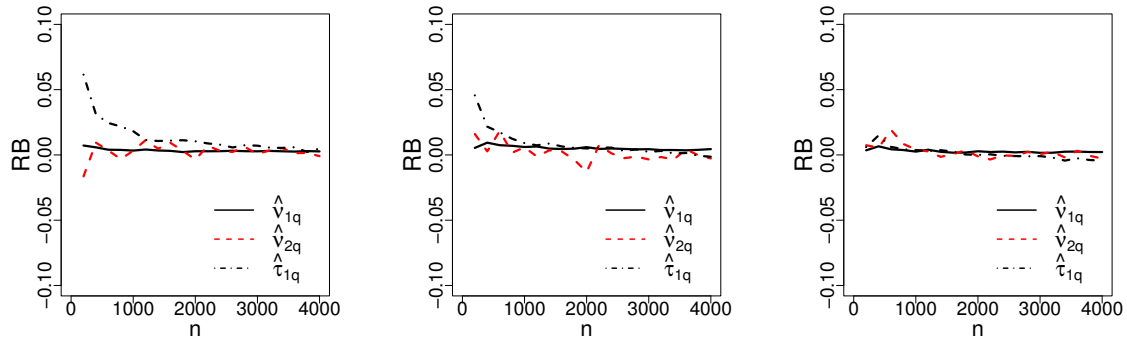

(a) $q = 0.1$ (b) $q = 0.5$ (c) $q = 0.9$

Figure 52 – SD on the 500 estimates of the components $\widehat{\boldsymbol{\nu}}_q$ and $\widehat{\boldsymbol{\tau}}_q$ obtained in the RPMOG model under different sample sizes.

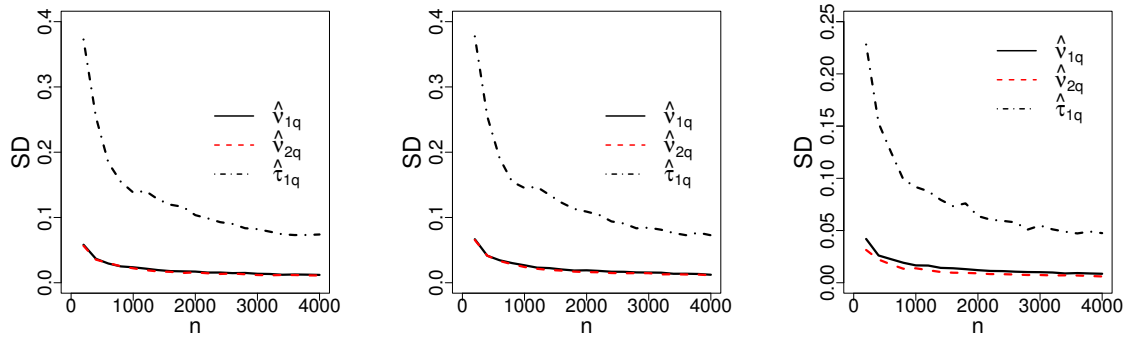

(a) $q = 0.1$ (b) $q = 0.5$ (c) $q = 0.9$

Figure 53 – RMSE on the 500 estimates of the components $\widehat{\boldsymbol{\nu}}_q$ and $\widehat{\boldsymbol{\tau}}_q$ obtained in the RPMOG model under different sample sizes.

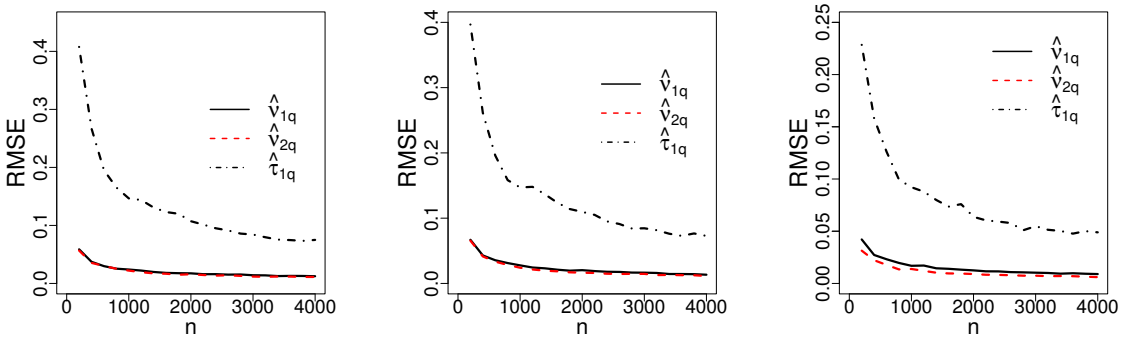

(a) $q = 0.1$ (b) $q = 0.5$ (c) $q = 0.9$

Figure 54 – Mean of the asymptotic SE on the 500 estimates of the components $\widehat{\boldsymbol{\nu}}_q$ and $\widehat{\boldsymbol{\tau}}_q$ obtained in the RPMOG model under different sample sizes.

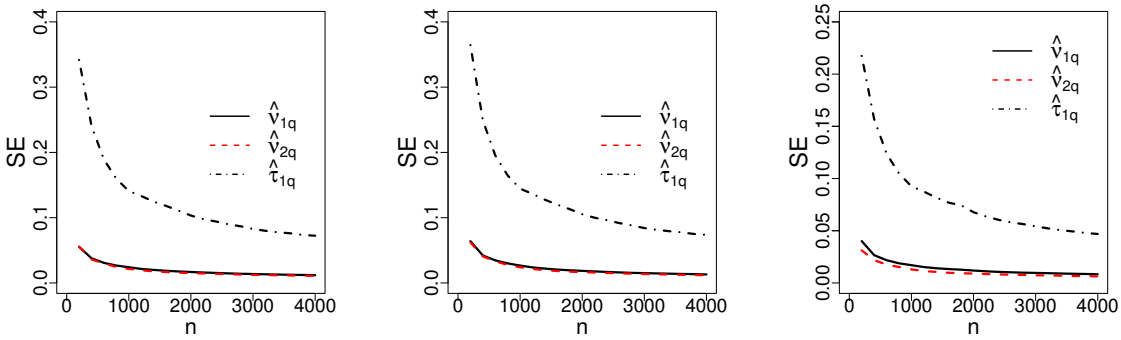

(a) $q = 0.1$ (b) $q = 0.5$ (c) $q = 0.9$

Figure 55 – 95% CP of the components $\widehat{\boldsymbol{\nu}}_q$ and $\widehat{\boldsymbol{\tau}}_q$ obtained in the RPMOG model under different sample sizes.

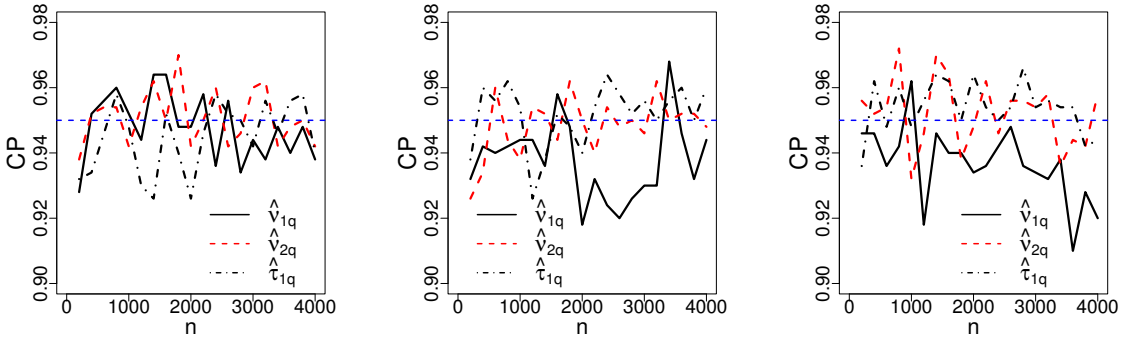

(a) $q = 0.1$ (b) $q = 0.5$ (c) $q = 0.9$

Figure 56 – Smooth function mean on the 500 estimates obtained in the RPMOG model under different sample sizes and $q = 0.1$.

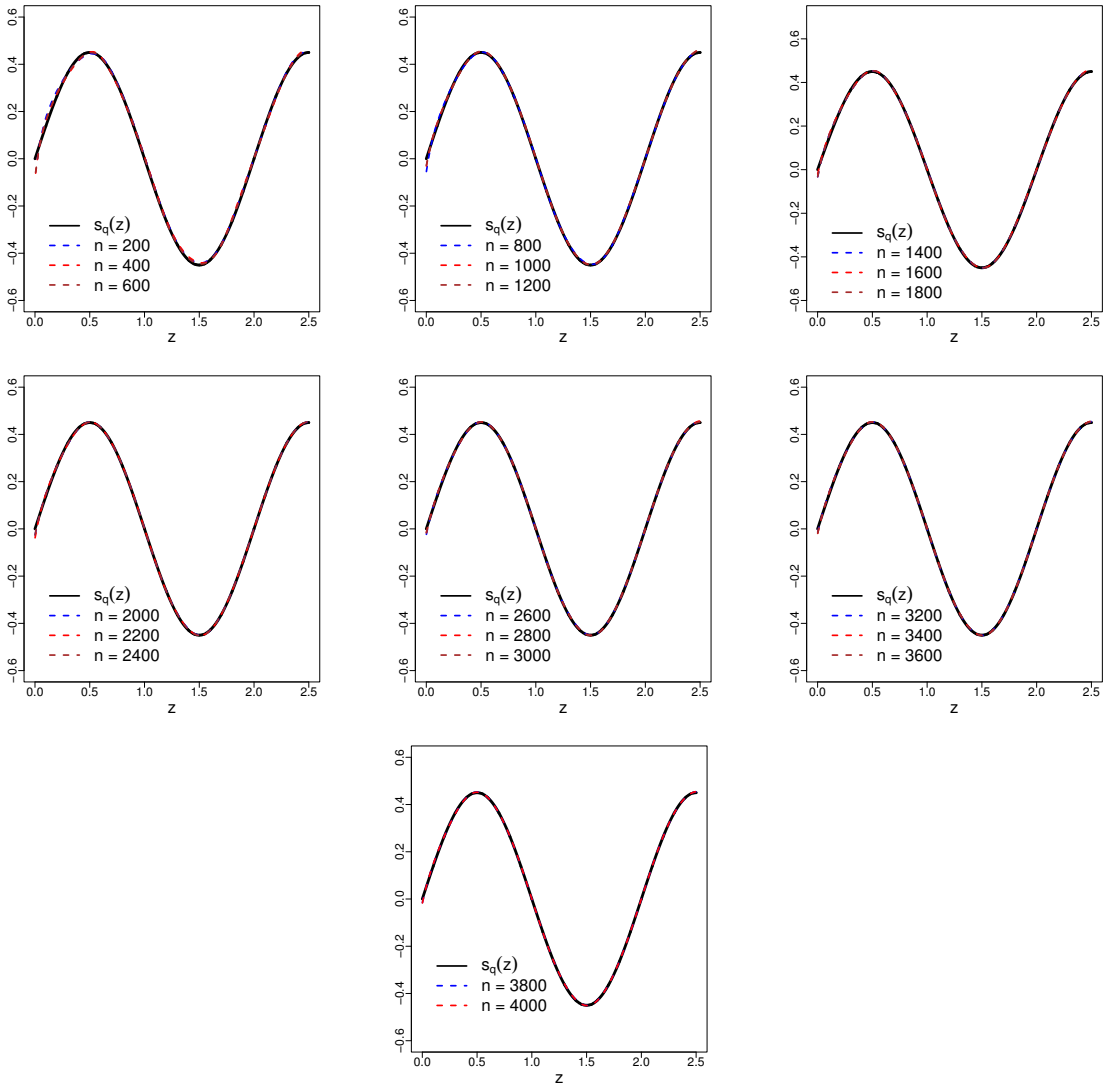

Figure 57 – Smooth function mean on the 500 estimates obtained in the RPMOG model under different sample sizes and $q = 0.5$.

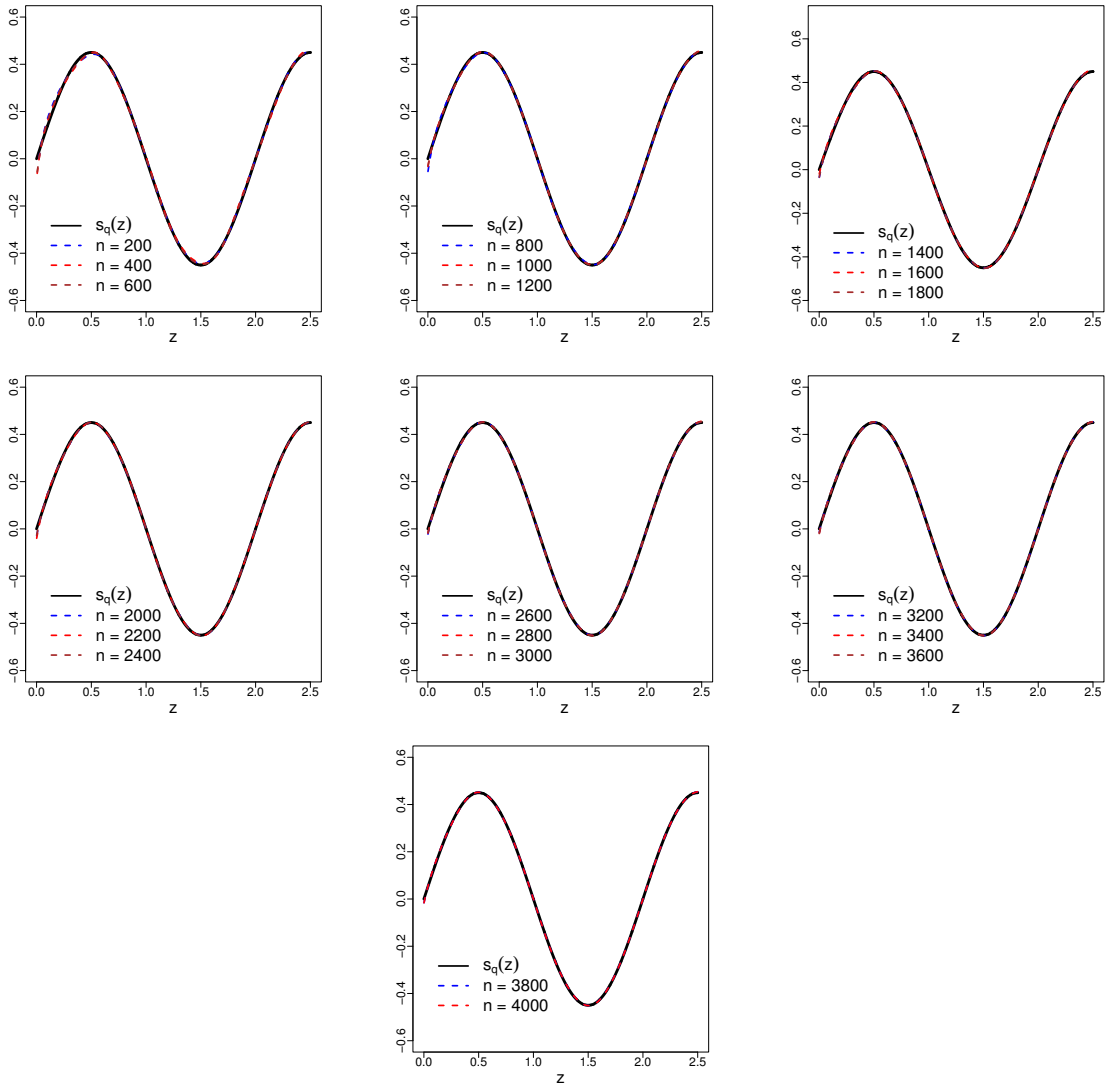

Figure 58 – Smooth function mean on the 500 estimates obtained in the RPMOG model under different sample sizes and $q = 0.9$.

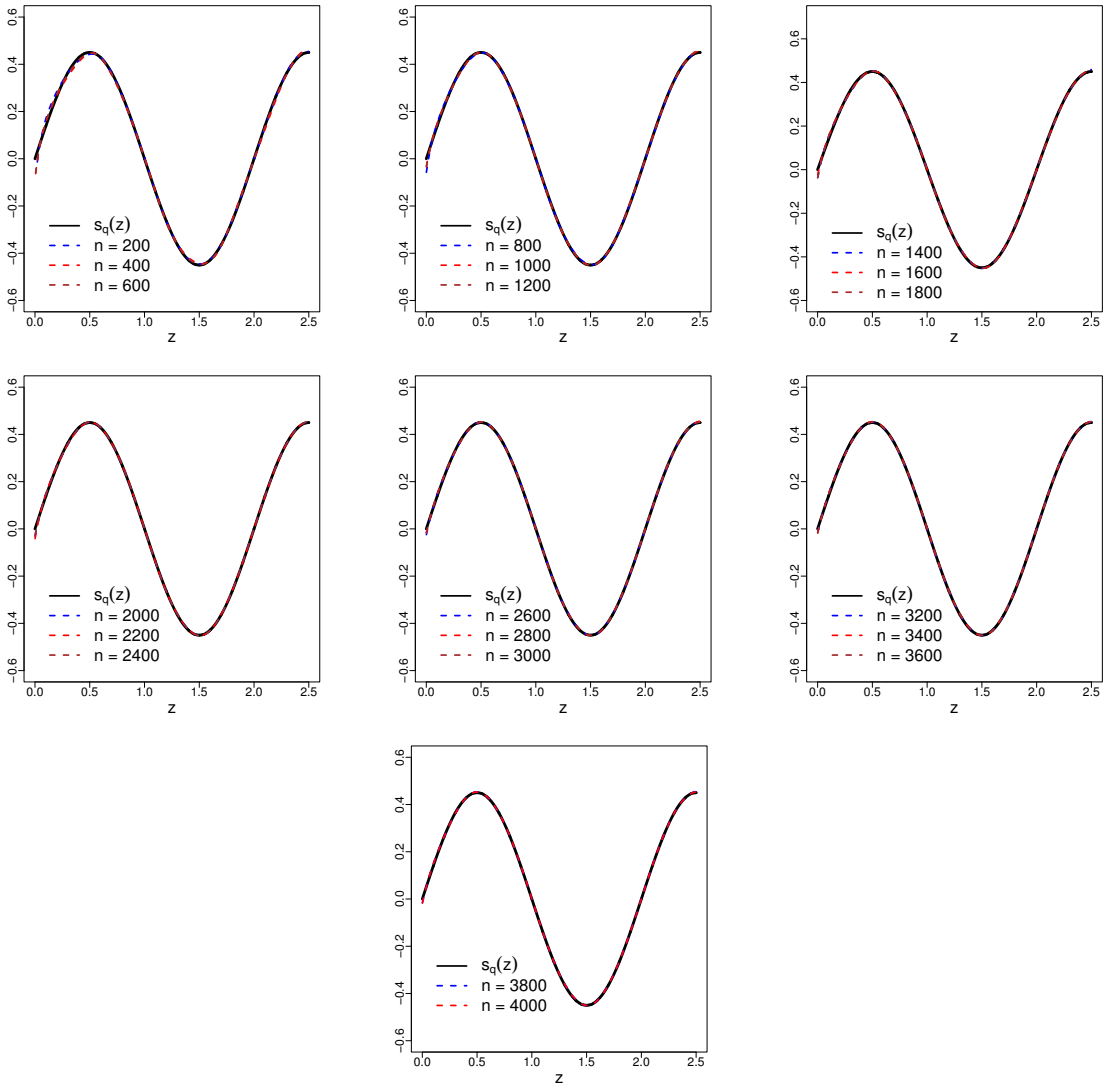

Figure 59 – SE_i/SE_{i+1} and $\sqrt{n_{i+1}/n_i}$ rates for the parameters indicated in the nonparametric QR model under RPMON distribution.

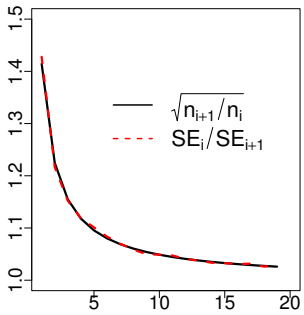

(a) $\widehat{\nu}_{1q}$ with $q = 0.1$

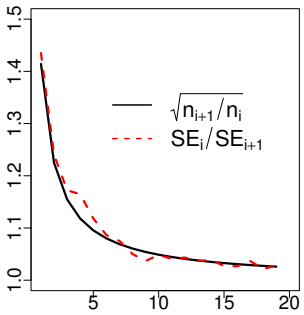

(b) $\widehat{\nu}_{2q}$ with $q = 0.1$

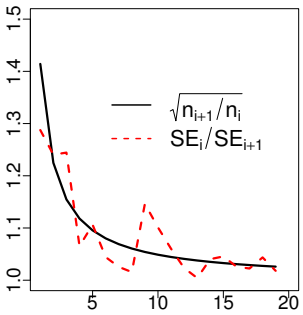

(c) $\widehat{\tau}_{1q}$ with $q = 0.1$

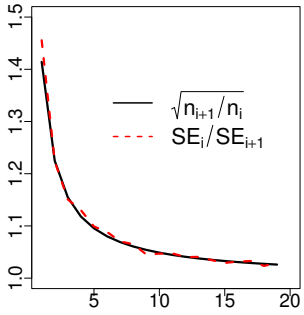

(d) $\widehat{\nu}_{1q}$ with $q = 0.5$

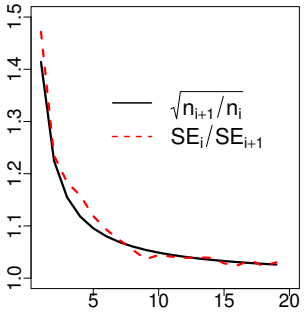

(e) $\widehat{\nu}_{2q}$ with $q = 0.5$

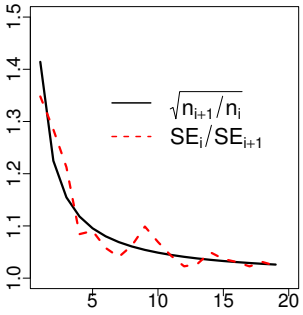

(f) $\widehat{\tau}_{1q}$ with $q = 0.5$

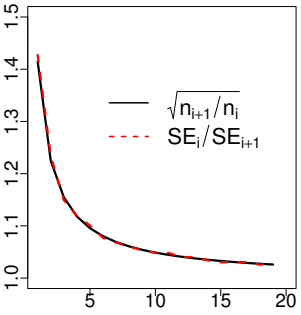

(g) $\widehat{\nu}_{1q}$ with $q = 0.9$

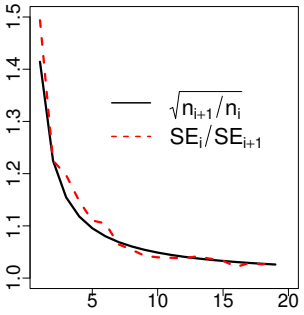

(h) $\widehat{\nu}_{2q}$ with $q = 0.9$

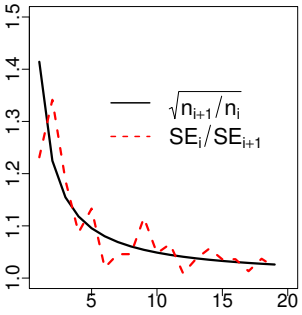

(i) $\widehat{\tau}_{1q}$ with $q = 0.9$

Figure 60 – $\mathrm{SE}_i/\mathrm{SE}_{i+1}$ and $\sqrt{n_{i+1}/n_i}$ rates for the parameters indicated in the nonparametric QR model under RPMOG distribution.

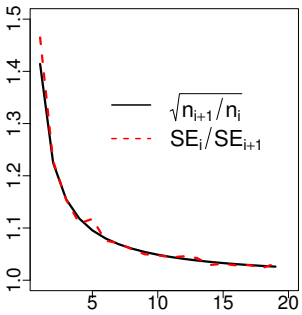

(a) $\widehat{\nu}_{1q}$ with $q = 0.1$

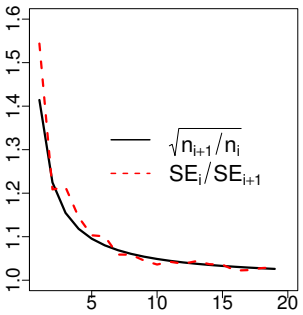

(b) $\widehat{\nu}_{2q}$ with $q = 0.1$

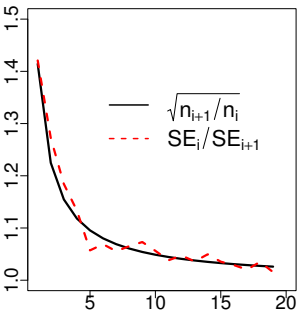

(c) $\widehat{\tau}_{1q}$ with $q = 0.1$

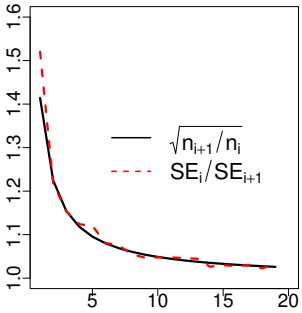

(d) $\widehat{\nu}_{1q}$ with $q = 0.5$

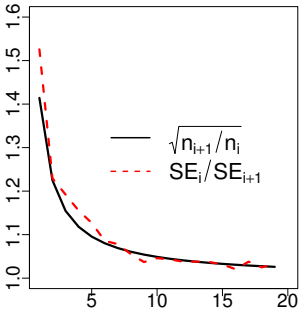

(e) $\widehat{\nu}_{2q}$ with $q = 0.5$

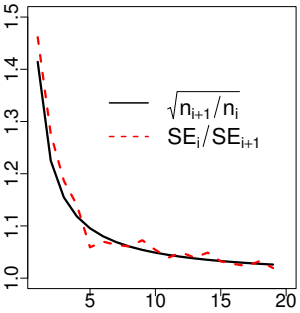

(f) $\widehat{\tau}_{1q}$ with $q = 0.5$

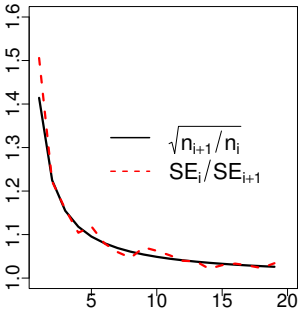

(g) $\widehat{\nu}_{1q}$ with $q = 0.9$

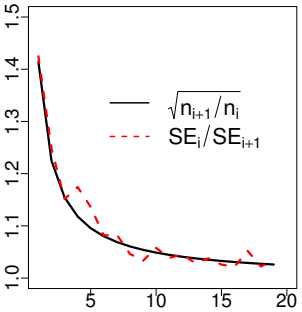

(h) $\widehat{\nu}_{2q}$ with $q = 0.9$

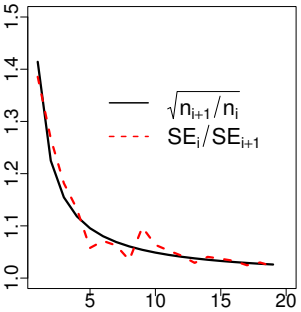

(i) $\widehat{\tau}_{1q}$ with $q = 0.9$

APPENDIX

C

PENALIZED OBSERVED INFORMATION MATRIX

This appendix shows the calculations of elements $\ddot{\ell}_{\xi_{iq}}$, $\ddot{\ell}_{\xi_{iq}\sigma_{iq}}$, $\ddot{\ell}_{\xi_{iq}\alpha_{iq}}$, $\ddot{\ell}_{\sigma_{iq}}$, $\ddot{\ell}_{\sigma_{iq}\alpha_{iq}}$ and $\ddot{\ell}_{\alpha_{iq}}$ presented in Section 4.2.3 of Chapter 4.

The remaining elements of the penalized observed information matrix of the PLQR model are as follows:

$$\begin{aligned}
\ddot{\ell}_{\xi_{iq}} &= \frac{\partial^2 \ell_i(\xi_{iq},\sigma_{iq},\alpha_{iq})}{\partial^2 \xi_{iq}^2} \qquad \text{(C.1)}\\
&= \psi_{1iq}^2\left[\frac{f_0''(u_{iq})}{f_0(u_{iq})} - \frac{f_0'^2(u_{iq})}{f_0^2(u_{iq})}\right] + 2\psi_{1iq}^2\left[\frac{f_0(u_{iq})(1-\alpha_{iq})}{\alpha_{iq}+(1-\alpha_{iq})F_0(u_{iq})}\right]^2\\
&\quad - 2\psi_{1iq}^2\left[\frac{f_0'(u_{iq})(1-\alpha_{iq})}{\alpha_{iq}+(1-\alpha_{iq})F_0(u_{iq})}\right],\\
\ddot{\ell}_{\xi_{iq}\sigma_{iq}} &= \frac{\partial^2 \ell_i(\xi_{iq},\sigma_{iq},\alpha_{iq})}{\partial\xi_{iq}\partial\sigma_{iq}} \qquad \text{(C.2)}\\
&= \psi_{1iq}^2\left[\frac{f_0'(u_{iq})}{f_0(u_{iq})}\right] + \psi_{1iq}^2\psi_{2iq}\left[\frac{f_0''(u_{iq})}{f_0(u_{iq})} - \frac{f_0'^2(u_{iq})}{f_0^2(u_{iq})}\right] - 2\psi_{1iq}^2\left[\frac{f_0(u_{iq})(1-\alpha_{iq})}{\alpha_{iq}+(1-\alpha_{iq})F_0(u_{iq})}\right]\\
&\quad + 2\psi_{1iq}^2\psi_{2iq}\left[\frac{f_0(u_{iq})(1-\alpha_{iq})}{\alpha_{iq}+(1-\alpha_{iq})F_0(u_{iq})}\right]^2 - 2\psi_{1iq}^2\psi_{2iq}\left[\frac{f_0'(u_{iq})(1-\alpha_{iq})}{\alpha_{iq}+(1-\alpha_{iq})F_0(u_{iq})}\right],\\
\ddot{\ell}_{\xi_{iq}\alpha_{iq}} &= \frac{\partial^2 \ell_i(\xi_{iq},\sigma_{iq},\alpha_{iq})}{\partial\xi_{iq}\partial\alpha_{iq}} \qquad \text{(C.3)}\\
&= 2u_{\alpha_{iq}}\psi_{1iq}\left[\frac{f_0'(u_{iq})(1-\alpha_{iq})}{\alpha_{iq}+(1-\alpha_{iq})F_0(u_{iq})}\right] - u_{\alpha_{iq}}\psi_{1iq}\left[\frac{f_0''(u_{iq})}{f_0(u_{iq})} - \frac{f_0'^2(u_{iq})}{f_0^2(u_{iq})}\right]\\
&\quad - 2\psi_{1iq}\left[\frac{f_0(u_{iq})(1-\alpha_{iq})}{\alpha_{iq}+(1-\alpha_{iq})F_0(u_{iq})}\right]\left[\frac{1-F_0(u_{iq})+(1-\alpha_{iq})f_0(u_{iq})u_{\alpha_{iq}}}{\alpha_{iq}+(1-\alpha_{iq})F_0(u_{iq})}\right]\\
&\quad - 2\psi_{1iq}\left[\frac{f_0(u_{iq})}{\alpha_{iq}+(1-\alpha_{iq})F_0(u_{iq})}\right],
\end{aligned}$$

and

$$\ddot{\ell}_{\sigma_{iq}} = \frac{\partial^2 \ell_i(\xi_{iq},\sigma_{iq},\alpha_{iq})}{\partial^2 \sigma_{iq}^2} \tag{C.4}$$
$$= \psi_{1iq}^2 + 2\psi_{1iq}^2\psi_{2iq}\left[\frac{f_0'(u_{iq})}{f_0(u_{iq})}\right] - 4\psi_{1iq}^2\psi_{2iq}\left[\frac{f_0(u_{iq})(1-\alpha_{iq})}{\alpha_{iq}+(1-\alpha_{iq})F_0(u_{iq})}\right]$$
$$- 2\psi_{1iq}^2\psi_{2iq}^2\left[\frac{f_0'(u_{iq})(1-\alpha_{iq})}{\alpha_{iq}+(1-\alpha_{iq})F_0(u_{iq})}\right] + 2\psi_{1iq}^2\psi_{2iq}^2\left[\frac{f_0(u_{iq})(1-\alpha_{iq})}{\alpha_{iq}+(1-\alpha_{iq})F_0(u_{iq})}\right]^2$$
$$+ \psi_{1iq}^2\psi_{2iq}^2\left[\frac{f_0''(u_{iq})}{f_0(u_{iq})} - \frac{f_0'^2(u_{iq})}{f_0^2(u_{iq})}\right],$$

$$\ddot{\ell}_{\sigma_{iq}\alpha_{iq}} = \frac{\partial^2 \ell_i(\xi_{iq},\sigma_{iq},\alpha_{iq})}{\partial\sigma_{iq}\partial\alpha_{iq}} \tag{C.5}$$
$$= 2u_{\alpha_{iq}}\psi_{1iq}\psi_{2iq}\left[\frac{f_0'(u_{iq})(1-\alpha_{iq})}{\alpha_{iq}+(1-\alpha_{iq})F_0(u_{iq})}\right] - u_{\alpha_{iq}}\psi_{1iq}\psi_{2iq}\left[\frac{f_0''(u_{iq})}{f_0(u_{iq})} - \frac{f_0'^2(u_{iq})}{f_0^2(u_{iq})}\right]$$
$$- 2\psi_{1iq}\psi_{2iq}\left[\frac{f_0(u_{iq})(1-\alpha_{iq})}{\alpha_{iq}+(1-\alpha_{iq})F_0(u_{iq})}\right]\left[\frac{1-F_0(u_{iq})+(1-\alpha_{iq})f_0(u_{iq})u_{\alpha_{iq}}}{\alpha_{iq}+(1-\alpha_{iq})F_0(u_{iq})}\right]$$
$$- 2\psi_{1iq}\psi_{2iq}\left[\frac{f_0(u_{iq})}{\alpha_{iq}+(1-\alpha_{iq})F_0(u_{iq})}\right],$$

$$\ddot{\ell}_{\alpha_{iq}} = \frac{\partial^2 \ell(\xi_{iq},\sigma_{iq},\alpha_{iq})}{\partial^2 \alpha_{iq}^2} \tag{C.6}$$
$$= u_{\alpha_{iq}}^2\left[\frac{f_0''(u_{iq})}{f_0(u_{iq})} - \frac{f_0'^2(u_{iq})}{f_0^2(u_{iq})}\right] + u_{\alpha_{iq}\alpha_{iq}}\left[\frac{f_0'(u_{iq})}{f_0(u_{iq})}\right] - 2u_{\alpha_{iq}\alpha_{iq}}\left[\frac{f_0(u_{iq})(1-\alpha_{iq})}{\alpha_{iq}+(1-\alpha_{iq})F_0(u_{iq})}\right]$$
$$+ 4\left[\frac{f_0(u_{iq})u_{\alpha_{iq}}}{\alpha_{iq}+(1-\alpha_{iq})F_0(u_{iq})}\right] - 2u_{\alpha_{iq}}^2\left[\frac{f_0'(u_{iq})(1-\alpha_{iq})}{\alpha_{iq}+(1-\alpha_{iq})F_0(u_{iq})}\right] - \psi_{3iq}^2$$
$$+ 2\left[\frac{1-F_0(u_{iq})+(1-\alpha_{iq})f_0(u_{iq})u_{\alpha_{iq}}}{\alpha_{iq}+(1-\alpha_{iq})F_0(u_{iq})}\right]^2,$$

where

$$u_{\alpha_{iq}\alpha_{iq}} = \frac{q(1-q)}{(1+q\alpha_{iq}-q)^2}\left[\Psi_0' - \frac{2q\Psi_0}{(1+q\alpha_{iq}-q)}\right], \qquad \Psi_0' = \frac{q(q-1)\Psi_1\Psi_0^3}{(1+q\alpha_{iq}-q)^2}$$

and

$$\Psi_1 = f_0'\left(F_0^{-1}\left(\frac{\alpha_{iq}q}{1+q\alpha_{iq}-q}\right)\right) \text{ for } i = 1,\ldots,n \text{ and } q \in (0,1) \text{ fixed.}$$

Note that the expression of the second derivative of $f_0(u_{iq})$, denoted by $f_0''(u_{iq})$ within Equations (C.1)-(C.6) is shown in Table 3 of Chapter 2.


ICMC
USP
SÃO CARLOS